STUDY OF MICRO-GRINDING OF GLASS USING ON-MACHINE FABRICATED POLYCRSYTALLINE DIAMOND (PCD) BY MICRO-EDM

ASMA PERVEEN

(B.Sc. in Mechanical Engineering, BUET)

A THESIS SUBMITTED

FOR THE DEGREE OF DOCTOR OF PHILOSOPHY

DEPARTMENT OF MECHANICAL ENGINEERING

NATIONAL UNIVERSITY OF SINGAPORE

2012

Declaration

I hereby declare that the thesis is my original work and it has been written by me in entirely.

I have duly acknowledged all the source of information which have been used in this thesis.

This thesis has also not been submitted for any degree in any university previously.

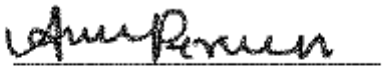

Asma Perveen
6 September 2012

Acknowledgments

I wish to express my deepest and heartfelt gratitude and appreciation to my Supervisors, Professor Wong Yoke San and Professor Mustafizur Rahman for their valuable guidance, unconditional support, continuous encouragement and for being the source of inspiration throughout the tenure. Their comments and advice during the research have contributed immensely towards the success of this work. In addition, their patient guidance and suggestions have also helped me in learning more.

I would also like to take this opportunity to show my thanks to the National University of Singapore (NUS) for supporting my research by providing the research scholarship and to the Advanced Manufacturing Lab (AML) and Micro Fabrication Lab for the state of the art facilities and support, without which this present work would not be possible.

I owe my deepest gratitude to the following staffs for their sincere help, guidance and advice: Mr. Tan Choon Huat, Mr. Lim Soon Cheong, Mr. Wong Chian Long, Mr. Sivaraman Selvakumar and Mr. Yeo Eng Haut, Nelson from Advanced Manufacturing Lab (AML). Special thanks go to Mr. Tanveer Saleh and Javahar from Mikrotools, a NUS spin off company, for their help with the machine set-up and technical assistance provided during different period of my research.

I would like to offer my appreciation for the support and encouragement during various stages of this research work to my lab mates and friends. My appreciation goes to Mohammad Pervej Jahan, Mohammed Muntakim Anwar, Rajib Saha, Mohammad Ahsan Habib, Fahd Ebna Alam, Tamanna Alam, Aklima Afzal, Kazi Monzure Khoda, Aziz Ahmed, Saikat Das, Mohammad Iftekher Hossain, Aslam Hossain, Jahidul Islam, Md. Mazharul Haque, Ashim Kumar Debnath, Saidur Rahman Bakaul, Mahjabeen Sultana, Chandra Nath, Indraneel Biswas, Muhammad Tarik Arafat, Anower Hossain, Wang Xue, Jingjing, Dang, Xinqian, Arif, Chanaka Dilhan Senanayake, Lubecki Tomasz Marek,

Subrata Saha, Khalid, Rumki, Jerry, Ranjan, Sujib and many more. Special thanks to all of them for being so supportive for the past four years. Last but not the least, my heartfelt gratitude goes to my dearest mother Mrs. Anowara Begum, for her loving encouragement and best wishes throughout the whole period and my father, Md. Ruhul Amin Khan, for his mental support and encouragement that kept me strong to face numerous challenges. I am also deeply indebted to my loving elder sisters, Nasima Khan Bakul, and Sabina Yesmin Bina for their inspiration and my brothers, Hasnanur Rahman Shadeen, Sakin Amin Khan and Jubaed Hossain, for always being there for me. Without them this journey might not be possible. I will be ever grateful to them for their kind support.

Table of Contents

Summary

This research mainly aims to study and develop a multi-process approach to improve and enhance the machining of brittle materials like glass using a PCD tool. A combined block-EDM and micro-grinding process is proposed where the micro-grinding process is applied to the glass following the block-EDM operation on PCD tool. The intregrated block-EDM and micro-grinding process is conducted in a single setup, which does not involve the taking out of the PCD tool after fabrication and hence can improve the accuracy in the fabrication of micro-features on glass. Firstly, the experimental investiagation has been performed to find the optimum block-EDM parameters for the PCD tool preparation considering the better surface finish on the glass material. Using the optimum tool, in depth investigation has been carried out to find out the optimum grinding condtions. It is envisaged that considering the machining time, optimum parameters for micro-EDM was found to be 120 V, 1000 pF and 30 µm feed length. An axial depth of cut of 2 µm and feed rate of 1 µm/min was found to be optimum in terms of cutting forces and achieved surface finish. In addition to this, BK7 glass was also found to provide better machinability based on cutting force and surface roughness (12.79 nm) analysis among three different kinds of glasses. Other than optimum machining condition, feasibility of fabrication of different geometry of grinding tools along with desired size and their effect on grinding glass has been studied. It is found that with the concept of block micro-EDM and application of the specifically designed block, microelectrodes of conical, triangular, square or rectangular, circular and D-shaped tool were possible to fabricate successfully in a single set-up which eliminates the usage of another machine when different shape micro-structure is needed on the glass material. In addition to this, it is found that the D-shape tool demonstrated better performances among all the four tools(circular, D-shaped, triangular, square) considered in terms of cutting force, roughness value, side surface and wear rate due to its geometry, with enhanced chip removal form the machined surface.

Thirdly, in order to comprehend the usage time of this newly developed on-machine fabricated PCD tool in case of glass machining, wear analysis and monitoring the wear process has been carried out also. The G ratio for this PCD micro tool was found to be nearly 940 indicating the greater wear resistance of the tool even against the abrasive material like glass. Edge chipping and abrasive wear were found to take place on the tool surface in the three steps of wear progression, which is initial, intermediate and severe. Moreover, the continuous monitoring of

AE signal is found to give an indication of tool topographic condition, i.e. sharpness and bluntness of PCD cutting edge during micro-grinding. In addition to this, glass cutting mechanism has been investigated using surface and sub-surface condition analysis to understand the effect of machining condition in this process. It is found that the ground surface consists of four different types; (a) smooth; (b) fractured; (c) smeared; (d) ploughing striations. Both the damage depth and surface roughness are found to be influenced by the depth of cut, feed rate, and spindle speed. In addition, two major types of grinding damage have been identified to likely be chipping damage and micro-cracking damage. Lateral, median and cone cracks are found to be existed in the sub-surface. The crack size varies from below to above 1µm.

Finally in this thesis, a new predictive analytical modified model for micro grinding process has been developed considering single grit interaction for calculating process force. Then, on the basis of this predictive model, a comparison between the experimental data and analytical prediction was performed in the case of overall micro-grinding forces in x, y and z direction. Although, there is pretty much deviation in the predicted value of the micro grinding forces, these differences can be reduced considering more parameters in the model which can be considered in future work.

The research works conducted in this project will be eminently helpful to promote better understanding while implementing this newly developed hybrid process, and to improve its robustness in the field of precision manufacturing. The investigation conducted in this thesis will be certainly supportive for the PCD tool users to understand the importance of choosing fabrication parameters that works in better associations with the glass grinding parameters and to utilize the full effectiveness of the PCD tool for precision finishing of brittle material like glass. In addition, the combined established relation among tool wear, cutting force and AE signal is new and useful analysis, which are more essential to necessitate offline dressing for tool wear compensation. Morover, the knowledge of the damage generation and propagation promotes the importance of selecting optimum parameters for finishing of a particular brittle work pieces.

Nomenclature

C = Capacitance (pF)

V =Gap voltage (V)

Δr-=Decrease in tool radius

G= Volume of material removal per unit volume of wheel wear

d_{si}= Mean of the tool diameter before and after wear

b_1 = Grinding width

V_s=Volume of radial wheel wear

V_w=Volume of material removal

K_c =Fracture toughness

H = Hardness

E = Elastic modulus

b = A constant which depends on tool geometry

y_c. =An average depth

f = Cross-feed

d_c =Critical penetration depth for fracture initiation

$C_{d(z')}$=dynamic cutting edge density

ν = Feed rate

$\bar{h}$ = Minimum chip thickness

α_{cr} = Critical rake angle

$Cs(z)$= Static cutting density

A= Empirical constant

Z=Radial distant measured into the wheel

d_c = Average grain diameter

Vt= Total volume on the periphery of the wheel engaged in the work piece

Vsh= Total kinematic shadow volume generated by active cutting edge

N_g =Total number of grain

d_{geq} = Equivalent grain diameter

b_c = *Cutting width of grain*

a_c = *Cutting length of grain*

t= Grain depth of cut

V=Spindle speed

HB= Brinall hardness number

f_{brnl} =*Indentation force*

d = Ball diameter

b = Diameter of impression.

β = *Friction angle*

ϕ =*Shear angle*

σ_s = *Shear strength*

f_{cgx} = *Chip formation force in tangential direction*

f_{cgy} = *Chip formation force in normal direction*

f_{pgx} = *Plough force in tangential direction*

f_{cgy} =*Plough force in normal direction*

f_n =*Force acting normal direction for each grain*

f_t =*Force acting tangential direction for each grain*

F_n =*Total force in normal direction*

F_t =*Total force in traverse direction*

F_l =*Total force in longitudinal direction*

μ_p = *Friction co-efficient*

B= Work piece width

D= Tool diameter

Lists of Figures

Lists of Tables

Chapter 1

Introduction

1.1. Machining of Glass and Ceramics: Importance and challenges

1.1.1. Importance

In recent past, there have been increased interests in the use of the advanced ceramics and glass materials such as alumina, silicon nitride, silicon carbide, BK7 and soda lime glass materials with unique metallurgical properties to meet the demands of extreme applications. While these materials are harder, tougher, brittle, less heat sensitive and/or more resistant to chemicals, corrosion and fatigue, these are more difficult to machine (Agarwal and Rao, 2008). These difficult-to-cut brittle materials have been widely used these days not only in the automotive industries but also in the public welfare industries like biomedical, optics (Foy et al., 2009). Therefore, the machining of difficult-to-cut materials has become an important issue in the field of manufacturing. As the indentation test proves that, when the penetration depth is less than certain critical value, most brittle materials like glass also undergoes plastic deformation. Hence, it is possible to machine difficult to cut brittle material in ductile mode without any fracture. This fact leads to the new possibilities of machining brittle material with optical surface finish by traditional machining process which eliminates the necessities of secondary finishing process. Since these difficult-to-cut materials possess excellent mechanical properties which can be useful in many important applications, machining of them in ductile mode can open up opportunities of utilizing them comprehensively.

1.1.2. Challenges in machining of Glass

Owing to brittleness and hardness, optical glass is one of the materials that is most difficult to cut. Besides silicon, glass is widely used substrate material in micro system

technology, particularly in the manufacturing of micro fluidic devices for biological analysis and biotechnical applications due to its beneficial and functional material properties (Daridon et al., 2001; Petersen et al., 2004). Compared to silicon, the use of glass in micro-total-analysis-system (μTas) offers several benefits like optical transparency for visual inspection, on line optical detection as well as its good dielectric properties to withstand high voltages used in electro kinetically driven flows and separation. Other beneficial properties of glass are its good chemical resistance, high thermal stability; chemical inertness that makes glass the most widely used substrate for the fabrication of DNA arrays. Therefore machining of glass has become one of the major concerns of the manufacturer for the last few decades. Fabrication of precise microstructures in a controlled fashion particularly in glass for micro fluidics device is challenging. This difficulty of making structure in glass is reflected in the wide variety of non-conventional techniques for glass micromachining along with some conventional technologies. Significant researches have been carried out on glass micro fabrication technology which involves mainly photolithography and chemical etching. Being isotropic material, glass can be wet etched with buffered HF in a non-directional manner. Dry chemical etching of glass is also possible in typical a SF_6 plasma which is hindered due to slow etching rate (Li et al., 2001). Etching techniques have a hazardous problem, since the etching material contains atoms of lead or sodium which produce nonvolatile halogen compounds as reaction product. Although deep reactive ion etching with inductively coupled plasma source producing high density plasma at low pressure has been used for silicon channels, it is not well developed enough to apply for similar structures in glass materials. Due to the brittleness and poor thermal properties of most glasses, there is a risk of micro-cracking and other collateral damages such as debris and poor surface quality in Laser micromachining of glass (Nikumb et al., 2005). Mechanical machining techniques specialized for brittle material such as abrasive jet machining which is based on mechanical removal from a substrate by a jet of particles allowing to get complex and controlled shapes of eroded structure is hindered due to rough surface and limited to larger components (Belloy et al., 2000; Plaza et al., 2003; Schlautmann et al., 2001; Slikkerveer et al., 2000).

Brittle materials are difficult to mechanically micro machined by cutting process like milling due to the damage resulting from material removal by brittle fracture leading to rough surface which requires further polishing. Although high speed milling is widely used in metallic mold industry, it is difficult to apply it in machining glass due to extreme hardness and strength. In order to overcome the technical difficulties in these above mentioned machining techniques and to reduce the high costs associated with the elevated hardness and intrinsic brittleness, new machining approaches are increasingly attempted for the machining of optical glass, particularly for applications where dimensional accuracy with complex geometries are primary requirements. Vertical micro-grinding is one of the important and cost-effective methods of machining this extremely hard and brittle material. Material removal by ductile mode instead of brittle fractures is made possible by using polycrystalline diamond tools. Therefore, vertical micro-grinding has been considered as one of most effective methods of machining glass.

1.3 Background (Motivation)

In order to reduce the size of parts and products in the electronics, computer, and biomedical industry, mmanufacturing technology has been advanced to higher level of precision to satisfy the increasing demand. New processing concepts, procedures and machines have become indispensable to fulfil the increasingly stringent requirements and expectations. Mechanical micro-machining is one of the promising technologies which can assure large benefits and equally great challenges in fabrication of micro-scale parts. Existing micro-machining processes can be broadly classified into mechanical micro-machining, chemical mechanical micro-machining, high energy beams-based machining, and scanning probe micro-machining as shown in Fig. 1.1(Liang, 2004).

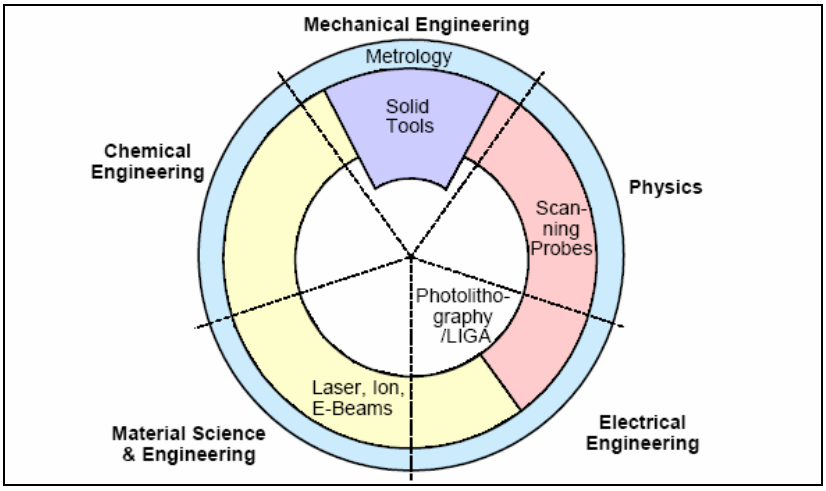

Fig.1. 1: Disciplinary areas for various micro manufacturing.

Mechanical micro-machining using a miniaturized machine tool is one type of research direction among these technologies, which has a number of inherent advantages. These advantages includes the significant reduction of required space and energy consumption for the machine drive; the improvement of machine robustness against external error sources due to increase in thermal, static, and dynamic stabilities; increased positioning accuracy due to decreased overall size of the machine; and a greater freedom in the selection of work piece materials, the complexity of the product geometry, and the cost of investment.

In general, mechanical micro-machining consists of various material removal processes. Within these processes, micro-grinding is the typical final process step and like conventional grinding, it also provides a competitive edge over other processes in micro-scale parts fabrication such as micro sensors, micro actuators, micro fluidic devices, and micro machine parts. Since conventional grinding wheels are very large compared to target products, their capability is usually limited to grinding simple parts as envisaged in Fig. 1.2.

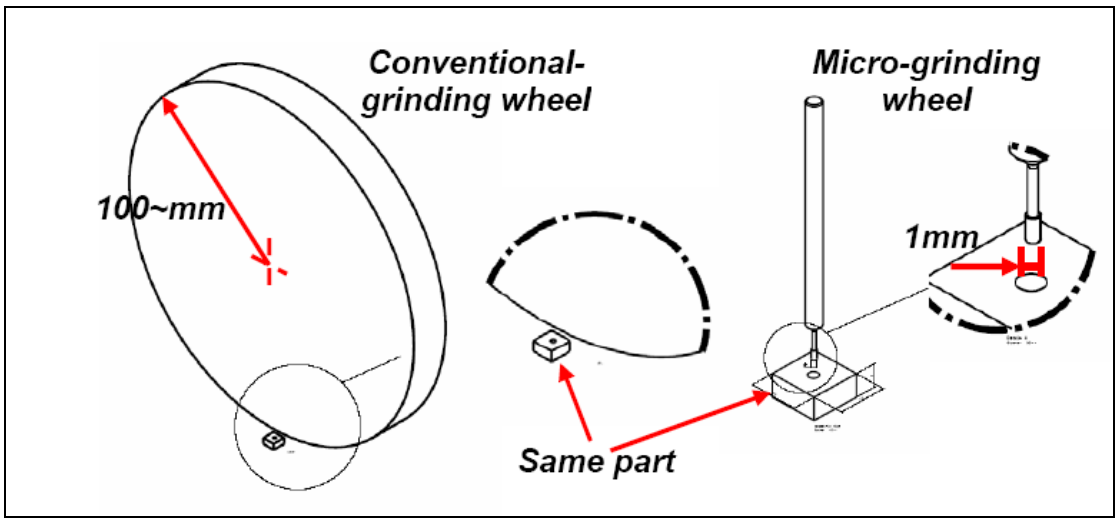

Fig.1. 2: Fabrication of micro-scale parts using conventional and micro grinding.

On the contrary, although a micro-grinding process resembles a conventional grinding process, this process is distinctive because of the size effect in micro-machining whereas the mechanical and thermal interactions between a single grit and a work piece are related to the phenomena observed in micro-machining, which are summarized in Table 1.1.

Since the diameter of the grinding wheel reduces, the negligible parameters in the conventional grinding process such as ploughing forces and grinding wheel deformation has become more significant in micro-grinding. Even though the boundary between micro and conventional grinding is not comprehensible, micro-grinding is not the simple reduction of the conventional grinding process. Furthermore, the quality of the parts produced by applying this process is subjected to the process conditions, micro-grinding wheel properties, and microstructure of materials (Hyung Wook Park, 2008) . Again, the micro tools properties are dependent on the fabrication process used. Micro-tools made of PCD offer new promise for micro-machining of hard and brittle materials like conventional grinding wheel. In recent years, machining of difficult-to-cut materials is an important issue in the field of manufacturing.

Table 1. 1: Characteristics of the micro-grinding process

	Macro-grinding	Micro-grinding
Ratio of the depth of cut to the grit radius	50-100	0.1-1
Ploughing Effect	Not significant(≈ 0%)	Significant (≈20−30%)
Friction on the interface	$\mu = \mu_c$	$\mu = \mu_c$ (*depth of cut)*+μ_p(ploughing friction co-efficient)
Rake angle	Constant negative	Variable negative
Material removal rate	$10^n \sim 10^{-1} mm^3/mm.s$	$10^{-1} \sim 10^{-3} mm^3/mm.s$

Since these difficult-to-cut materials possess excellent mechanical properties which can be useful in many important applications, machining of them can open up opportunities of utilizing them comprehensively. Among the difficult-to-cut materials PCD is an extremely hard material used extensively in manufacturing because of its superior wear and corrosion resistance. Therefore machining of PCD has become one of the major concerns of the manufacturer for the last few decades (Mahdavinejad, 2005). However the fabrication of these hard tools by mechanical process like diamond grinding gives rise to difficulties associated with the high cost of diamond wheel, large consumption of diamond and arduous processing. On the other hand, whereas the efficiency of traditional cutting process is restricted by the mechanical properties of material and the complexity of work piece geometry, electro discharge machining being a thermal erosion process, is not subjected to such strain. EDM now a days is extensively and successfully applied for machining difficult to work material (A.G.Mamalis, 2004). Some researchers tried to fabricate tools with WEDG. When compared with other methods such as WEDG and mesh electrode method, the EDM block electrode method has a lower investment cost and is easier to set up. More importantly, it can also produce electrodes on the machine and this greatly reduces the installation error and cost (Nachiappan Ravi and Han. Huang, 2002). Hence the PCD tool produced by this block EDM method can be useful in micro-grinding of hard and brittle materials like glasses.

In addition, the need for fabricated micro-features in glass has been increasing to generate diversified functionalities on optical devices and bio-fluidics devices. Micro-channels are integral part of micro-fluidic devices, which are used for various applications such as lab-on-chip, bio-MEMS (MEMS denotes micro-electromechanical system) based sensors, etc. These micro-channels are used for seamless integration of sample collection, separation, and detection of various biological and chemical species on a single chip with fluidic pumps and valves integrated with the system. Fundamental understanding of liquid flow through micro-channels is important to predict the performance and behaviour of micro-fluidic devices. Depending on the manufacturing technique or due to adhesion of biological particles from the liquids, the channel surface has certain degree of roughness. The surface roughness ranges from 0.1 micron to 2 micron and this surface roughness of micro-fluidic channel affects the flow characteristics in the channel. Higher roughness of this channel results in higher flow interruption. So, surface roughness is very important in the glass micro-channel (Mitra, 2008) . Although some manufacturing process such as chemical etching has been used to fabricate micro-patterns on glass, the process takes a longer time around (597-723 minutes) and it is hazardous. Photolithography gives surface roughness up to micro level and the process is not cost effective (Takashi Matsumura, 2005) .

Therefore, the development of a process which can produce smooth glass surface is of prime importance in the field of machining glass. This process should be applicable to small parts and also micro-fluidics devices which comprises the main field of application of glass.

1.4. Significance of research

Although grinding has several advantages over other machining processes and several researches have been carried out for last few decades on the conventional grinding of

brittle materials, micro-grinding of brittle materials using on-machine fabricated grinders is still a relatively new area to be further explored. Hence, a number of issues remain to be solved before this vertical micro-grinding process can become a reliable, effective and economical process for manufacturing micro components and parts with micro-features on glass using on machine fabricated PCD tools.

Brittle materials like glass and ceramics are expected to revolutionize the industry due to their unique and highly favorably properties. Presently, the industries that are shifting to utilize ceramic and glass based materials for their products are mold manufacturing, biomedical, semiconductor, lens manufacturing, automobile engines and aerospace sector. Due to their superior properties, glass and ceramics have potential to replace metal and other materials currently being used for aforementioned sectors. These brittle materials offer excellent wear resistance and high temperature resistance characteristics. Due to these characteristics, modern mold making industry is using ceramics and glass to manufacture molds. High hardness, excellent wear resistance and high temperature resistance of these materials impart longer life to the molds. However the machining of brittle materials is cost-prohibitive and is the only obstacle in their immediate application. Mainly ceramics and glass are machined through polishing, honing and grinding to obtain the optical surface finish. Optical and superior surface finish is the requirement of many ceramic based products due to the nature of their intended application. Therefore, it has been found that, although requirements for micro-features in difficult to- cut materials have made grinding a cost-effective manufacturing process, grinding itself cannot fulfill all the requirements of the product performance alone. There is a need to investigate the feasibility of introducing other processes in association with conventional grinding to meet the increasing demands and challenges. Fortunately the ongoing research in this field is developing new technology to machine brittle materials in ductile mode to produce high quality surface finish. The development of process which can provide micro-features with good surface quality and better dimensional accuracy at high machining efficiency is of prime importance. One of these technologies involves the usage of polycrystalline diamond tool for micro-grinding of glass. In this regard, this

study considers micro-EDM based multi-process machining techniques which may improve the performance of the machining of glass in order to make it a more feasible process. Although, several researchers has used PCD for girnding of brittle materials, litlerally noone has come up with the idea of combining the on-machine fabrication of PCD tool using block EDM and then microgrinding of brittle material. which also facilates the offline dressing of tool as well. Therefore, micro-grinding of glass material using on machine fabricated PCD tool can provide a new passage for ductile mode machining of brittle materials. The results of this thesis should present the structured knowledge of micro-grinding of glass using super-abrasive particle in a PCD tool form. The investigation of micro-grinding of glass would help the research community to further understand the optimization of machining process, tool wear conditioning, and sub-surface damage condition involved with this newly developed method. Finally, all of this information would be useful for researchers to further explore this newly developed micro-grinding process using on-machine fabricated PCD tool in single setup. The main implication of this research is that these block-EDM based multi-processes should have significant contribution in the machining of glass materials and the processes should be applicable to small parts as well as die and mold making, where glass is primarily used nowadays.

1.5. Research Objectives

The aim of this research is to develop a multi-machining process for shaping PCD tool by EDM for effective micromachining of brittle glass. The principal approach is to incorporate a combination of block-EDM and grinding process in a single setup that will attain the aforementioned target. In this context, a number of objectives have been established to accomplish the primary aim as follows:

I. Experimental studies of micro-grinding of glass material.
   (a) To study the effect of different operating parameters for the EDM of Polycrystalline diamond (PCD) blank and to achieve the optimum

condition of different parameters for tool preparation.

(b) To invesitgate the effect of micro-grinding parameters on the performance of the PCD tool in glass micro-grinding.

(c) To machine micro features on glass with mirror finish and high accuracy.

II. The feasibility of making different shape tool for glass grinding and investigating their effect on grinding of glass.

III. Understanding the performance of PCD tool in vertical micro-grinding of optical glasses.

(a) Wear mechanism studies of PCD tool while micro-grinding of glass.

(b) On-machine monitoring of tool conditioning.

IV. Investigation of sub-surface damage analysis of BK7 glass during micro-grinding.

V. Modeling of the micro-grinding force

1.6. Organization of Thesis

The report comprises of nine chapters. Chapter one introduces the significance of the research as well as the objectives of the project. Chapter two discusses the principle of EDM, comparison and advantages of micro-EDM over other micro-machining processes for the machining of PCD. Then different tool fabrication methods are discussed. In addition, various works on fabrication of micro features on the hard materials like glass are also discussed in this chapter. Chapter two ends with indicating the limitations of the previous research works and how the proposed research aims to address some of the limitations. The experimental set up and procedures are discussed in chapter three. In chapter four, identification of operating parameters for improved performance of block-EDM of PCD and comparative study on the performance of tool while grinding 3 different hardness glasses are investigated. Chapter five covers the newly approached tool fabrication process and tool geometry effect on micro-grinding of glass. Details experimental investigation of PCD wheel wear process has been highlighted in chapter 6.

Chapter 7 includes the sub-surface damage analysis of glass. Chapter eight includes the cutting force modeling of micro-grinding process.The last chapter discusses the conclusion and contributions of the thesis, and also explores the possible future works. The list of references and publications has then been enumerated.

Chapter 2

Literature Review

2.1. Introduction

This chapter presents a review of literature in relevant areas to the proposed works. These works provide an overview of past and current research relating to micro-scale machining of brittle and hard materials which covers micro-scale machining using solid tools and fabrication of micro-scale precision tools.

2.2. Glass Machining

Machining of precise microstructures in a controlled fashion made out of glass, in particular in glass for micro-fluidics (Becker et al., 2002; Daridon et al., 2001) is challenging. The difficulty of making structures in glass is reflected in the wide variety of non-conventional techniques for glass micromachining along with some conventional micro-fabrication technologies.

2.2.1. Application of Glass Microstructures

Besides silicon, glass is a widely used substrate material in micro-system technology, in particular in the manufacturing of micro fluidic devices for biological analysis and biotechnical applications (Freitag et al., 2001; Petersen et al., 2004) as it provides beneficial structural and functional material properties. With comparison to silicon, the use of glass in micro-total- analysis-systems (μTAS) applications is advantageous with regard to its optical transparency which allows for visual inspection and on-line optical detection (good fluorescence properties) as well as its good dielectric properties used in a number of applications which allow it to withstand the high voltages used in electro kinetically driven flows and separations (e.g. capillary electrophoresis). Some other beneficial properties of glass are its good chemical resistance, high thermal stability, chemical inertness and established schemes for surface modification and fictionalisation

(silane modification) (Daridon et al., 2001) which make glass the most widely used substrate for the fabrication of DNA arrays. The use of glass substrates may also improve the long-term chemical stability of the devices in comparison with silicon-based systems. Many applications also require the high mechanical strength and the good mechanical stability of glass.

2.2.2. Fabrication of Glass Microstructures

Glass micro-fabrication technologies include photolithography and chemical etching. Glass is an isotropic material that is wet-etched with buffered HF in a non-directional manner. Therefore, structures with curved sidewalls and relatively low aspect ratio are produced by isotropic wet etching (Bu et al., 2004; Corman T, 1998; Gretillat et al., 1997; Li et al., 2001; Mourzina et al., 2005; Nikumb et al., 2005; Stjernstrom and Roeraade, 1998). Dry chemical etching of glass is also possible in typically a SF6 plasma(Belloy et al., 2000) but the structure depth is limited by a slow etch rate. There are many problems in etching materials which contain atoms of lead or sodium (glass, PZT, etc.) as they yield non-volatile halogen compounds (PbF2, NaF, etc.) as the reaction product. High speed directional etching of silicon by deep reactive ion etching (DRIE) with inductively coupled plasma source, which produces high-density plasma at low pressure, can be used for silicon channels but is still not sufficiently developed for producing similar structures in glass or quartz (DRIE).

Laser micromachining of glass is hindered by the brittleness and poor thermal properties of most glasses, resulting in a risk of micro-cracking and producing other collateral damage such as debris and a poor surface quality (Schlautmann et al., 2001). The two main ways to overcome this limitation are to use short wavelengths (UV) that can be focused down to smaller spot size or use lasers with ultra-short pulse duration that reduce thermal effects. Mechanical machining with techniques specialized in brittle materials such as powder blasting (also known as abrasive jet machining) is based on the mechanical removal from a substrate by a jet of particles (Moronuki N, 2002; Plaza et al.,

2003; Slikkerveer et al., 2000; Yan et al., 2002). Powder blasting allows making complex and controlled shapes of the eroded structure. Moreover, the erosion rate is much higher than with standard wet-etching processes. Another technique which is used here is micro-ultra-sonic machining (MUSM) which exploits the ultrasonic frequency vibration of a tool to force abrasive grains to erode a substrate (Dietrich et al., 1996; Etoh et al., 2003). Brittle materials are difficult to mechanically micro-machine by cutting processes like milling due to damage resulting from material removal by brittle fracture which leads to rough surfaces requiring subsequent polishing steps. Material removal by ductile regime instead of brittle fractures is made possible by using polycrystalline diamond tools. Mechanical sawing, though limited to simple straight patterns has also proved successful (Moronuki N, 2002).

There exists a variety of silica-based oxide glass materials such as soda-lime glass, borosilicate glass, pure silica glass (quartz glass). Some special variety of glass is amenable to anisotropic photo structuring. So it does not require an intermediate photo resist layer for patterning. It is commercially available through various suppliers and is patterned by photolithography using a mask (Brokmann et al., 2002; Gimkiewicz and Gerhard, 1997; Masuda et al., 2003; Mori R, Oct 2003) or by direct laser writing (Cao et al., 2009; Iliescu et al., 2005; Morgan et al., 2004). Typical approaches like wet chemical etching and mechanical structuring are not suited to achieve fine (<10 lm) and high aspect ratio (>10) structures. In Addition, micro-electrochemical discharge machining (ECDM) was studied in order to improve the machining of 3D micro-structures of glass. To minimize structures and obtain good surface microstructures, the effects of the electrolyte, the pulse on/off-time ratio, the voltage, the feed rate, the rotational speed, and the electrolyte concentration in the drilling and milling processes were studied(Lin et al., 2001).

2.3. Fundamentals of grinding and cutting principle

Grinding is a complex abrasive cutting process, related to machining with geometrically unspecified cutting edges. Grinding interface involves a material removal by the contact between grinding wheel with a randomly structured topography with work pieces. Each grain removes a chip from the surfaces of the work pieces material and generates a surface finish.

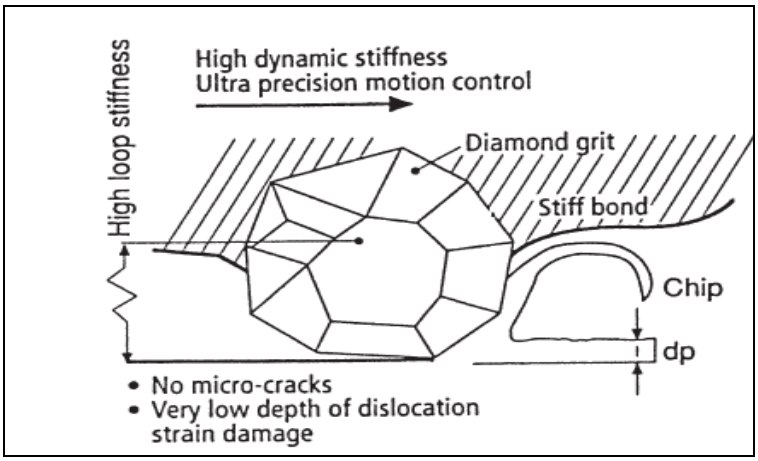

Fig. 2. 1: The mechanism of ductile or shear mode grinding of brittle materials.

Grinding refers to material removal by individual grains whose cutting edge is bounded by force and path. Fig. 2.1 shows initial cutting interface which is characterized by elastic deformation, followed by plastic flow of work piece material. The interface friction condition and cutting speed have a significant influence on chip formation. A consistent cutting mechanism description therefore comprises complex penetration relationships between two hard materials, elasto-plastics mechanics and aspect of tribiology, all of which influences the kinematics and contact condition (Kopac and Krajnik, 2006).

2.3.1. Ductile regime machining

Improvements in machining tolerances have enabled researchers to expose the ductile material removal of brittle materials. Under certain controlled conditions, it is possible to machine brittle materials like ceramics using single- or multi-point diamond tools so that material is removed by plastic flow, leaving a crack-free surface (Fig. 2.1). This process

is called ductile regime machining. Ductile regime machining follows from the fact that all materials will deform plastically if the scale of deformation is very small. Another way of viewing the ductile regime machining problem is that described by Miyashita (Miyashita, November 1985), as shown in Fig. 2.2. The material removal rates for grinding and polishing are compared and there is a gap in which neither technique has been utilised. This region can be termed the micro-grinding gap since the region lies in between grinding and polishing. This gap is important because it represents the threshold between ductile and brittle grinding regimes for a wide range of materials like ceramics, glasses and semiconductors.

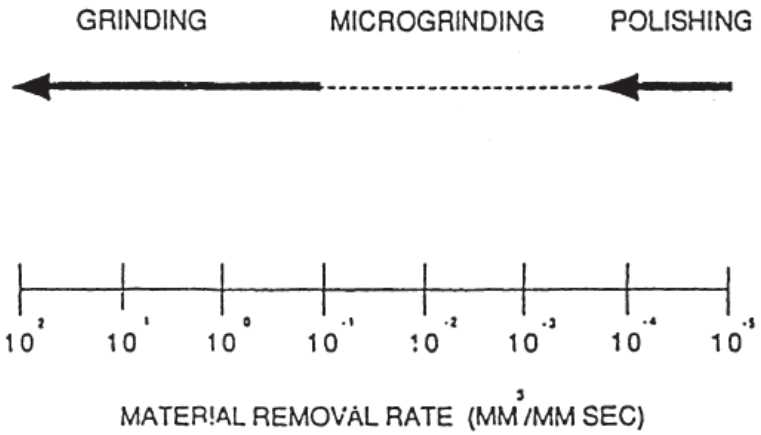

Fig.2. 2: Achievable material removal rates in abrasive machining.

Principle of ductile regime machining

The term energy balance is used to describe transition from brittle to ductile transition during machining of brittle between strain energy and surface energy(T. G. Bifano, 1992). For brittle machining, localized fractures produced during the application of load are of great interest. The indentation cracks generated during indentation machining play an important role in ductile mode machining (S. Blackeley, 1990).

A critical penetration depth *d*c for fracture initiation is described as follows (V.C. Venkatesh, 1995).

$$d_c = b(K_c/H)^2(E/H) \quad \text{.....(1)}$$

Where *K*c is the fracture toughness, *H* is the hardness, *E* is the elastic modulus and *b* is a constant which depends on tool geometry. Fig. 2.3 shows a projection of the tool perpendicular to the cutting direction. According to the energy balance concept, fracture damage will initiate at the effective cutting depth and will propagate to an average depth *y*c. If the damage does not continue below the cut surface plane, ductile regime conditions are achieved. The cross-feed *f* determines the position of *d*c along the tool nose. Larger values of *f* move *d*c closer to the tool centreline.

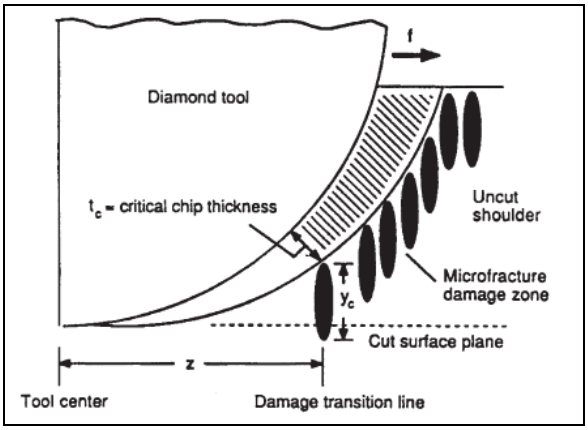

Fig.2. 3: Projection of the tool perpendicular to the cutting direction

Another interpretation of ductile transition phenomena is based on cleavage fracture due to the presence of defects (T. Nakasuji, 1990). The critical values of a cleavage and plastic deformation are affected by the density of defects/dislocations in the work material. Since the density of defects is not so large in brittle materials, the critical value of fracture depends on the size of the stress field. Fig. 2.4 shows a model of chip removal with size effects. When the uncut chip thickness is small, the size of the critical stress field is small to avoid cleavage. Consequently a transition in the chip removal process from brittle to ductile may take place depending on the uncut chip thickness.

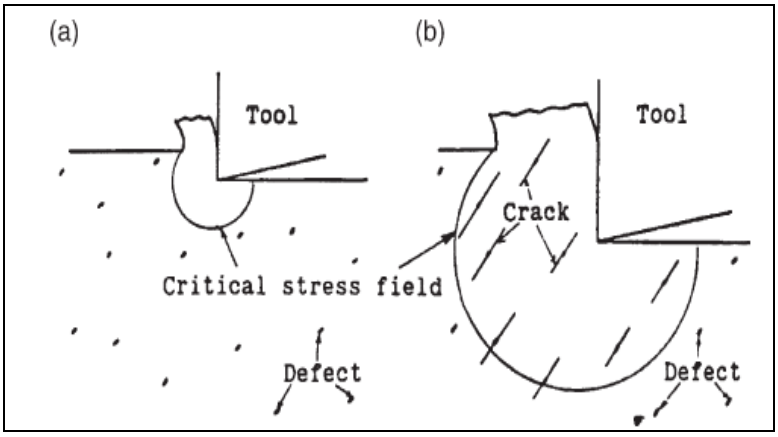

Fig.2.4: Model of chip removal with size effects. (a) Small depth of cut; (b) large depth of cut.

Material removal mechanisms in ductile regime machining

Machining generates a useful surface by intimate contact of two mating surfaces, namely the work piece and abrasive tool. However, the micromechanics of material removal differ from material to material depending upon the microstructure of both work piece and tool material. Generally, during high-precision machining of brittle materials, tools having large negative rake angles are used (as high as -30°). The negative rake angle provides the required hydrostatic pressure for enabling plastic deformation of the work material beneath the tool radius. During conventional machining with a single-point tool, the rake angle will be positive or close to 0°. With positive rake angle, the cutting force will generally be twice the thrust force. Hence the deformation ahead of the tool will be in a concentrated shear plane or in a narrow plane as shown in Fig. 2.5. During the grinding process, it is generally agreed that the tool will have a large negative rake angle and also that the cutting force is about half of the thrust force [Fig. 2.5(b)]. In ultra-precision machining of brittle materials at depths of cut smaller than the tool edge radius, the tool presents a large negative rake angle and the radius of the tool edge acts as an indenter as shown in Fig. 2.5(c). This represents indentation sliding of a blunt indenter across the work piece surface. This is similar to a situation where the tool is rigidly supported and cuts the work piece under a stress such that no median vents are generated

but the material below the tool is plastically deformed due to large hydrostatic pressure as in Fig. 2.5(d)(P.S.Sreejith, 2001).

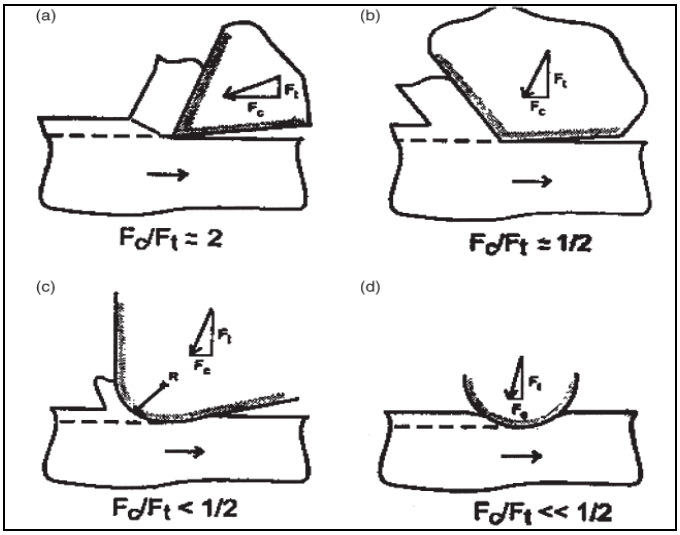

Fig.2. 5: The progression of tool and work piece interactions: (a) conventional cutting, (b) grinding, (c) ultra-precision machining at small depth of cut and (d) indentation sliding.

2.3.2. Material removal in glass and ceramics

The ductile grinding of optical glass is considered as the most perfect adaptation of a machining method to the material (W. Konig, 1990). Glass is an inorganic material super cooled from the molten state to the solid state without crystallising. Glasses are non-crystalline (or amorphous) and respond intermediate between a liquid and a solid; i.e., at room temperature they behave in a brittle manner but above the glass transition temperature they behave in a viscous manner. The high brittleness of glass is due to the irregular arrangement of atoms. In crystalline materials like metals, the atoms have a fixed arrangement and regularity described by Miller indices, whereas glass structure does not show any definite orientation (Fielder, 1988).

The unique physical and mechanical properties of ceramics such as hardness and strength, chemical inertness and high wear resistance have contributed to their increased application in mechanical and electrical components. The advanced ceramics for

structural and wear applications include alumina (Al2O3), silicon nitride (Si3N4), silicon carbide (SiC), zirconia (ZrO2) and SiAlON. The nature of atomic bonding determines the hardness of the material as well as the Young's modulus. For ductile metallic-bonded materials the ratio E/H is about 250, while for covalent bonded brittle materials the ratio is about 20. The ratio will lie in between these values for ionic bonded materials. Low density and low mobility of dislocations are the reasons for the high hardness of some of brittle materials.

Depending on the atomic bond, different material removal mechanisms arise (T. G. Bifano, 1992). The metals, those are characterised by metallic bonds where the valence electrons are shared freely between the atoms of a structure, are machined typically in the ductile regime. The machining of glasses and ceramics, if performed in the brittle regime, causes vertical cracks during application of the cutting load and lateral cracks during removal of the load. The formation of lateral cracks causes chipping, which is the main mode of material removal. But the formation of vertical cracks causes a substantial amount of subsurface damage. However, if a very small depth of cut is chosen, even brittle materials like glass and ceramics can be machined in the ductile regime. Glasses and ceramics can be machined in a ductile manner if the depth of cut is kept below 10 nm (S. Blackeley, 1990). The mechanics of material removal in ceramics and glasses consists of brittle fracture and plastic deformation. The former is similar to indentation on a brittle material by a hard indenter causing lateral and median cracks. The latter is analogous to the chip formation process in metal grinding, which involves scratching, ploughing and formation of chips. The loading at the cutting point and the properties of the work piece are the factors that control the extent of brittle fracture. According to the ductile machining hypothesis, all materials (including brittle) will undergo a transition from brittle to ductile machining region below a critical depth of cut. The energy required to propagate cracks is believed to be greater than the energy required for plastic deformation below the critical depth of cut region. Hence plastic deformation is the predominant mechanism of material removal at this region (T. Nakasuji, 1990). Ductility generation is

very essential for material-adapted machining of high performance ceramics/glasses. During ductile regime grinding, it is assumed that when grains impact the material, heat concentration occurs at the immediate contact area of the edge due to low heat conduction within the material. This, along with high compressive stress, is sufficient to cause local ductility for plastic deformation (W. Konig, 1990). In Ductile regime machining not all material removal takes place in a ductile fashion as the name seemingly suggests. Material removal takes place due to combine effect of plasticity and extensive micro-fracture. Ductile regime machining is interplay between tool profile geometry and feed rate and also the critical depth parameter that determines fracture initiation. Pure ductile response will occur only along the apex of the tool tip where the effective depth of cut is less than the critical depth of cut (Y.J. Yuan, 1993). In finishing of brittle materials like Ge and Si by turning, grinding, polishing, etc., the response of material is very important and affects the quality of the surface. The material response in turn depends on the magnitude and size of the stress field and also on the response of the work material and cutting combination during the process. While studying on brittle– ductile transition, Yoshikawa(Yoshikawa, 1967) classified the stress field into four domains as shown in Fig. 2. 6:

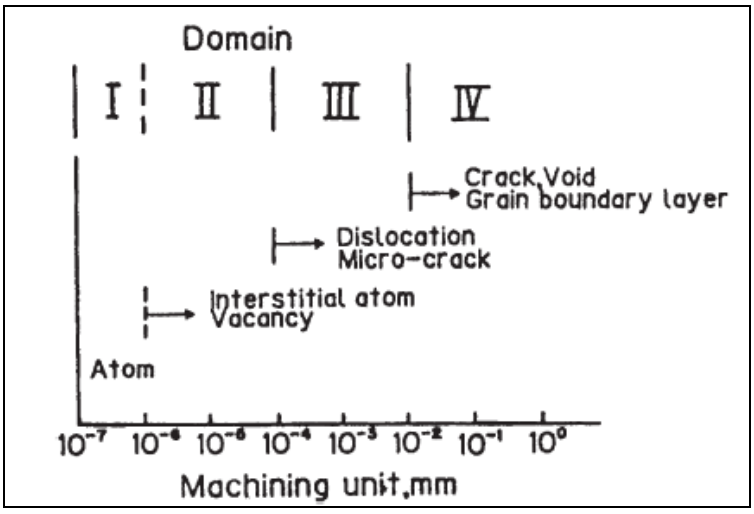

Fig.2. 6: Factors affecting deformation and fracture of materials [49].

1. Domain I — material removal takes place not only by mechanical action but also by chemical/temperature effects. Only a very small quantity of material is removed.
2. Domain II — here no dislocation is present and the material is assumed as an ideal crystal. Dislocations are created prior to brittle fracture. After the creation of dislocations, the crystal is assumed to behave as in Domain III.
3. Domain III — plastic deformation occurs at this domain followed by crack initiation at the deformation zone.
4. Domain IV — material removal takes place only due to cracks.

Thus, it can be concluded that at extremely small depth of cut material removal takes place by erosion/chemical action, followed by plastic deformation/micro-fracture depending on the conditions.

2.3.3. Subsurface mechanical damage

High dimensional accuracy and good surface integrity are frequently required in some of structural ceramic components. Although advances have been made in the near-net shape technology, grinding with diamond wheels is still the method of choice for the machining of these structural ceramics. Unfortunately, the ground ceramic components are most likely to contain a deformed layer, surface/subsurface micro-cracks, phase transformation, residual stresses and other types of damage. The major form of machining damage usually occurs as surface and subsurface damage (Agarwal and Rao, 2008). Sub-surface mechanical damage (SSD) consists of surface micro-cracks created during grinding and/or polishing of brittle materials surfaces, such as glass. These surface cracks, typically identified macroscopically as scratches and digs, are often hidden below an index-matched Bielby layer or have closed (i.e., healed); hence they are not always detectable by visual inspection or standard optical microscopy until exposed by chemical etching (Beilby, 1921). In some applications, the removal or minimization of SSD is required for improving the material strength (e.g., spacecraft, underwater windows/barriers, and other military applications) where the surface flaws determine the ultimate strength or for reducing/eliminating laser-induced damage (e.g., high-peak-

power laser applications. The creation of SSD can be thought of as the repeated indentation of mechanically loaded hard indenters (abrasives) sliding on the surface of an optic during various cutting, grinding and polishing processes. The initiation and growth of the three basic types of cracks (lateral, radial, Hertzian) resulting from a single, static indenter as a function of load, material properties of the indenter and substrate are known.

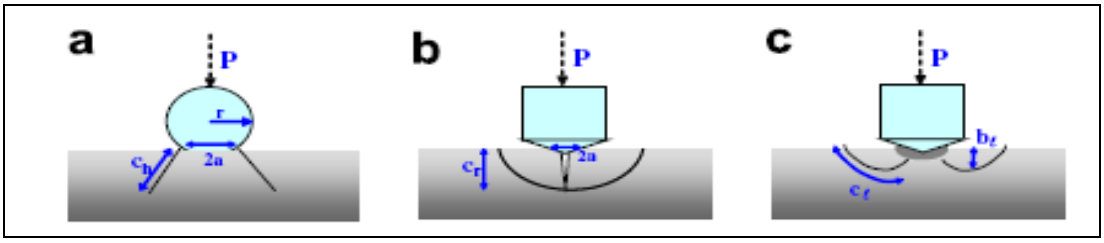

Fig.2. 7: Schematic illustration of the fracture geometry of the idealized fractures created by static indentation: (a) Hertzian cone crack from a blunt indenter; (b) radial or median cracks from a sharp indenter; (c) lateral crack from a sharp indenter.

Hertzian cracks are cone shaped cracks that are created from a spherical indenter; radial cracks are semi-circular crack in shape and perpendicular to the glass surface from a sharp indenter; and lateral cracks are cracks that run generally parallel to the glass surface which are also typically created by a sharp indenter. By their geometry, it is clear that formation of lateral cracks will largely lead to material removal and will contribute significantly to the observed surface roughness. Hertzian and radial cracks, on the other hand, will largely contribute to deeper SSD and potentially to some material removal through the intersection with other cracks(I.Hutchings, 1992.; Lawn, 1993) .

Malkin and Hwang have studied and analyzed the mechanism of material removal in ceramic grinding using indentation fracture mechanics approach and the machining approach. With the aid of first approach they showed that median/radial cracks are usually associated with strength degradation, and lateral cracks with material removal

(Malkin and Hwang, 1996). Xu et al. have focused on exploring the mechanism of material removal and the effects of machining-induced damage on strength of advanced ceramics and demonstrated that it can be controlled by approximately tailoring the microstructure. These findings have suppressed the formation of strength degrading cracks and also have accelerated easy, well-controlled material removal by grain dislodgement during machining (Xu et al., 1995). Zarudi and Zhang (Zarudi and Zhang, 2000) carried out experimental and theoretical investigation on subsurface damage in alumina by ductile-mode grinding. They reported that the distribution of the fractured area on a ground mirror surface, having RMS roughness in the range from 30 to 90 nm, was dependent on both grinding conditions and the pores in the bulk material. Interaction of abrasive grains of the grinding wheel with pores resulted in surface pit formation. Therefore, initial microstructure of a material is the limiting factor for achievable surface quality by ductile-mode grinding. The investigation showed that median and radial cracks did not appear and hence were not the cause of fracture as were usually thought. Factors influencing surface quality of brittle materials, during ultra-precision grinding were investigated and analyzed theoretically in details by Chen et al. (M.J. Chen, 2004). Grinding experiments were also carried out to compare the outcome of theoretical analysis for the brittle materials. The results suggested that primary influencing factor on surface quality was average abrasive grain size of the diamond wheel and the influence of the wheel speed and feed rate were secondary. Zhao et al. (Zhao et al., 2007) investigated surface and subsurface integrity of diamond ground optical glasses. They used a machine tool featuring high close-loop stiffness to conduct the ultra-precision machining of fused silica and fused quartz assisted with electrolytic in-process dressing (ELID). An acoustic emission sensor and a piezoelectric dynamometer were used to monitor the grinding process to correlate the processing characteristics with the generated surface and subsurface integrities, which were characterized by atomic force microscope, scanning electronic microscope, and nano-indentation technique. From experimental results they showed that for optical glasses the fracture toughness value could be used to predict the machinability and its larger value always indicates better surface and subsurface integrity.

For case study grinding process in optical glass, the smaller amplitude and RMS values of acoustic emission signal, smaller grinding forces and the ratio of normal force to tangential force, resembles to a better surface and subsurface integrity. Nanometric quality surfaces with minimal subsurface damage depth can be generated for fused quartz with the aid of selected machining parameters and a very fine grain-sized diamond grinding wheel. Detailed knowledge on the effect of the grinding process on surface integrity gives the opportunity for a better exploitation of ceramic materials by improved process conditions.

The X-ray diffraction techniques were studied by Pfeiffer and Hollstein (W. Pfeiffer, 1993) to determine the damage induced in ground silicon nitride and alumina. From their studies they set up correlations between micro-plastic deformation and amount of damage. From their investigations they showed that bending strength is dominated by machining- induced damage in the case of lapped and ground alumina and of ground silicon nitride. The effect of damage can be compensated by machining-induced compressive residual stresses in the case of lapped silicon nitride. One important laggings of the X-ray diffraction technique is that it cannot differentiate subsurface damage from the bulk structures, and also the effects of the damage on the residual strength and surface tribological properties of a ground component. The scope is still left for further improvement to provide more precise and reliable prediction.

Daniels(Daniels, 1989) has investigated the influence of surface grinding parameters such as diamond abrasive type, wheel speed and down feed on the rupture strength of silicon carbide. He showed that more severe grinding conditions, like power consumptions and higher normal force, has less effect on reducing the mean rupture strength of the material. The most prominent outcomes inferred from these results were that grinding conditions could be changed to optimize the process without significant structural damage to the work material. Some other techniques like flexural strength testing, fractography, and non-destructive inspection were considered to be useful for

assessing subsurface damage. Ahn et al. (Ahn et al., 1996) applied the ultrasonic technique and the thermal wave measurement technique to detect the subsurface lateral cracks (at larger scale) associated with indentations in glass and silicon nitride. Service life of a ceramic component, in a wear and corrosive environment, could be usually affected by these types cracks produced during the grinding process. Therefore, Ahn et al suggested applying these techniques for small cracks developed during the grinding process. Shen et al.(Y. Shen, 2003) studied the force and energy characteristics in grinding of advanced ceramics. Two typical ceramics were ground with a resin bonded diamond wheel on a precision surface grinder under different grinding conditions. The normal and tangential force components operating on the grinding wheel, the force ratio, the specific grinding energy in grinding of ceramics were analyzed based on measured power used by the spindle. Ceramic materials were mainly removed in the fracture mode, while most of the energy was expended by ductile. Friction between the diamond wheel and ceramics were taken into account in material removal mechanisms for ceramic grinding. But applications of advanced ceramics in industrial scale have been restricted mainly due to machining difficulties and associated high cost with the use. Therefore great efforts were made towards the development of efficient mode grinding technology (Annamalai et al., 1993; F. Klocke, 1999; H.K. Tonshoff, 1999).

High-speed grinding has been studied in order to achieve high material removal rate in the ceramics grinding. In high-speed grinding process, reduction of maximum chip thickness can be achieved with an increase in wheel speed, and thus reducing the grinding force(F. Klocke, 1997) . This would cause the ductile flow by reducing the tendency for brittle fracture (J.A. Kovach, 1993). On the other hand, the increased speed will cause the increase in the depth of cut or the feed rate to obtain the higher material rate, without deteriorating the ground surface integrity.

Feasibility study on the applications of high speed in the low-damage grinding of the advanced ceramics was studied by Kovach et al. Hwang et al. (L. Yin, 2005; T.W.

Hwang, 1999) investigated the machining characteristics of silicon nitride under high speed grinding conditions. Main focus of this investigation was on the wheel wear mechanism, at low material removal rate. Klocke et al.(F. Klocke, 1999) studied various process strategies for the high-speed grinding of aluminum oxide and silicon infiltrated silicon carbide at high removal rates. The results demonstrated that fracture strength of the machined ceramic components are not decreased at high-speed grinding having high removal rates. Yin et al. (L. Yin, 2005) investigated grinding of alumina and alumina–titania at high removal rate (up to 16.6mm^3/s per mm) with respect to material removal and basic grinding parameters using a resin-bond 160mm grit diamond wheel at the speeds of 40 and 160 m/s, respectively. The results show that the material removal for the single-phase polycrystalline alumina and the two-phase alumina–titania composite revealed identical mechanisms of micro-fracture and grain dislodgement under the grinding conditioned selected. Surface roughness and morphology for both materials ground at either conventional or high speed were found to be same. Material removal rate increment did not necessarily downgrade the surface roughness for the two materials at both speeds. At any grinding speeds and specific removal rates, the grinding forces for the two ceramics demonstrated similar characteristics. Regardless of removal rates, both normal and tangential grinding forces and their force ratios at the high speed were found lower than those at the conventional speed. It was also shown that high-speed grinding exerted a great amount of coolant induced normal forces in grinding zone, which were four to six times higher than the pure normal grinding forces irrespective of all the removal rates. However, in these works (H. Huang, 18–20 July, 2001; H. Huang, 26–30 May, 2002; L. Yin, 2005; T.W. Hwang, 1999), no detailed investigations of the effects of high-speed grinding conditions on the material removal mechanisms and the surface integrity of advance ceramics have been reported.

Machining characteristics and surface integrity of advanced ceramics, viz. alumina, alumina–titania, and yttria partially stabilized tetragonal zirconia by Huang and Liu (H. Huang, 2003) under high speed deep grinding conditions. They focused to explore the

material removal mechanisms involved in the grinding processes. They reported that grain dislodgement or lateral cracking along grain boundaries are the dominating factors for material removal in grinding of alumina and alumina–titania. In case of Zirconia material removal was via both local micro-fracture and ductile cutting.

Zhang et al. (B. Zhang, 2003) conducted the study on diamond grinding of advanced ceramics, including hot-pressed silicon nitride, hot-pressed alumina, slip-cast zirconia, and pressure-less sintered silicon carbide. Three destructive inspection techniques and progressive lapping technique combined with scanning electron microscopy (SEM), and transmission electron microscopy (TEM) were applied to assess and characterize grinding-induced damage in these ceramics. As a result, pulverization and micro-cracking grinding damages were identified. Damage depth was found to be related to the properties of ceramic materials, especially their brittleness. Damage penetration characteristics were outlined from their experiments. They showed that for a given grinding condition, damage penetrated deeper in less brittle materials than in more brittle materials. In addition, two types of grinding induced micro-cracks were identified, scattered and clustered. All four types of materials tested under various grinding conditions exhibited scattered micro-crack, while clustered type was only associated with less brittle materials subjected to relatively aggressive grinding conditions. The grinding characteristics and mechanism of material removal during surface grinding of silicon carbide by diamond-grinding wheel were investigated by S. Agarwal et al. The surface and subsurface characteristics of the ground silicon carbide showed that the material removal associated with this material was primarily due to the dislodgement of individual grains, resulting from micro-cracks along the grain boundaries. This advantageous phenomenon can subsequently reduce the grinding force and specific grinding energy. This led to an important outcome in ceramic manufacturing so that the silicon carbide could be efficiently ground without causing a significant loss to the surface integrity.

2.3.4. Tool wear

One major problem of glass micro grinding is the tool wear caused by the hardness of material. The tool wear process can be divided into three main wear mode, namely Attritions wear, grain fracture, and bond fracture. Attritions wear which involves dulling of abrasive grains and the growth of wear flats by rubbing against the work pieces was found to be directly related to the grinding forces. Grain fracture refers to the removal of abrasive fragments by fracture within the grain and bond fracture occurs by dislodging the abrasive from the binder (Malkin and Guo, 2008).

Grinding wheel wear is usually expressed by the G-ratio, which is defined as the volume ratio of material removal to the wheel wear. G-ratios cover an extremely wide range of values (from below unity to up to 60,000). Most experimental studies of grinding wheel wear involve the measuring event of the G-ratio and the specific grinding energy for particular set of grinding conditions. While this approach has had partial success in the optimization of grinding conditions, very little has been learnt about the fundamental aspects of grinding wheel wear. Furthermore, small changes in grinding conditions often lead to the larger unexplained differences in the G-ratio (Malkin and Cook, 1971).

Recent researches on micro-grinding have mainly focused on assessing its tool life and wear mechanism, since the performance of the micro grinding wheel is more sensitive to the tool wear than those of conventional size. The tool wear of electroplated micro-grinding wheels in side grinding of porcelain and zirconia was investigated by Ohomori et al.(Yin et al., 2004). The wear mechanism of the metal bonded micro grinding wheel in end grinding of zirconia was studied by Feng et al. (Feng, 2007). Onikura et al. investigated its performance in end grinding of silicon suggesting that electroplated micro-grinding wheel wears too fast for the practical applications (Onikura, 2003). Luo et al. analyzed the wear of resin bond diamond wheel while grinding of tungsten carbide and found that interrupted cutting causes higher grinding ratio while continuous cutting

causes poor grinding performance (Luo et al., 1997). Bai et al. (Bai et al., 2004) and Philbin et al. (Philbin and Gordon, 2005) has studied the wear mechanism of PCD cutter for laminated floor and wood based composites.

However in practice, ductile regime machining of glass material is often limited by rapid wear of the diamond tool. Although a diamond tool can be used to cut nonferrous metals such as aluminum and copper for a distance up to a few hundreds of kilometers, (Hamada, 1985) when cutting glass an initially sharp tool will wear and become worn out rapidly. As the geometry of the contact zone between tool and the work pieces is extremely important for the attainment of perfect geometric shape, the wear of the diamond tool become a limiting factor in developing machining process for glass. Tool wear not only raises machining cost but also degrades product quality. The problem becomes particularly serious when machining large volume of components (C.K.Syn, April 1998). For this reason better understanding of the performance of the diamond tools in glass machining will result in significant production cost savings. Various researchers in the past have made their valuable contributions to the understanding of the process that take place when a diamond tool wears. However most of the work carried out has involved the wear of diamond tool in cutting metal materials. Up to date, there is very little literature available on the tool wear during glass micro-machining.

Tool condition monitoring (TCM) plays an important role in improving reliability and promoting automation of the manufacturing process. One of the important tools of TCM is the tool failure detection which includes cracking chipping and fracture of the tool during machining. Several systems are commonly used based on the forces, acoustic emission, current and temperature. During ultra-precision machining on optical glass, material removed from the work piece at a very low material removal rate, the uncut chip thickness usually being at nanometer level to achieve minimal surface roughness. Power consumption, vibrations, force signal show very low sensitivity and low signal to noise ratio due to the involvement of low level force signal. Though, the systems based on the

cutting forces are considered to be the most promising, however in spite of the availability of the some of the commercial systems these are still considered not reliable enough, they require double checking by other different system. Moreover the dynamometer is costly and its installation is rather inconvenient and might weaken the machine structure. Therefore some other approaches have been used for tool condition monitoring, among them is the Acoustic emission signal which has been applied and to some extent has been successful. It is even better suited for monitoring very fast events than force measurement (Bifano and Yi, 1992; Dornfeld and He Gao, 1984; Hundt et al., 1994). The AE signal has been classified into continues and burst type. The raw AE signal usually contain high frequency component which cannot be handle easily when using conventional signal processing equipment. An appropriate method for analyzing the AE signal based on the root mean square signal is often used and suitable for using with traditional signal processing system with much lower sampling frequency (Jemielniak and Otman, 1998). AE waves can be detected using AE sensor, which is mounted near the surface. The source of AE signal are the combination of elastic impact, friction, indentation crack, bond fracture, chip fracture, grain fracture, and grain removal at wheel work piece interface. Previous research indicated that, worn grit wheel loading heavy friction; hard bonded material can result in high AE energy. From the aspect of wheel loading, ploughing, and sliding contribute to the main source of emission energy (Mokbel and Maksoud, 2000; Ravindra et al., 1997). Choi et al fused AE and cutting force in their attempt to develop a real time CMS for turning operations(Choi et al., 1999). Similar work conducted by Jemielniak and Otman used statistical signal processing algorithm to identify the root mean square skew and kurtosis of the AE signal in order to detect catastrophic tool failure (Jemielniak and Otman, 1998). Kakade et al used AE signal to predict tool wear and chip form in milling operation by selecting AE parameters (Kakade et al., 1994). Analysis of signal concluded that AE signal could able to distinguish clearly cutting actions of a sharp and worn or broken tool. As for continuous monitoring, no suggestions were made, presumably because the method was deemed unsuitable.

2.4. Micro-EDM

There are several methods for micro electrode fabrication processes for micro-EDM machine. This section explores those techniques to explore the feasibility of using those methods in the field of micro-EDM for fabricating micro features.

Ravi et al reported on the development of an electro-discharge machining (EDM) block electrode method for the fabrication of microelectrodes with symmetrical sections, e.g. tapered, and circularly stepped, rectangular and triangular. In the EDM process, a newly developed machining strategy is applied for the fabrication of micro features. The machining is carried out with multi-pass machining to reduce the volume of material removed, and thus to reduce the possibility of electrode breakage. This strategy is found to be feasible for producing microelectrodes of various symmetrical sections down to a few tens of micrometers (Nachiappan Ravi, 2002) . From experiment, it is revealed that sparking energy and electrode rotational speed have considerably small influence a little on electrode diameter and feeding length was found to be inversely proportional to diameter at reverse polarity (Nachiappan. Ravi, 2002).

Egashira et al fabricated 20 micron diameter micro-tools of cemented carbide with a D-shaped cross-section and cutting edge radius of 0.5μm by wire electro discharge grinding (WEDG). However, the fabricated tool has the drawback of having curve cutting edge compare to commercial available cutting tool (Egashira and Mizutani, 2002) . Moreover, H S Lim et al fabricated on machine micro electrode tools with high aspect ratio by using stationary block electrode, rotating block electrode and wire electrode. The simplest method to machine a tool electrode is a stationary block. Wire of 0.07 mm in diameter can be used as a sacrificial electrode. When there is a dimensional change in the sacrificial electrode, the diameter of the tool electrode fabricated is usually unpredictable (Lim et al., 2003) .

F. T. Weng et al developed a multi-EDM grinding process to fabricate micro-electrodes. Rod electrodes of copper with diameter 3.00mm were cut to be 0.15mm on wire-EDM machine at first step. EDM grinding process was used to grind micro-electrodes to fine diameter bellow 20micron at second step. Micro-electrode can be fabricated through proposed multi-EDM process. Nevertheless a single process may not achieve desired micro size (Weng et al., 2003). Guohui et al presented a new fabrication method for tungsten microelectrode by means of pressure difference of plasma between cathode and anode in a single electrical discharge. Proposed method greatly shortens the microelectrode fabrication time and effectively improves the reliability of the microelectrode. Tungsten microelectrode of 350 micron in length and 30micron diameter was fabricated in this method on the top of tungsten wire of 0.125mm in diameter which can be used as a drilling tool in micro EDM of a probe for scanner and measurement device (Cao et al., 2005). Another novel technique for fabricating efficiently precision cutting tools made from polycrystalline super hard materials is reported by A.G. Mamalis et al. For this purpose, a two-stage electro-discharge machining (EDM) was applied on diamond polycrystalline, by employing first wire-electrode EDM for rough cutting and subsequently rotational disc-electrode EDM for finishing operations. Experimental results obtained clearly indicate the applicability of the proposed two-stage technique for fabricating precision cutting tools that can be used for the production of machined components made from glass and plastics, ceramics, composite materials and non-ferrous metals, at an industrial scale (Mamalis et al., 2004).

Another interesting fabrication process to build a unique micro-spherical diamond tool by using EDM combined with co-deposition of Ni-diamond composites was proposed by Jung-Chou Hung et al. Here, tungsten carbide rod machined to required shape by WEDG and then using EDM forming a sphere was formed on the electrode tip due to surface tension. ECM was also done to remove crater formed due to EDM. Finally, NI-diamond deposition took place on the tool tip. This tool can be used to machining molds (Jung-Chou and et al., 2008). Shun-Tong Chen et al established another process quiet similar to

that one proposed by Hung et al, where micro-EDM with precision co-deposition was used to form a micro-electrode. Metal substrate was micro-EDMed to 50 micron diameter and diamond particle of 0-2 micron grains are electroformed on the surfaces of substrate. This miniature tool was used for ZrO_2 ceramics grinding (Shun-Tong and et al., 2008). Again, in order to machine micro aspheric molds and dies made of ceramics, micro milling tools made of polycrystalline diamond (PCD) are developed. H. Suzuki developed polycrystalline diamond (PCD) micro milling tool. At first the PCD wafer was bonded with a silver alloy on to a cemented carbide substrate and the bonded PCD plate was cut to small cylindrical chips by wire EDM. The PCD chip was bonded on to a cemented carbide shank with a silver alloy. Finally, the end face and side face of the PCD chip was ground and polished with a diamond wheel, and the cutting edges were ground and polished with a sharp diamond wheel. Some micro aspheric molding dies made of binder-less tungsten carbide were cut with the PCD milling tool developed (Suzuki et al., 2007). Morgan et al demonstrates that PCD tools shaped by μEDM are also effective for micro machining brittle glass materials. This is significant since glasses are commonly used in tooling for micro molds, micro fluidics, lab-on-chip devices and bio-MEMS devices. Micromachining does not require a mask, enabling short lead-times for prototype devices. These important applications justify effort to advance micro machining with PCD tools. Prior to using PCD tools for micromachining, Morgan et al prepared the tools (shaped) with a three-step process consisting of wire EDM, wire electro discharge grinding (WEDG) and μEDM with a polished flat surface. This process enables a wide variety of tool geometries that can be used for drilling and milling operations. Furthermore, the surface roughness of the tool is controllable with adjustments in the capacitance and voltage during μEDM, which suggests that the tools can be optimized for material removal rates and surface finish (Chris and et al., 2004).

2.4.1. Principles of EDM

Electrical discharge machining (EDM) is based on the material erosion of electrically conductive materials. It is given through the series of specially discrete high-frequency electrical discharges (sparks) between the tool and the work piece (Llanes et al., 2001). When sparks are generated the electrode materials will erode and in this way material removal is realized. Every discharge (or spark) melts a small amount of material from both of them. Part of this material is removed by the dielectric fluid and the remaining solidifies on the surface of the electrodes. The net result is that each discharge leaves a small crater on both work piece and tool electrode (Allen and Lecheheb, 1996).

In the EDM process, as the electrode charged with a high-voltage potential, come close to the work piece, an intense electromagnetic flux or 'energy column' is formed and eventually breakdown the insulating properties of the dielectric fluid (Guitrau, 1997). The voltage then drops as current is produced, and the spark vaporizes anything in contact with it, including the dielectric fluid. The area struck by the spark will be vaporized and melted, resulting in crater being formed. Thus metal is predominantly removed by the effect of intense heat locally generated and collapse of the vaporized dielectric. Melting and vaporization actions are the causes of removing material in the EDM process

2.4.2. Micro-EDM and Its Types

The basic mechanism of the micro-EDM process is essentially similar to that of the EDM process with the main difference being in the size of the tool used, the power supply of discharge energy and the resolution of the X-, Y- and Z-axes movement (Masuzawa, 2000). In micro-EDM the discharge energy is reduced to the order of 10^{-6} to 10^{-7} Joules in order to minimize the unit material removal. At low energies the net metal removal efficiency (measured volume/maximum volume that can be removed) has been found to be near 1.0 whereas at higher energy, the efficiency is found to fall off rapidly until 0.15.

Current micro-EDM technology used for manufacturing micro-features can be categorized into four different types (Pham et al., 2004):

- Die-sinking micro-EDM, where an electrode with micro-features is employed to produce its mirror image in the work piece.
- Micro-wire EDM, where a wire of diameter down to 0.02mm is used to cut through a conductive work piece.
- Micro-EDM drilling, where micro-electrodes (of diameters down to 5–10μm) are used to 'drill' micro-holes in the work piece.
- Micro-EDM milling, where micro-electrodes (of diameters down to 5–10μm) are employed to produce 3D cavities by adopting a movement strategy similar to that in conventional milling.

There is another variant of micro-EDM called micro-WEDG (wire electro-discharge grinding) in which grinding is done using EDM mechanism. An overview of the capabilities of micro-EDM is provided in the table 2.1(Masuzawa, 2000) :

Table 2. 1: Overview of the micro-EDM varieties

Micro-EDM variant	Geometric Complexity	Minimum feature size	Maximum aspect ratio	Surface quality R_a (μm)
Drilling	2D	5 μm	~ 25	0.05 – 0.3
Die-sinking	3D	~ 20 μm	~ 15	0.05 – 0.3
Milling	3D	~ 20 μm	~ 10	0.5 – 1
WEDM	2 ½ D	~ 30 μm	~ 100	0.1 – 0.2
WEDG	Axi-sym.	3 μm	30	0.8

2.4.3. Advantages of micro-EDM over other micromachining processes

Compared to traditional micromachining technologies micro-EDM has several advantages such as (Reynaerts et al., 1997):

- EDM requires a low installation cost compared to lithographic techniques.
- EDM is very flexible, thus making it ideal for prototypes or small batches of products with a high added value.
- EDM requires little job overhead (such as designing masks, etc.).
- EDM can easily machine complex (even 3D) shapes.
- Shapes that prove difficult for etching are relatively easy for EDM

2.5. Concluding remarks on the Literature review

From the detailed literature review the following conclusions can be drawn which are considered in as this research proposal:

- Recently, micro-grinding is becoming an alternative shaping process for brittle and hard material like glasses, especially, for manufacturing complex component shapes with high precision and good surface integrity. But no research has been reported on micro-grinding of glass material using on-machine fabricated PCD tool.
- However, the main drawback of the micro-grinding of glass is that, its surface burr, and subsurface micro cracks, which have resulted from brittle mode cutting. Several researchers used ductile mode machining to avoid this entire problem. Still there is room for further exploration of this hybrid type of micro-grinding process.
- The poor surface integrity of the ground glass often leads to mechanical degradation of these materials and the poor surface quality hampers the fluid flow in the micro fluidic channel. Hence, the quality and integrity of surface finish of ground glasses resulting from micro-grinding using PCD tool are of critical interest. But very few works have been done on improving the surface of micro-

ground glasses. Moreover, tool wear during glass grinding is a very important issue to investigate, as the tool will experience severe wear due to abrasive nature of glass material.

- As a result, the ways of improving the surface finish of glasses are required which can be a contribution to the micro-grinding of glass. Since the tool preparation method and tool corner wear during micro-grinding have great influence on the surface quality of ground glasses, focus should be put on these two aspects. From literature review, it was found that if tool has low surface roughness it will generate lower roughness of the ground surface. In addition, bottom of the tool needs to be dressed so that rubbing effect does not significantly affect surface quality.

Chapter 3

Experimental Setup and Methodology

3.1 Introduction

This chapter describes the experimental set up and experimental procedures used in the micro-grinding of glass reported in this thesis. The overview of the setup includes brief description of the machine tool, work piece, electrode and dielectric materials. Description of various measurement methods and equipment are also provided in the final section.

3.2 Experimental Setup

3.2.1. Multi-purpose Miniature Machine Tool

A multi-purpose miniature machine tool that has been developed for high-precision micro-machining at National University of Singapore (NUS) has been used for conducting the block-EDM on PCD tool material and also micro grinding of glass has been performed using the on-machine fabricated PCD tool. This machine is energized by a pulse generator which can be switched to both transistor type and RC-type, and is capable of performing micro-EDM, micro-turning, micro-milling, micro-grinding and micro-ECM by changing a suitable attachment where required. The maximum travel range of the machine is 210 mm (X) × 110 mm (Y) × 110 mm (Z) with the resolution of 0.1 μm in X, Y & Z direction. Each axis has an optical linear scale with a resolution of 0.1μm, and closed-loop feedback control ensuring accuracy of sub-micron level.

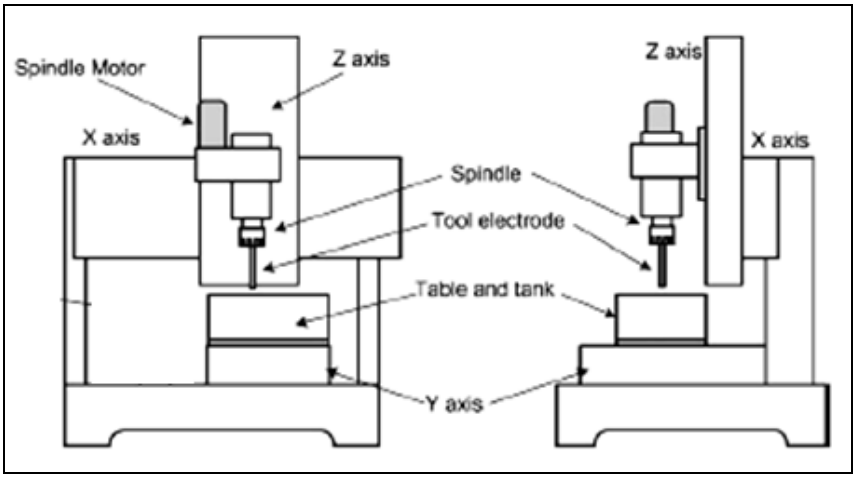

Fig.3. 1: Structure of the desk-top miniature machine tool used for the micro-EDM

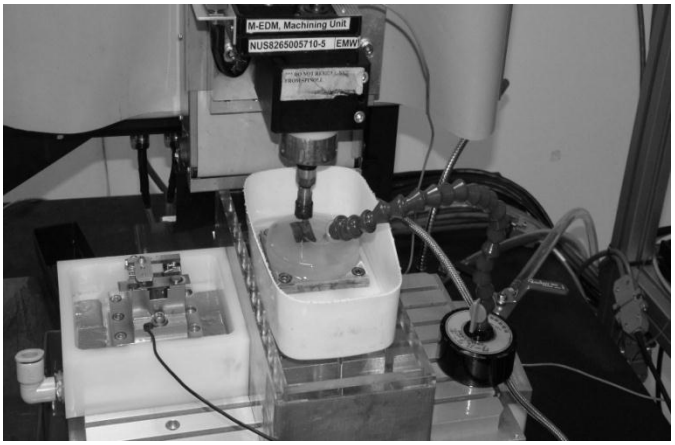

Fig.3. 2: A Detailed view of the set-up with micro-EDM attachment.

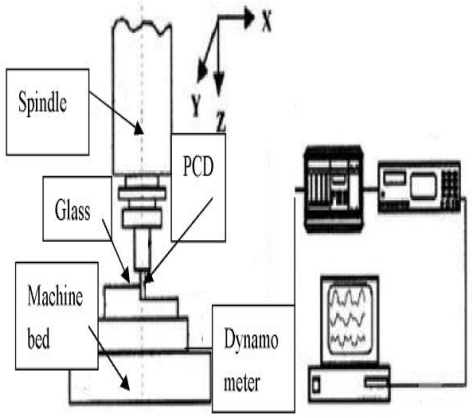

Fig.3. 3: A schematic view of the set up for Glass Micro-milling.

The Machine is capable of using variable high speed, middle speed and low speed spindles for micro-milling, micro-turning and micro-grinding on the machine. The low speed spindle is electrically isolated from the body of the machine so that electrical machining, such as EDM and ECM, can be performed on the machine. The motion controller can execute a program downloaded from the host computer independently; thus a good EDM gap control can be achieved in a real time. Experimental set up for block EDM on PCD is given in Fig. 3.2. While doing Glass micro-grinding, specimen is prepared in circular blank and mounted on top of the three–component force dynamometer (KISTLER type9345) fixed on the machine table. The dynamometer is connected to a charge amplifier (KISTLER type 5007) from which the output voltage signals are fed into a digital data recorder and the signals are recorded at a sampling frequency of 180 KHz. The schematic diagram of the experimental set up is shown in Fig. 3.3.

3.2.2. Work piece material

3.2.2.1. Glass

The work piece material used in this study is three different types of glasses (Bk7, Lithosil, N-FS14 glass). The work piece was fabricated and ground to 12.0 mm thickness with diameter 80.0 mm. The three glasses tested in this study represent a relatively wide cross section of those glass encountered practically in real life. Lithosil is known as one of the hardest glass which is difficult to machine. NSF-14 is softer glass and easy to material removal, whereas BK-7 glass is harder glass. The properties of the work piece material are shown in Table 3.1.

Table 3. 1: Properties of Work piece material

Glass	E(Gpa)	Kc(Mpa$\sqrt{m}$)	Hk(Kg/mm^2)	Tg(◦c)
Lithosil(fused silica)	72	0.74	615	980
BK7	82	0.85	610	559
N-SF14	88	0.7	515	566

3.2.2.2. Polycrystalline Diamond (PCD)

PCD is increasingly used in high volume machining due to the superior tool life. PCD is synthesized from extremely tough inter grown mass of randomly oriented diamond crystals bonded to a tungsten carbide substrate. It is manufactured by sintering together micron sized diamond grains at high pressure and temperature in the presence of a solvent/crystal metal, usually cobalt or cobalt/nickel alloy. During the sintering process, the voids between PCD grains are filled with cobalt binder. Unlike cemented tungsten carbide, however individual diamond grains actually bond to one another. The result is a tough hard product that will retain its shape and strength if some of the metal matrix is removed. In the case of tungsten carbide, when the binder phase is removed, the tungsten carbide grain breaks away from parent materials and from each other's. For PCD, if the

matrix is eroded grains are still held together by the bonding between them (Philbin and Gordon, 2005).

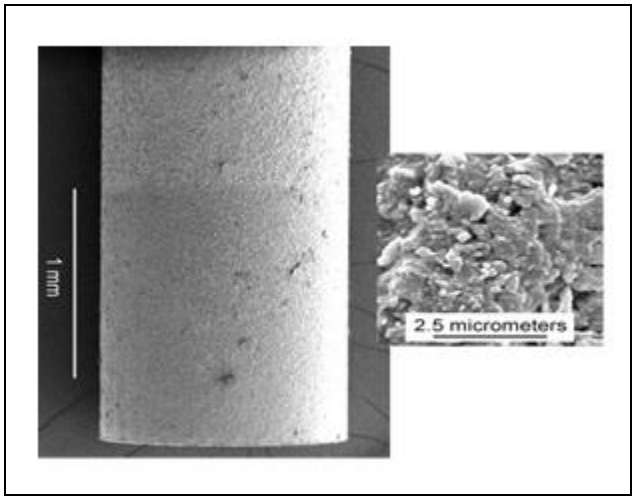

Fig.3.4**:** SEM micrograph of a ⌀ 1 mm PCD tool with tungsten carbide shank.

3.2.3. Electrode material For PCD

The tool electrode material for PCD used in this study is pure tungsten of length 4.5 cm, width 1.3cm and height 0.5cm with negative polarity. The properties of the electrode material are given in the following Table 3.2. For glass grinding PCD works as tool. This pure tungsten is chosen due to its high melting point which will cause low wear of tool electrode.

Table 3. 2: Properties of Electrode material

Material	Tungsten
Composition	99.9 % W
Density	19.3 g/cm^3
Melting point	3370 ^{0}C
Relative conductivity (to Silver)	14.0
Specific resistance	56.5 μΩ
Thermal expansion coefficient	4.6 × 10^{-6} K^{-1}

3.2.4. Dielectric fluid

The dielectric fluid used in this study is EDM oil having relatively high flash point, high auto-ignition temperature, low viscosity and high dielectric strength. This fluid is clear mineral oil exhibiting good resistance to oxidation, contains very low aromatics contents, low volatility and low pour point creating possibility of outside storage and low viscosity ensures evacuation of chips material. The properties of the EDM oil are shown in the Table 3.3.

Table 3. 3: Properties of the Dielectric fluid

Dielectric fluid	EDM oil
Density	0.77 g/cm^3
Flash point	259 ^{0}F
Auto ignition temperature	410 ^{0}F

Table 3. 4: Dynamometer specification

Measurement range	Fx,Fy,Fz:-250 to 250N
Sensitivity	Fx,Fz:-26pF/N,Fy:-13pF/N
Linearity all ranges	≤0.4(%FSO)
Fixed frequency	fx,fy,fz:5.1,5.5,5.6kHz
Operating Temperature range	0-70◦C

Fig.3. 5: Kistler precision capacitive dynamometer.

3.3. Experimental procedures

3.3.1. Micro-electrode fabrication

Prior to using PCD tools for micro grinding, the tool was first fabricated with a two-step process of block micro-EDM and scanning micro-EDM in order to ensure a polished flat surface. A sacrificial tungsten block with high wear resistance was used for the tool fabrication. During fabrication using micro-EDM, the PCD tool was set in positive polarity and the tungsten block was used as negative polarity as shown by Jahan et al. (2010)(Jahan et al.). When a voltage is applied between the PCD rod and block, an intermittent spark occurs between the inter-electrodes gap. The spark causes a rise in the surface temperature of both the block and the rod to a point where the temperature exceeds the melting point of the materials. Consequently, a small amount of material is removed from both the electrodes and flushed away from the machine zone using side flushing. Since, diamond is not an electrically conductive material; the electrical discharges take place between the conductive electrode material and conductive cobalt. Consequently, the conductive cobalt material is removed during the EDM process and to expose new or fresh surface of PCD grains for the next grinding process. This removal of cobalt material will leave the space between PCD grains which can subsequently work as chip storage place during grinding process. Sometimes the PCD grain will also fall off from the tool surface due to the excessive removal of the entire cobalt bonds around them as well. The fall of diamond grain will accelerate the material removal process during EDM process as next spark will be exposed to the conductive cobalt material again, but it will enhance the wear progression during grinding process. In this process, surface roughness can be controlled by varying capacitance and voltage. PCD tool was fabricated to nearly 600 µm size using different energy during different experimentation.

3.3.2. Micro-grinding of Glass

After the fabrication of PCD tool with desired shape and surface finish using micro-EDM, the tool was used for glass micro grinding on the same machine without changing

the tool from collet. During experiment, different feed rate, depth of cut and spindle speed were used depending on the aim of experiment. While glass micro-grinding, the work piece was mounted on top of a three-component force dynamometer (KISTLER type 9345) fixed on the machine table. The dynamometer was connected to a charge amplifier (KISTLER type 5007) from which the output voltage signals were fed into a digital data recorder and the signals are recorded at a sampling frequency of 180 KHz. Using the dynamometer and oscilloscope, the touching of tool bottom on the glass surface is made confirm. The specifications of the dynamometer used in this study are listed in table 3.5. Figure 3.2 shows the photograph of the set up representing glass micro-grinding with micro-EDM-fabricated PCD tool. Grinding forces and acoustic emission signal were recorded and optical images of tool were taken in between the experiments. The assessment of actual grinding tool wear was conducted by inspecting its topography and the channel geometry with FESEM and white light interferometer (Wyko NT2000). The white light interferometer has resolution of 0.1nm in vertical and 0.825µm in horizontal direction.

3.4. Equipment used for measurement and analysis

For measuring the dimensions, the Keyence VHX digital Microscope (VH-Z450) was used. Moreover, to obtain images of surface quality a Scanning Electron Microscopy (SEM) (JSM-5500.JEO Ltd) was used. An energy Dispersive X-ray (EDX) machine associated with the SEM was also used to investigate the surface properties changes of the work pieces material after micro-EDM process. The average surface roughness (Ra) and the distance between the highest pick and the lowest valley (R_{max}) were measured using the Atomic Force Microscopy (AFM) technique, which scans the samples over an area of 40µmX40 µm. A Seiko Scanning probe microscope was used for this purpose. To monitor the grinding conditions, an oscilloscope aided with electronic data recorder was used as well.

3.4.1. Atomic force Microscope (AFM)

Atomic force microscope (SEIKO scanning probe microscope) (Figure 3.6) is used to measure the surface roughness and distance between highest peak and lowest valley. Atomic force microscopy (AFM) technique scans the samples in an area of 40μmX40μm and displays the surface roughness of that area. Moreover it can also measure the peak to valley height of a line drawn across the surface. The microscope is able to scan an area of maximum 90μmX90μm. The radius of the probe tip is about 10 nm. This machine consists of two units – one is a probe station with a CCD camera and the other is a monitor for captured data processing with pre-installed windows supported software.

Fig.3. 6: Atomic Force Microscopes.

3.4.2 Scanning Electron Microscope (SEM) and Energy Dispersive X-ray (EDX) Machine

A Scanning Electron Microscope (SEM) (JSM-5500, JEOL Ltd,), as shown in Figure 3.7, was used to examine the surfaces obtained by using the RC setup. The microscope with one electron beam can be operated with a resolution of 4 nm. The maximum values of magnification and accelerating voltage which can be attained by the microscope, are 50,000X and 30kV respectively. The probe current ranges from 10-12 to 10-6A. An Energy Dispersive X-ray (EDX) machine associated with the SEM was also used to investigate the properties of the work piece material.

Fig.3. 7: Scanning Electron Microscope (SEM) also with Energy Dispersive X-ray (EDX) device

3.4.3 Keyence VHX Digital Microscope

Surfaces of machined work piece were observed under the Keyence VHX Digital Microscope (VH-Z450). This has two separate attachments with magnifications of 25X-175X and 450X-1000X. This has the ability of give 3D surface profile. It also has a feature to capture the

image directly to the computer and offer on-screen measurement. The 450X-3000X lens was used to capture pictures of the surface. This machine consists of two units – one is a digital photo taker with an optical microscope and another is a monitor for captured digital data editing with pre-installed windows supported software. The picture of Keyence microscope is given in Figure 3.8.

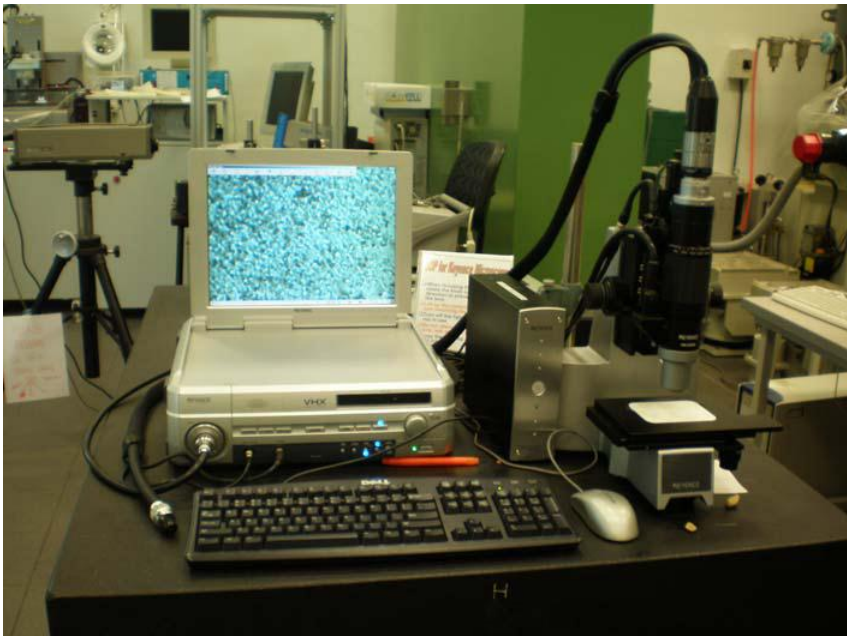

Fig.3. 8: Keyence VHX Digital Microscope

3.4.4 Taylor Hobson Machine

The Taylor Hobson Talysurf Model 120 stylus profiler is a precision metrology instrument used for measuring surface texture is shown in figure 3.9. All measurement functions are programmable and extensive analysis functions are available in the Windows-based measurement/analysis software. This machine was used to measure the surface roughness of the ground surface in this study. Due to its range limitation it is mainly suitable for measuring surface roughness of flat surface where probe range in z

direction is not big. Even though this machine was used for measuring surface roughness due to its better reliability taking shorter sampling length to keep the stylus range within limit. Detail specifications of this machine are given in table 3.5.

Fig.3. 9: Picture of the Taylor Hobson Talysurf Model 120.

Table 3. 5: Specification of the Taylor Hobson machine

Traverse speeds	1.0 mm / sec and 0.5 mm/sec (+/- 5%)
Column traverse	450 mm
Stylus range	6 mm range
Stylus tip radius	1.5 - 2.5 micron
Stylus force over full range	0.7 - 1.0 mN

Chapter 4

Experimental Studies of Micro-grinding of Glass

4.1. Introduction

The need for fabricated glass has been increasing to generate diversified functionalities on optical devices and bio-fluidics devices. In recent years, besides silicon, glass materials have important applications in micro-fluidics and micro-electromechanical systems (MEMS) as it can provide advantages like optical transparency, good fluorescence properties, dielectric properties, good chemical resistance, high thermal stability and high mechanical strength as demonstrated by Daridon et al. (2001)(Daridon et al., 2001). Micro-channels are integral part of micro-fluidic devices, which are used for various applications such as lab-on-chip, bio-MEMS-based sensors, etc. Depending on the manufacturing techniques, the channel surface has certain degree of roughness and this surface roughness of micro-fluidic channel affects the flow characteristics in the channel as demonstrated by Waghmare and Mitra (2008) (Waghmare and Mitra, 2008). Therefore, the development of processes which can produce smooth surface is of prime importance in the field of machining glass. This process should be applicable to small parts and micro-fluidics devices that comprise the main field of application of glasses.

For certain applications, like DNA micro arrays used in DNA analysis, glass component with micro-features are typically produced by photolithography and etching process which is time consuming and may involve hazardous chemical. Although chemical etching has been used to fabricate micro-patterns on glass materials, the process is hazardous and takes longer time. In addition, some problems associated with chemical etching are slow etch rate, presence of non-volatile halogen compounds and overall the process is difficult to apply except silicon channel as demonstrated by Malek et al. (2005) (Khan Malek et al., 2007). Similarly, photolithography process of glass fabrication needs longer machining time with surface roughness in micro level, and also the process is not

cost effective as mentioned by Matsumura et al. (2005) (Takashi Matsumura, 2005). In order to solve these problems associated with photolithography and etching process, mechanical micromachining processes may be approached which is much faster compared to other processes and non-hazardous. However, high hardness and brittleness of glass make this mechanically micromachining process problematic due to damage resulting from material removal by brittle fracture, cutting force-induced tool deflection, breakage and tool wear as demonstrated by Morgan et al. (2004) (Morgan et al., 2004). The forces arising from the cutting process significantly influence MRR, tool life and performance as well as achieved surface finish. Therefore, in recent years researches are being carried out on fabricating micro-features with high level of surface finish using different mechanical micromachining processes.

In order to reduce the arising cutting forces during machining and also to improve the surface finish and accuracy of the final structure, the size of the tools need to be minimized and fabricated on-machine. Moreover, fabricating on-machine cutting tool during mechanical micromachining has advantages like reduction of clamping error, run out error and position error. On-machine fabricated micro tools made of PCD can meet up this challenge of micromachining hard and brittle materials. A novel technique for fabricating precision cutting tools from polycrystalline super hard materials using micro-EDM is reported by Mamalis et al. (2004) (Mamalis et al., 2004). Several researches have been carried out on micromachining of hard and difficult-to-cut ceramics and carbides using PCD tool. Suzuki et al. (2007) (Suzuki et al., 2007) developed PCD micro-milling tool in order to machine molding dies made of binder-less tungsten carbide. Chen et al. (2008)(Shun-Tong and et al., 2008) used PCD tool for grinding ZrO_2 ceramics. PCD tool containing micron-sized diamond grains is manufactured by sintering under high temperature and pressure with metallic cobalt. The cobalt which fills the interstices between the diamond particles, serves as an electrically conductive network adequate for electro-discharge machining as demonstrated by Kozak et al. (1994) (Kozak J, 1994). Similarly, the mechanism of micro grinding phenomena using PCD tool was also

explained by Liu et al. (1997) (Liu Y H, 1999). For the on-machine fabrication of microelectrodes into different cross-sectional shapes, several micro-EDM-based technologies have been used. Masuzawa et al. (1985) (Masuzawa et al., 1985) has introduced wire electro discharge grinding (WEDG) process as a novel technique to fabricate microelectrode on-machine before using in micro-EDM. The mesh electrode method was also suggested by Masuzawa (2000) (Masuzawa, 2000), which can produce microelectrodes of different shapes. In addition, Allen et al. (1997) has shown that the block EDM method of fabricating microelectrode is simpler and more effective compare to other processes (Allen and Lecheheb, 1996). Among all the micro-EDM based processes, block-μEDM using a conductive block as sacrificial and the PCD rod as a work piece has been identified as being a simple and useful approach for fabricating microelectrodes, due to its low investment cost and quick set-up as demonstrated by Ravi and Huang (2002). In recent years, many researchers are focusing on the micro grinding of hard glasses and ceramics using diamond grinding wheels (Nachiappan. Ravi, 2002). Among them, Takahashi et al. (2000) have studied the micromechanics of diamond composites tools during the micro grinding of glass materials (Takahashi and Funkenbusch, 2000). It has been reported that the evolution of grinding performance is strongly related to both the process conditions and the glass type. In addition, research has been carried out by Gao et al. (2009) on the surface characteristics of nano-zirconia ceramics during micro grinding using diamond grinding wheel with the aid of ultrasonic vibration (Gao et al., 2009). An investigation on the micro grinding performance of BK7 glass material has also been reported by Sun et al. (2006)(Sun et al., 2006). Although extensive researches have been conducted on grinding of glasses using commercially available diamond grinding wheels, the application of micro PCD rod has not yet been studied extensively. Therefore, a number of issues remain to be solved before the micro grinding of glass using PCD tool becomes a well-accepted process, especially in industries. Moreover, research on the selection of optimum parameters for improved surface finish and reduced cutting forces during glass micro grinding is of prime importance.

Hence, this chapter intends to investigate the performance of PCD tool in micro grinding of three different glass materials (BK7, Lithosil and N-SF14) with varying hardness. The effect of micro-EDM conditions on tool surface during fabrication of PCD tool and its effect on the grinding performance are studied. In addition, experimental investigation has been carried out on the effect of grinding parameters on cutting forces and surface finish during micro grinding of different types of glass materials.

4.2. Methodology

Prior to using PCD tools for micro grinding, the tool was first fabricated with a two-step process of block micro-EDM and scanning micro-EDM in order to ensure a polished flat surface. A sacrificial tungsten block with high wear resistance was used for the tool fabrication. During fabrication using micro-EDM, the PCD tool was set in positive polarity and the tungsten block was used as negative polarity as shown by Jahan et al. (2010) (Jahan MP, 2009). When a voltage is applied between the PCD rod and block, an intermittent spark occurs between the inter-electrodes gap. The spark causes a rise in the surface temperature of both the block and the rod to a point where the temperature exceeds the melting point of the materials. Consequently, a small amount of material is removed from both the electrodes and flushed away from the machine zone using side flushing. In this process, surface roughness can be controlled by varying capacitance and voltage. After the fabrication of PCD tool with desired shape and surface finish using micro-EDM, the tool was used for glass micro grinding on the same machine without changing the tool from collet.

4.3. On-machine Fabrication of PCD Tool Using Micro-EDM

The commercial PCD is manufactured by sintering with micron size diamond grain under high pressure and temperature in the presence of a solvent/crystal metal like cobalt or nickel alloy. During the sintering process, the voids between PCD grains are filled with cobalt binder where individual diamond grains actually bond to one another. The effect is a tough and hard product. Even if some part of the metal matrix is removed it can retain its shape and strength as demonstrated by Philbin and Gordon (2005) (Philbin and

Gordon, 2005). The cobalt binder is removed during micro-EDM as it is conductive, whereas the PCD grain is exposed to the surface and can work as cutting edge during micro-grinding. However, as the surface finish of the fabricated tool can have significant influence on the micro-grinding performance, the effect of micro-EDM parameters is important to consider. Following section will present the effect of gap voltage, capacitance and depth of feed in each step on the machining time during the fabrication of PCD tool. A comparison on the performance of PCD tool in micro-EDM against widely used conductive tungsten rod was carried out to analyse the micro-EDM machinability of PCD.

4.3.1. Effect of Gap Voltage

Fig.4.1 (a) shows the effect of gap voltage on machining time during micro-EDM of PCD and tungsten (W) rod. It has been found that for both the materials, the machining time decreases significantly with the increase of gap voltage. This is due to the reason that with the increase of gap voltage the discharge energy per pulse is increased, which results in larger craters and causes more material removal from work piece. Keeping all other factors constant, an increase in voltage will result in increased energy per spark. It has been also observed that compared to pure tungsten, PCD material need higher machining time to be fabricated by micro-EDM. This is due to the higher electrical conductivity of tungsten materials which make it better machinable by micro-EDM. The non-conductive diamond particles of PCD material causes higher machining time during micro-EDM. One important observation at lower gap voltage is that the machining time for W becomes higher than that of PCD material. This is due to the reason that at lower gap voltage the spark gap between the electrodes becomes smaller, which prohibits flushing out of all the debris materials from the machined zone as demonstrated by Jahan et al. (2009a) (Jahan et al., 2009a). Therefore, the flushing out of cobalt binder in PCD tool becomes easier than that of tungsten at lower spark gap, which causes sudden increase in machining time for W material.

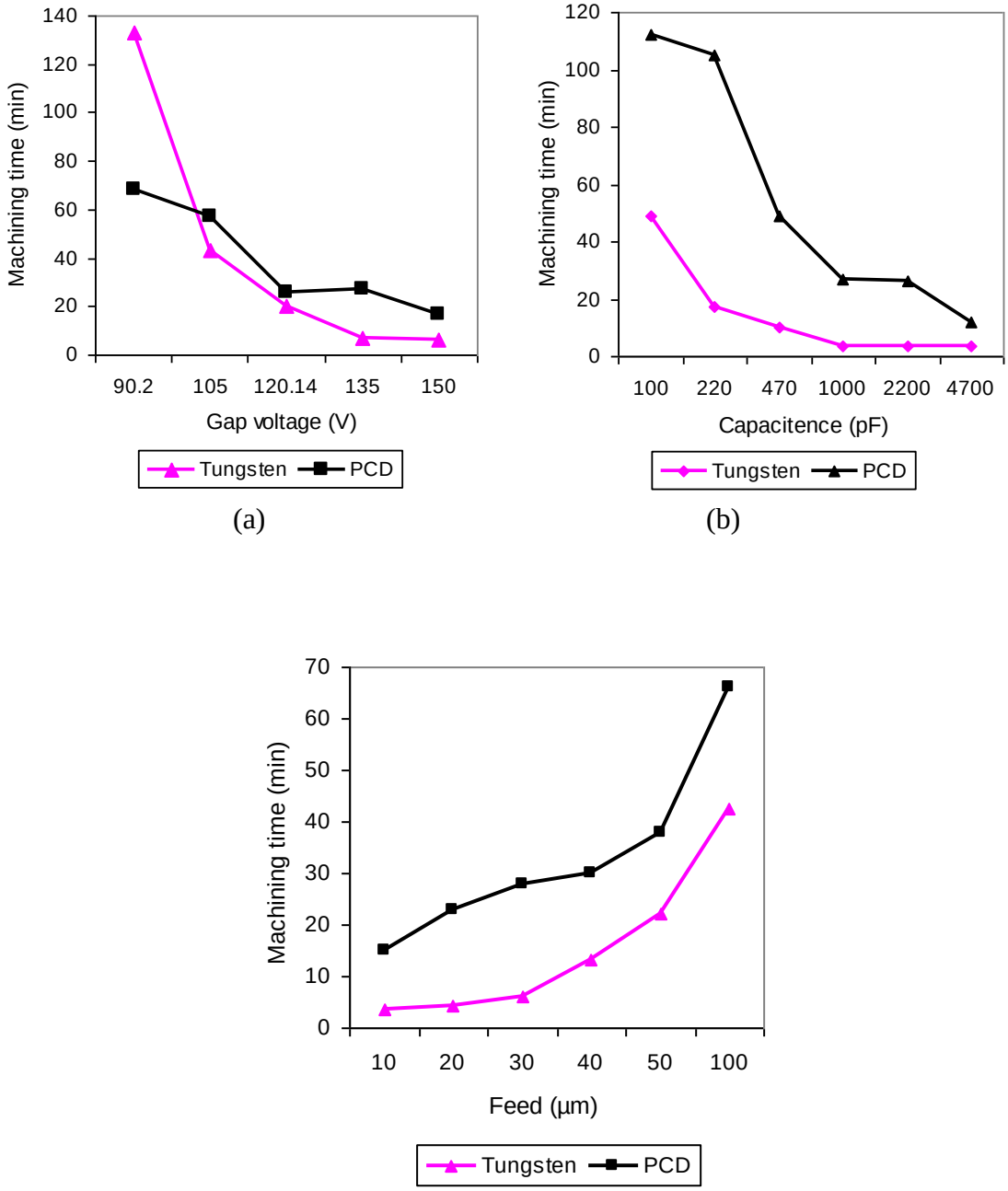

Fig.4. 1: Effect of operating parameters on machining time during the fabrication of PCD tool using micro-EDM.

4.3.2 Effect of Capacitance

The capacitor controls the charging and discharging process as well as the frequency of discharging. Therefore, the performance of the micro-EDM in RC-circuit is more influenced by the capacitance as demonstrated by Jahan et al. (2009b) (Jahan et al., 2009b). It has been found in Fig.4.1 (b) that with the increase of capacitance the machining time decreases significantly as the discharge energy increases. As the capacitance value becomes larger, the peak current also increases. Therefore, the larger capacitance results in deeper craters which increase the material removal. It has been observed that the trend of reduction of machining time with increase of capacitance is more sharp during micro-EDM of PCD compared to W. However, for all the settings of capacitance, the machining time is lower in micro-EDM of W rod. As the melting point of PCD is higher than tungsten, machining time is also higher in case of PCD when removing same amount of materials under same machining condition.

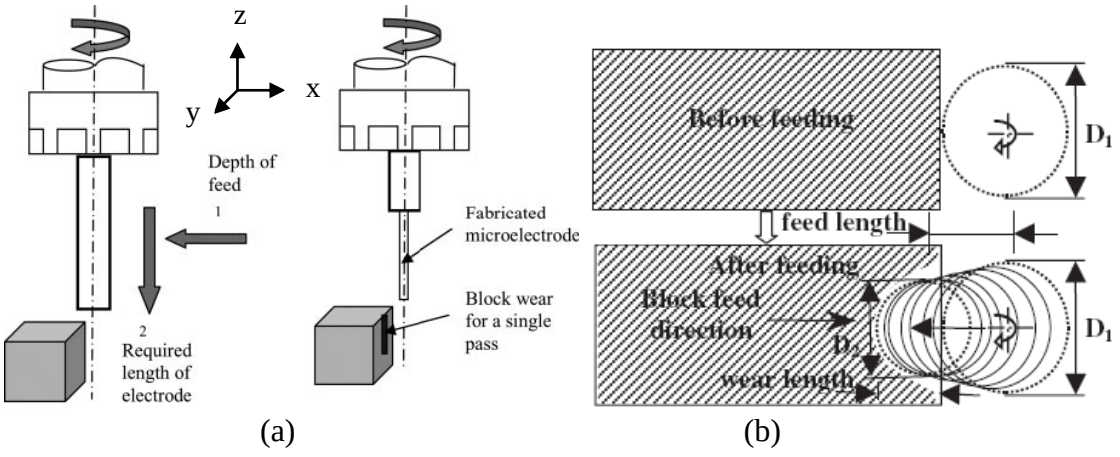

Fig.4. 2: (a) Schematic diagram representing on-machine fabrication of tool electrode using block-µEDM, (b) schematic showing the geometry of feed length and wear length.

4.3.3. Effect of Depth of Feed in Each Step

Depth of feed during tool electrode fabrication is the offset of the electrode length in X-axis to the sacrificial electrode [see Fig.4.2]. Fig.4.2 (a) shows the schematic representation of the block-µEDM process of tool fabrication. The geometric definition of feed length and wear length during the block-µEDM process are presented in Fig. 4.2(b) as demonstrated by Ravi and Chuan (2002) (Nachiappan. Ravi, 2002). Fig.4.1(c) shows the effect of electrode feed length on the machining time during micro-EDM of PCD and W rod. It is clear that the machining time will be higher for removing materials using a higher feed length, since more material has to be removed. However, if the tool fabrication is carried out in several steps, the overall machining time for fabricating a micro-electrode will reduce with increasing the feed length for a single step. Moreover, if a higher feed length is used during the final stages of fabrication, the fabricated tool can become more tapered. Therefore, the suggestion is that a higher feed length can be applied for rough machining at the first few steps of the fabrication process. However, during the final few steps of the fabrication process, the feed length should be kept low in order to improve surface finish and accuracy.

4.4 Effect of Fabricated PCD Tool Surface on Glass Micro grinding

After the tool fabrication process with micro-EDM, the on-machine fabricated tool is used to machine micro-slots on the glass surfaces using micro grinding process. During this grinding process, the surface roughness of the fabricated tool has significant effect. Therefore, to study the effect of PCD tool roughness on the grinding surface, three different tools were fabricated using three different levels of discharge energy in micro-EDM. The three settings of electrical parameters are selected in such a way so that they can be classified under higher, medium and lower levels of discharge energy. The bottom of the tools were machined using scanning micro-EDM operation at the same electrical setting to make sure that the bottom surface has same roughness as side wall surface of the PCD tool. After that, three pockets were machined on Lithosil glass using micro

grinding with same cutting condition of axial depth of cut 2 µm, feed rate10 µm/min and tool rotational speed of 2000 rpm.

Fig. 4.3 shows the comparison of the PCD tool surface after fabricating using three different levels of discharge energy settings. The optical images of the machined pocket surface on glass using fabricated PCD tools are shown in Fig. 4.4. The roughness profiles on the machined glass surface for three different tools are shown in Fig. 4.5. The surface roughness of the machined pockets was investigated using Taylor Hobson Profilometer (cut off length (Lc) of 0.08 mm, (Ls) 0.0025mm, bandwidth 30:1 and evaluation length of 1mm) to study the cutting regime transition based on the scanned surface profile. It is obvious that during micro-EDM, machining with higher discharge energy will produce relatively larger craters and generate rougher surface. Therefore, fabricated PCD tool using high energy settings [Fig. 4.3(a)] resulted in rough surface on machined micro-slots after micro grinding [Fig.4.4(a) and 4.5(a)]. On the other hand, the tool fabricated by both medium and low discharge energy settings generates smooth surfaces on the glass after micro-grinding. However, it has been observed that the tool obtained by medium discharge energy has still some deposited molten materials on the surface [Fig. 4.3(b)], which can generate sudden abrupt change in surface roughness profile due to scratching by those deposited debris particles [Fig. 4.5(b)]. However, the tool fabricated using lower discharge energy generates very smooth surface on the PCD tool [Fig.4.3(c)], which can produce burr-free nanosurface [Fig. 4.5(c)] without any adhesion of chips [Fig.4.4(c)]. This is due to the fact that PCD tool with smoother surface generates smaller chips on the glass materials during micro-grinding that can be easily flushed out from the machined zone. Therefore, the overall surface finish improves in addition to reduction in adhesion of chips on the glass surface. Table 4.1 presents a summary on the micro grinding performance of PCD tool fabricated using different levels of discharge energy in micro-EDM.

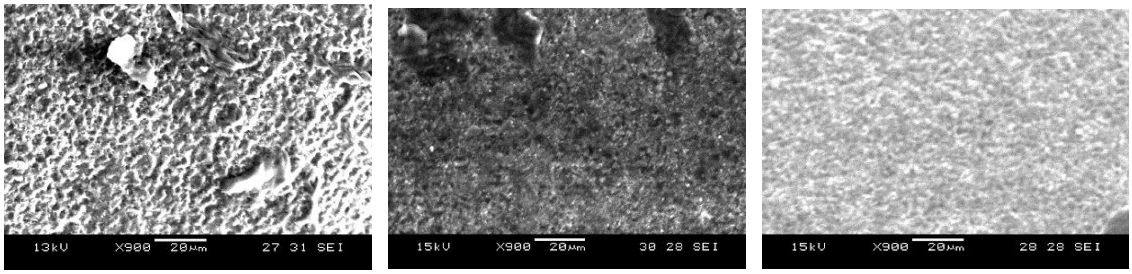

(a) C = 4700 pF, V=150 V (b) C = 1000 pF, V=110V (c) C = 100 pF, V=80 V

Fig.4. 3: Comparison of PCD tool surface fabricated by micro-EDM at different settings

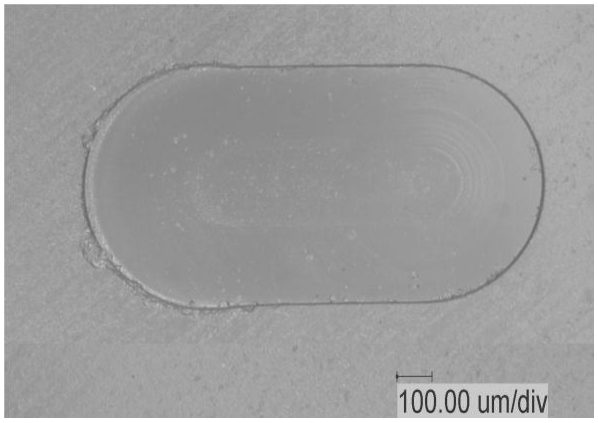

(a)

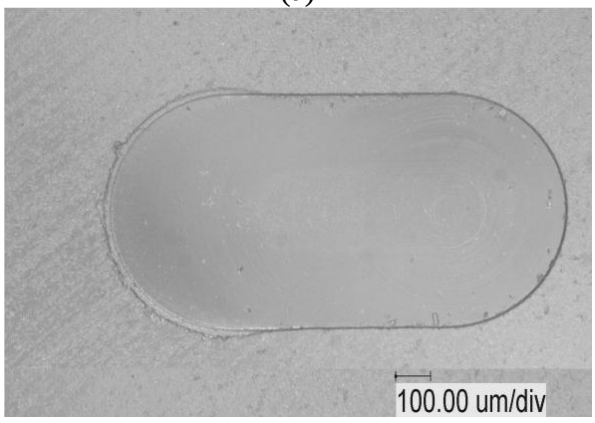

(b)

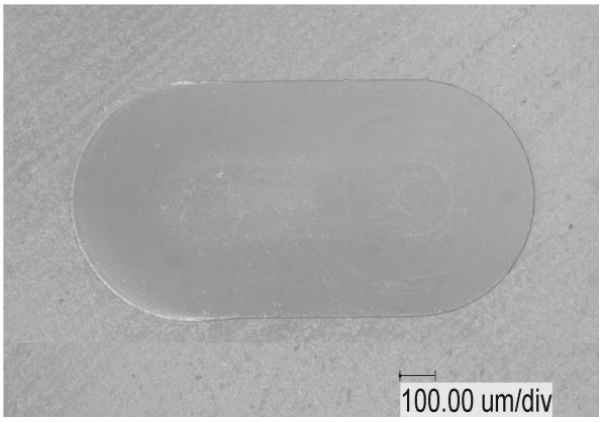

(c)

Fig.4. 4: Comparison of surface finish of the machined pocket with the three different PCD tool fabricated using different energy settings; (a) with tool machined using 4700pF, 150V, (b) with tool [1000pF, 110V] (c) with tool [100pF, 80V]

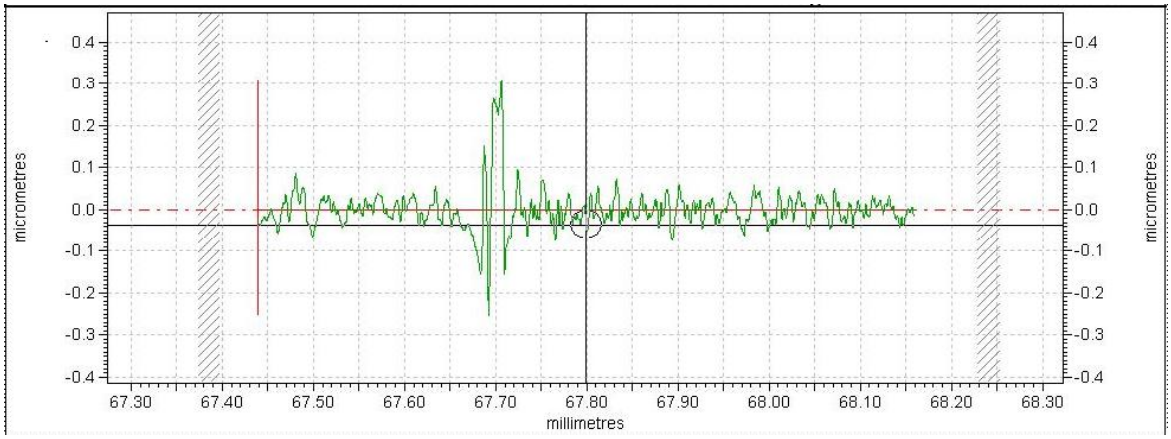

(a) Roughness profile (R_a = 60.2 nm) for the slot shown in Fig 4.4(a)

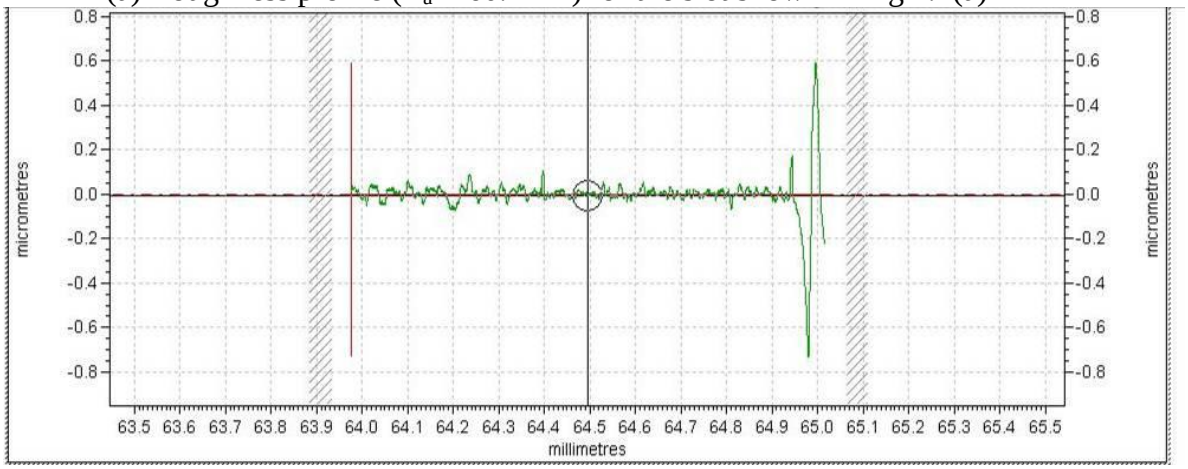

(b) Roughness profile (R_a = 35.5nm) for the slot shown in Fig.4.4 (b)

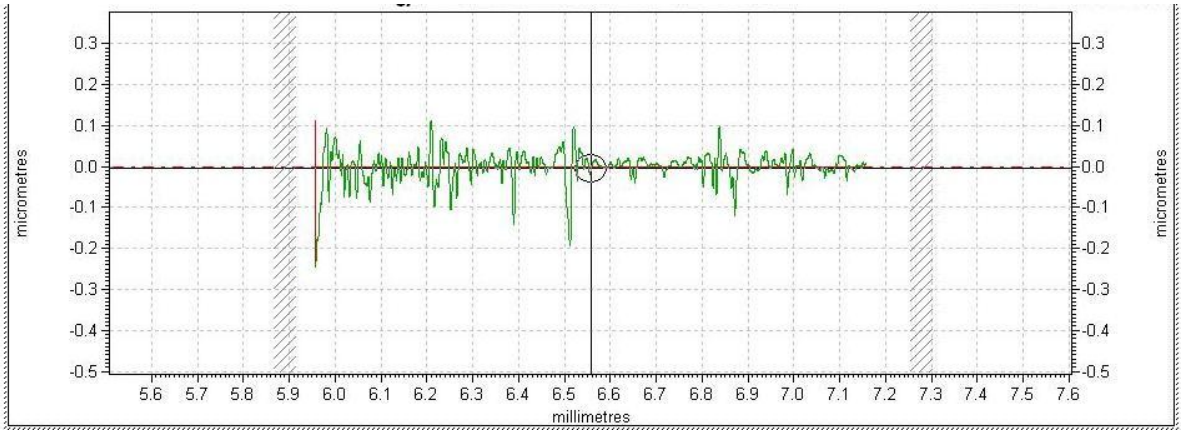

(c) Roughness profile (R_a = 22.9 nm) for the slot shown in Fig. 4.4(c)

Fig.4. 5: Comparison of surface roughness of slots machined by PCD tool with different settings

Table 4. 1: Comparison of roughness of PCD tools and machined slots with those tools

Discharge energy (D.E.) settings to fabricate PCD tool	Surface roughness of fabricated PCD tool at different D.E.	Roughness of the glass after micro-grinding with PCD tool
Higher D.E.: 52.87 µJ/pulse V: 150 V, C: 4700 pF	R_a = 1.90 µm, R_{max} = 10.25 µm	R_a = 60.2 nm, R_{max} = 0.191 µm
Medium D.E.: 6.05 µJ/pulse V: 110 V, C: 1000 pF	R_a = 1.19 µm, R_{max} = 7.73 µm	R_a = 35.5 nm, R_{max} = 0.159 µm
Lower D.E.: 0.15 µJ/pulse V: 80 V, C: 100 pF	R_a = 0.99 µm, R_{max} = 5.91 µm	R_a = 22.9 nm, R_{max} = 0.148 µm

4.5 Comparative Micro Grinding Performance of BK7, Lithosil and N-SF14 Glasses

4.5.1 Comparison of Cutting Forces

Machining of brittle materials like glasses using mechanical micromachining processes are difficult due to cutting force induced tool deflection and brittle fracture of glass materials. The forces arising from micromachining processes need important consideration as it can affect the material removal rate, surface finish and dimension of the microstructures. The following section will present a comparative analysis of cutting

forces generated along three axes during microgrinding of BK7, Lithosil and N-SF14 glasses using on-machine fabricated PCD tool of lower energy. The dimension of fabricated PCD tool was of 670 µm diameter and 1mm length. The effect of cutting conditions on the grinding forces has also been presented.

It can be observed from Fig. 4.6 that during microgrinding, the cutting forces experienced by Lithosil and BK7 glasses show some kind of pattern, whereas the forces experienced by N-SF14 show fluctuating trend. In fact the cutting force is supposed to increase with an increase in the axial depth of cut as demonstrated by Liu et al., (2008) (Liu et al., 2008). It is seen from Fig. 4.6(a) that the force along X-axis shows an increasing tendency for Lithosil glass material, whereas for BK7 glass the force is becomes constant after initial increment. This may be due to loosing diamond particles during grinding as demonstrated by Feng et al. (2009) (Feng et al., 2009). It can be also explained from brittle fracture point of view. The cutting force is expected to become constant after the occurrence of brittle fracture, as further cutting only induces fracture without any deformation as established by Cai et al. (2007) (Cai et al., 2007). However, as force ratio of X to Y axis is less than unity, brittle cutting mode was dominating for grinding, which will be also clear from optical image shown later in surface roughness section. However, no specific trend of cutting force along X-direction has been observed for micro-grinding of N-SF14 which might be due to adhered glass material on the tool bottom surface from the previous cut.

This adhered glass chip could be the result of thermal softening of glass material as NSF-14 has comparatively lower transition temperature than other two glasses (Table-4.1).As a result of this; welded center line is also found from the optical image of this glass. It has been found from Fig. 4.6(b) that for all three different glasses, force along Y axis increases gradually with the increase of depth of cut. It is also seen that for same experimental conditions, cutting force along Y-axis is higher for Lithosil glass compared to BK7 and N-SF14 glasses. This may be due to difference in hardness between these

glasses, as Lithosil is the hardest and N-SF14 is least hard glass material. Force acting in Z direction is about 10 times higher than the force acting in the X and Y direction [Fig.4.6(c)]. N-SF14 glass experienced less cutting force along Z axis compared to Lithosil and BK7 glass, which may be due to its lower hardness. It has been also observed that cutting forces along Z-axis for N-SF14 shows slightly decreasing but zigzag trends with the increase of depth of cut. In addition to lower hardness of N-SF14, the reason may be the flatness error of glasses which causes tool deflection and tool lift up. This flatness error also results in tool disengagement and irregular material removal as demonstrated by Torres et al. (2009) (Torres et al., 2009). As Lithosil and BK7 glass have hardness nearer to each other, they experienced quite similar force along Z axis.

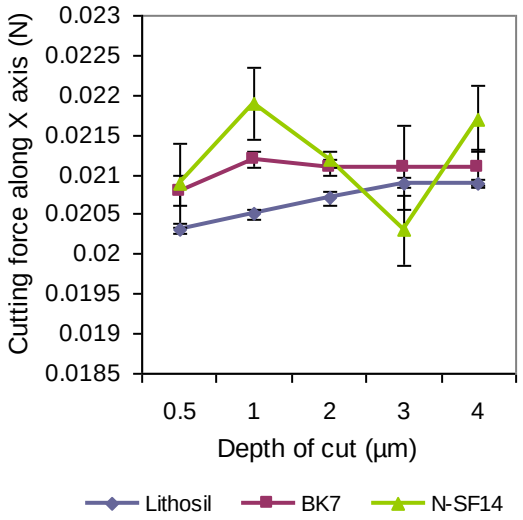

(a)

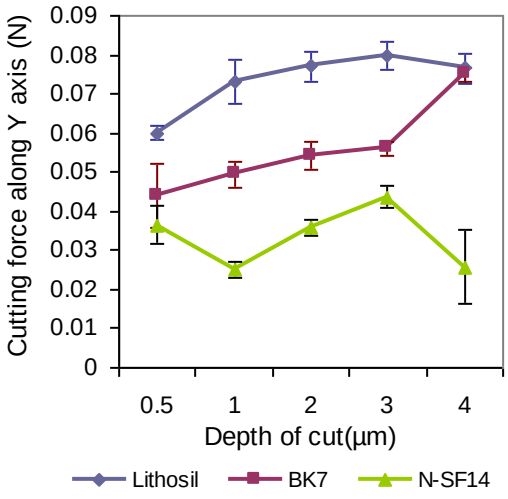

(b)

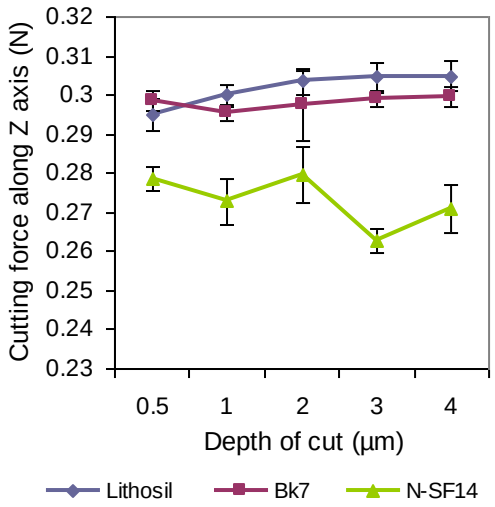

(c)

Fig.4. 6: Variation of cutting forces along (a) X-axis, (b) Y-axis and (c) Z-axis with depth of cut during micro-grinding of Lithosil, BK7 and N-SF14 glass materials

Fig. 4.7(a), (b) and (c) show comparison of 3 dimensional forces (forces along X Y and Z axis) as a function of feed rate during microgrinding of Lithosil, BK7 and N-SF14 glasses, where axial depth of cut was maintained at 1 µm. It has been observed that forces along Z axis was the dominant force during machining of glasses with PCD tool. Ratio of forces along X axis to Y axis was found less than unity which indicated that brittle mode cutting plays a dominant role as demonstrated by Cai et al. (2007) (Cai et al., 2007). As a result, change in feed rate did not significantly change forces acting along Z axis. Force acting along X axis increases slightly with the change of feed rate except NSF-14 glass. Significantly large fluctuation of force in Y-axis for Lithosil glass may be due to adhered chips on tool bottom surface from previous cutting. During micro grinding, the micro tool encounters more bending force due to its relatively smaller size of tool which may cause the tool fluctuation resulting in irregular material removal and changes in cutting force. This usually happens more once the tool bottom contains some of the material cut from previous cutting. Then the tool is supported by that smaller chip area. This adhered chip on the bottom of tool from previous cutting results in the reduction of axial depth of cut

consequently causes the reduction of cutting force even with increment of feed rate. Moreover, the higher hardness of the Lithosil glass is responsible for relatively more tool wear which also may contribute to the reduction of axial depth of cut as well as cutting force. Hence, while increasing the feed rate, reduced axial depth may cause this kind of sudden fall of cutting force.

For the other two glass materials, the cutting forces along Y-axis are almost constant. In this study, comparatively lower range of feed rate was used in order to maintain the grinding regime in the ductile mode cutting. Therefore, not much variation of cutting forces was observed within 1 – 25 µm/min feed rate in all three axes.

It can be concluded from the above discussion on cutting force analysis that, the cutting forces in Z-direction (major force component) is higher in case of Lithosil compared to BK7 and N-SF14, which was mainly due to the variation of hardness in different glass materials. On the other hand, large volume of N-SF14 materials can be removed with lesser tool wear using a PCD tool. However, the BK7 glass showed intermediate behavior. Moreover, as the feed force to cross feed force ratio was less than one, it can be said that brittle regime cutting was still dominating during the microgrinding process.

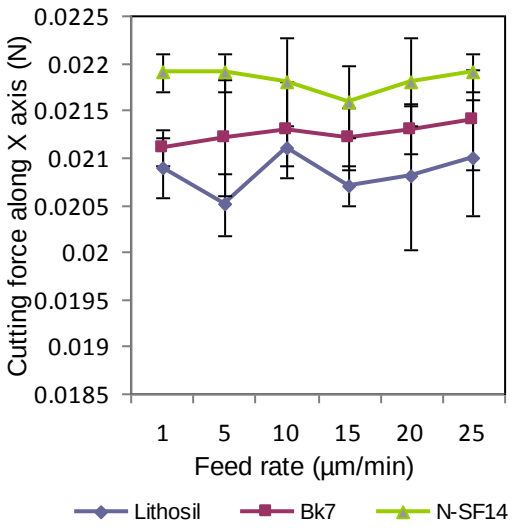

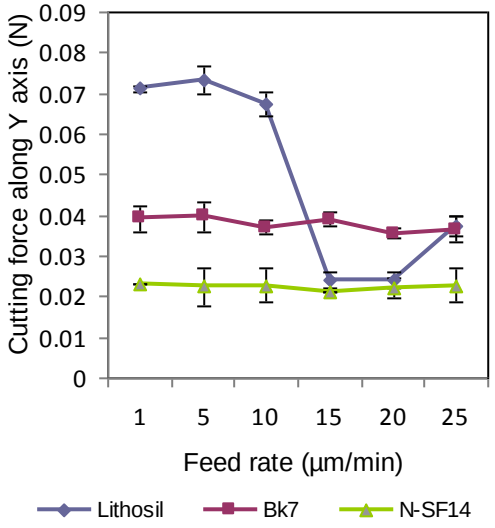

(a) (b)

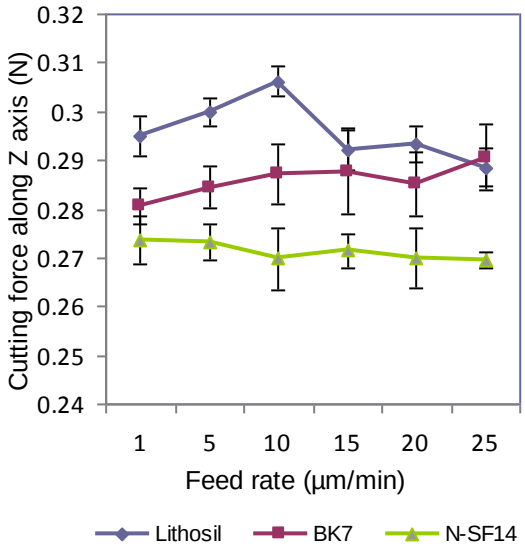

(c)

Fig.4. 7: Variation of cutting forces along (a) X-axis, (b) Y-axis and (c) Z-axis with feed rate during micro-grinding of Lithosil, BK7 and N-SF14 glass materials.

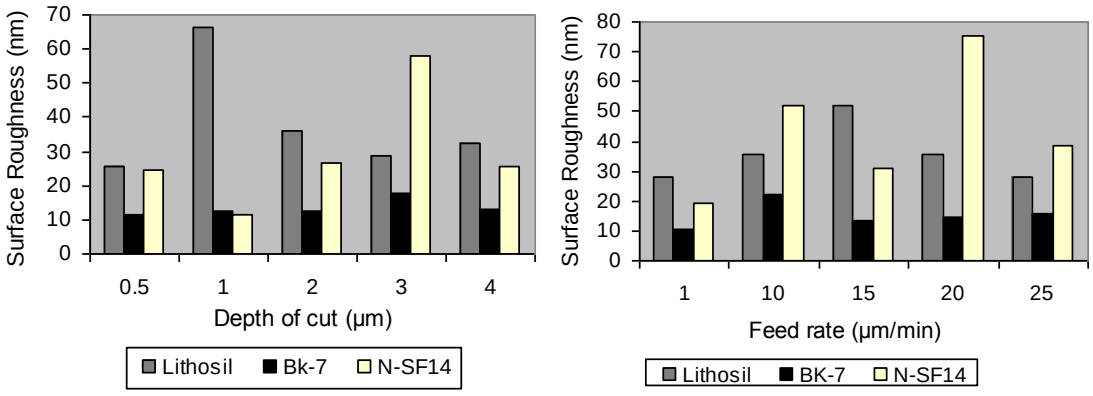

(a) (b)

Fig.4. 8: Comparison of surface roughness for different glass materials with respect to (a) depth of cut and (b) feed rate

4.5.2 Comparison of Surface Roughness

Fig.4.8 shows a comparison of average surface roughness obtained in different glass materials at various settings of axial depth of cut and feed rate. It has been observed that with the increase of depth of cut, the surface becomes rougher during grinding of Lithosil and N-SF14 glasses [Fig4.8 (a)]. However, there is little variation of surface roughness with increase of axial depth of cut in case of BK7. Similar results can be observed from Fig. 4.8(b), as BK7 glass was found to show little variation with increase of feed rate.

It can be observed from Fig. 4.9 that, for almost every micro channels, surface roughness has a decreasing tendency from entry to middle of the pocket along width direction, and from middle to exit the roughness is increasing. First phenomenon may be due to exceeding minimum un-deformed chip thickness of the work piece and second phenomenon may be attributed to the micro crack induced fracture as demonstrated by Foy et al. (2009) (Foy et al., 2009). In addition to microgrinding, some rubbing action may also take place, which contributes to the final surface roughness and surface or sub-surface defects. It is believed that rubbing will suppress fracture propagation but increase surface roughness, brittle machining will increase fracture propagation and surface roughness, and ductile machining will lead to a fracture-free, low surface roughness surface. Strictly speaking, rubbing is not responsible for any material removal, so only the cutting transition from brittle machining to ductile machining is usually of interest as demonstrated by Foy et al. (2009) (Foy et al., 2009)). In addition, the amounts of adhered materials are lower in case of BK7 glass, comparatively more in N-SF14 and almost none for Lithosil. The reason behind this might be the variation in transition temperature, which is higher for Lithosil glass, lower for BK7 and the lowest for N-SF14 glass [Table 3.1]. Due to lower transition temperature of NSF-14 glass material, some glass chips adhered on the ground surface with the generation of temperature during machining as demonstrated by Torres et al. (2009) (Torres et al., 2009).

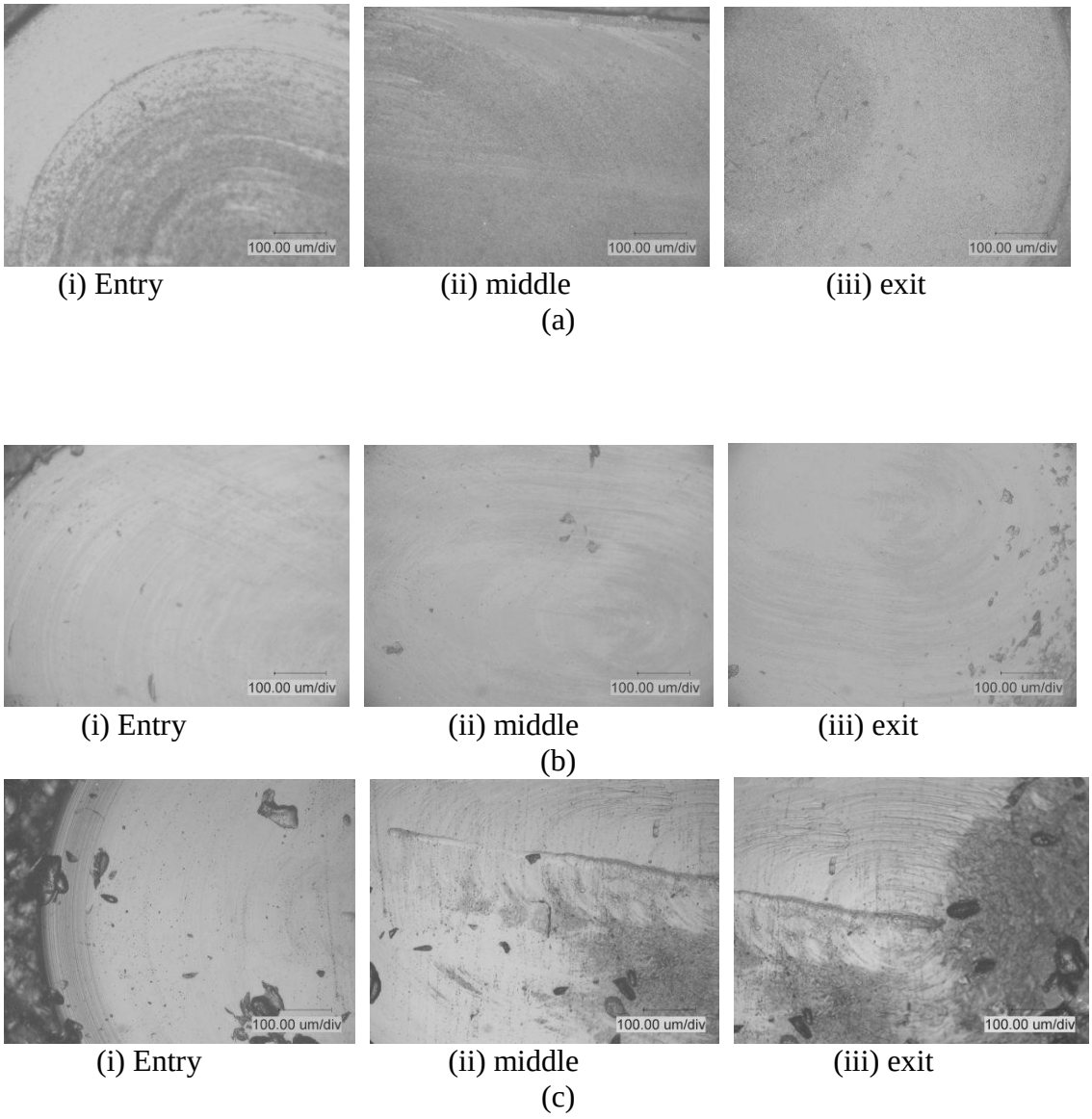

Fig.4. 9: Comparison of surface finish (optical image) between (a) Lithosil, (b) BK7 and (c) NSF-14 glasses at different location of the machined slots

Fig.4.9 also presents a comparison of machined surface for three different glass materials after microgrinding process using on-machine fabricated PCD tool. The PCD tool has been fabricated using the lowest energy settings (80 V, 100 pF), as fabricated tool using this setting was found to provide improved surface finish [see Figs.4.3 – 4.5]. It can be seen from Fig. 4.9 that both the Lithosil and BK7 glass provide surface finish with low

amounts of adhered glass chips. Among the three glasses, BK7 glass provided the lowest average surface roughness and Lithosil glasses produced surfaces with lesser amount of adhered glass chips. However, the slot produced in N-SF14 after micro-grinding using PCD tool was found to suffer from extensive adhesion of chips materials. It can be observed from Fig. 4.9(c) that in addition to adhesion of chips on the surface, a dragging track was observed in the middle portion of ground surface. The reasons for this scratching or dragging effect is due to the zero velocity effect at the center of PCD tool, which trap chips and drag them along the cutting path without cutting as demonstrated by Izman and Venkatesh (2007). This has been confirmed, as the PCD tool bottom was also dressed in two steps in order to ensure flat surface of the PCD tool. Moreover, with the increase of coolant pressure this mark tends to reduce to a great extent. However, in this study during microgrinding experiments higher volumetric coolant flow was used so that traces of drag lines are minimized, though still some traces was there like in Fig. 4.9c(ii). It has been observed that although Lithosil glass provides comparatively smoother surface, the traces of PCD tool path was noticeable on the machined surface [Fig. 4.9(a)]. On the other hand, the machined slots in BK7 glass have fewer tool path marks in addition to lower average surface roughness and fewer adhesions of chips. The better performance of BK7 glass may be associated with the higher fracture toughness of the materials. The higher the fracture toughness of a material, the bigger will be the fracture resistance. The higher fracture resistance allows better machinability in addition to lesser surface defects due to cutting forces. Moreover, due to higher facture resistance, microgrinding of BK7 glass involves more ductile material removal mode and more stable interaction between material and diamond grains resulting in less grinding force as demonstrated by Zhao et al. (2007) (Zhao et al., 2007).

The phenomena of adhering chips on PCD tool tips are supported by the observation of tool bottom surface and EDX analysis of PCD tool before and after micro grinding. Fig. 4.10 shows the EDX analysis of the PCD tool before and after micro-grinding of BK7 glass. It has been observed that there is significant amount of materials migrate from

glass materials to the PCD tool after the micro-grinding process. This is due to the attached chips of glass materials that adhered to the PCD tool during grinding. The percentage of parent materials (C: 74.10%, Co: 11.93%) of the PCD tool decreases (C: 61.90%, Co: 3.19%) in addition to increase in foreign materials after micro-grinding of BK7 glass due to adhered chips of glasses. These adhered foreign materials have close relationship with final surface finish, as increased amount of glass chips on PCD tool caused an increase in surface roughness of ground glass pockets in addition to making the surface faulty.

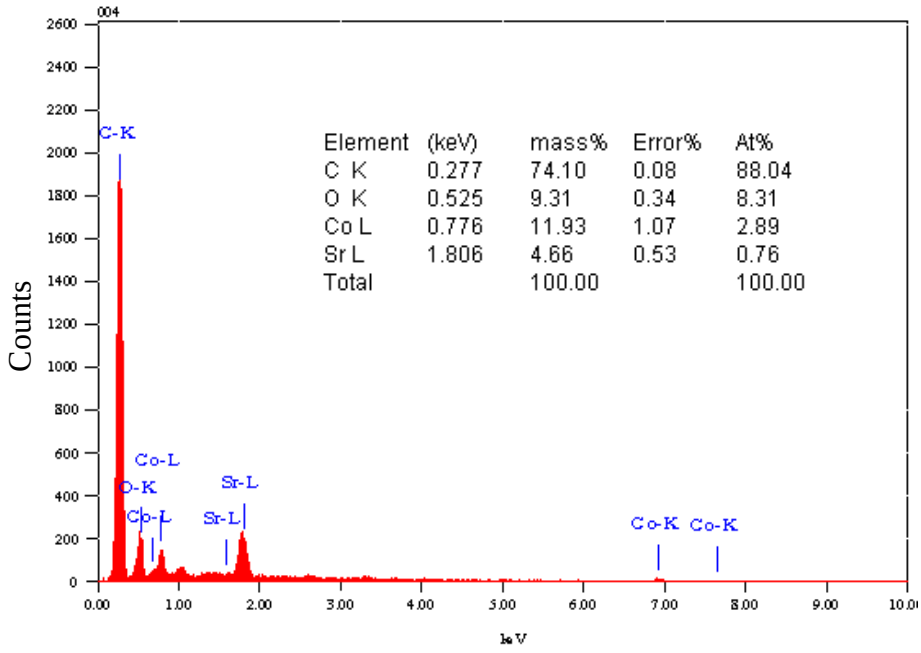

(a)

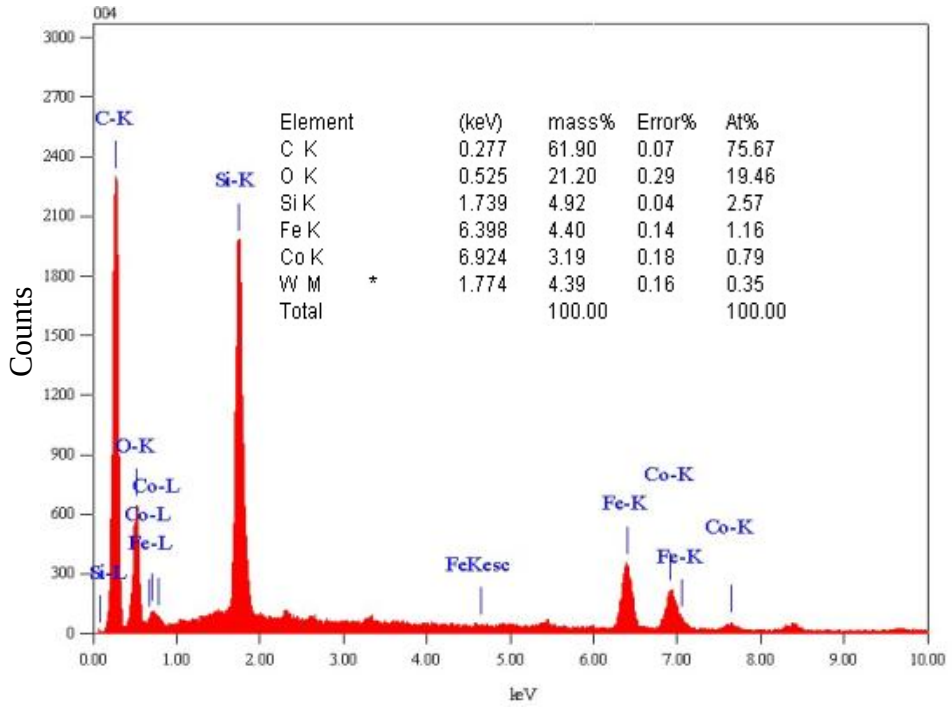

(b)

Fig.4. 10: Comparison of the material composition of PCD tool (a) before and (b) after micro-grinding of BK7 glass

In order to observe and compare the surface finish more comprehensively, a comparative analysis of 3D surface textures obtained by AFM is shown in Fig. 4.11 using an axial depth of cut of 2 µm and feed rate of 1 µm/min. It can be seen that for the same scale of crater heights 500 nm, the surface of BK7 shows lesser amounts of white peaks indicating smoother surface [Fig.4.11 (b)]. On the other hand, it is clearly observable that among the three glasses, Lithosil glass provides roughest surface [Fig. 4.11(a)]. The R_a of the surfaces shown in Fig. 4.11 was measured using a profilometer and found to be 35.9 nm for Lithosil, 12.79 nm for BK7 glass and 26.6 nm in case of N-SF14 glass material at the same grinding condition, i.e. axial depth of cut 2 µm and feed rate 1 µm/min.

Finally, using the optimum settings of PCD tool dressing and micro grinding conditions, micro-features were machined in BK7 glass. Fig. 4.12 shows the machining of characters

"N" and M" using micro grinding process with the on-machine fabricated PCD tool. It can be observed that the surface generated in the machined slots is smooth and clear from any adhesion of chips. The average surface roughness on the pockets is measured about 12 nm.

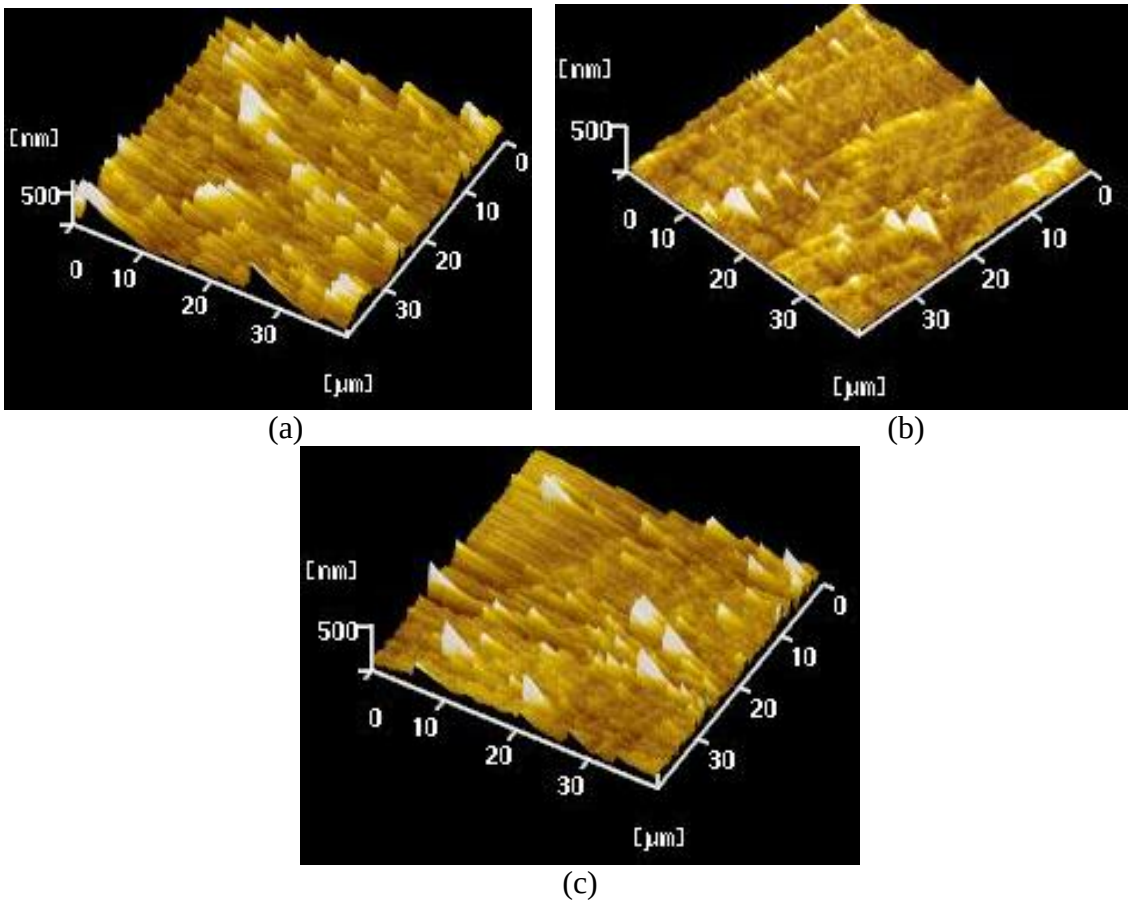

Fig.4. 11: Comparison of 3D surface texture (at d.o.c.: 2 µm, f: 1 µm/min) of (a) Lithosil, (b) BK7 and (c) N-SF14 glasses obtained by AFM

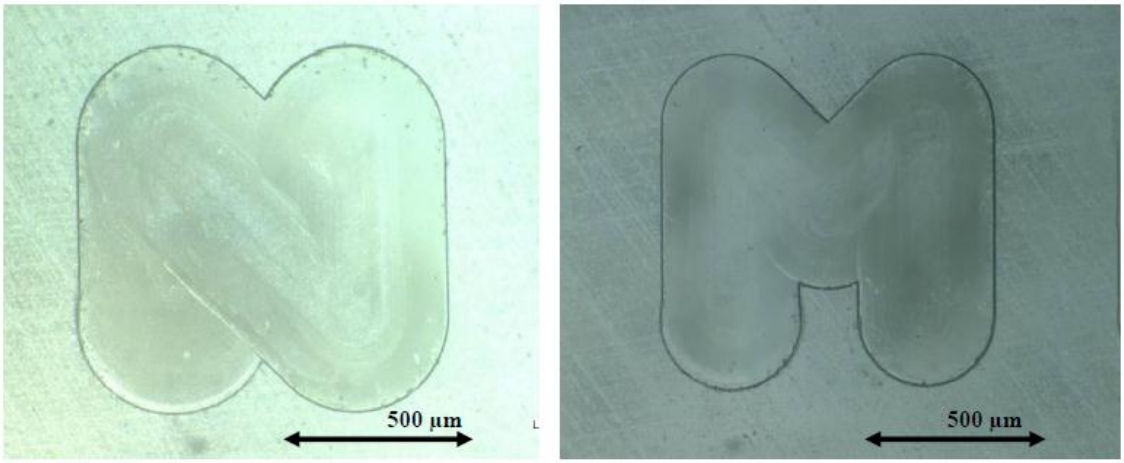

(a) (b)

Fig.4. 12: Fabrication of "N" and "M" slots on BK7 glass using micro-grinding process with on-machine fabricated PCD tool

4.6 Concluding Remarks

A comparative analysis on the micro-grinding performance of three commonly used glass materials: Lithosil, BK7 and N-SF14 glass was carried out using an on-machine fabricated PCD tool. The effect of micro-EDM conditions on tool fabrication, and its performance during microgrinding was studied. In addition, the effects of grinding parameters on cutting forces and surface roughness were investigated. Following conclusions can be drawn from this experimental investigation:

- The micro-EDM parameters have significant influence on the surface roughness and performance of the fabricated PCD tool during glass micro-grinding. Considering the machining time, optimum parameters for micro-EDM was found to be 120 V, 1000 pF and 30 µm feed length. Nevertheless, better surface roughness required the consideration of lower energy level. During the fabrication of PCD tool using micro-EDM, lower discharge energy produces smooth surface

on the PCD tool, which generates smaller chips on the glass surface during microgrinding and eventually generates better surface finish.

- The increase of axial depth of cut and feed rate results in increase of cutting forces along all axes, although some variations of forces are observed. Surface roughness was found to increase with the increase of axial depth of cut and feed rate. An axial depth of cut of 2 µm and feed rate of 1 µm/min was found to be optimum in terms of cutting forces and achieved surface finish.
- The cutting force is higher in case of Lithosil glass followed by BK7 compared to N-SF14. The BK7 glass showed intermediate behaviour by generating moderately lower cutting forces and causing lesser adhesion of glass chips at the bottom of PCD tool.
- For the slots machined by micro grinding using PCD tool, surface roughness is lowest at the middle of the slot with an increasing trend along the corners of the slots. In addition, some traces of scratching and dragging track was observed at the middle portion of the machined slot, especially in N-SF14 glass materials, as brittle mode cutting regime was found to dominate in this region.
- BK7 glass has better machinability during micro grinding with on-machine fabricated PCD tool based on cutting force and surface roughness analysis. Finally, smooth and defect-free surface with lowest average surface roughness of 12.79 nm has been achieved in the micro grinding of BK7 glass using micro-EDM-fabricated PCD tool.

Chapter 5

Effects of Cutting Tool Geometry on the Glass Micro-grinding Process

5.1. Introduction

Due to heavy industrial demand of three-dimensional complex micro-shapes, fabrication of different shape tool has got importance in addition to commercial ones. Generally, it has two purposes; on machine fabrication minimizes clamping error, and freedom of desired shape and size of tool. Several methods are available to meet these requirements. Among these methods, focused ion beam, mechanical diamond grinding and diamond turning have been most extensively used (Nakazawa, 1994). However, the fabrication of such tools by diamond grinding gives rise to difficulties, associated with high cost of diamond wheel due to large consumption of diamond. Besides this, diamond grinding is characterized by significant mechanical and thermal impact on the work piece resulting in the formation of split and flaw (Mamalis et al., 2004). As a result, conventional tool fabrication processes including grinding and turning which apply large force to work piece cannot be applied due to low strength of small sized tool (Egashira and Mizutani, 2002). In addition to this, focused ion beam is problematic as it has Gaussian distribution that causes material removal at the axis of beam rather than around the periphery (Friedrich et al., 1997). On the other hand, whereas the efficiency of traditional cutting processes is limited by the mechanical properties of the processed material and the complexities of work piece geometry, electro discharge machining is not subjected to such restrains. EDM, now a day is extensively and successfully applied for difficult-to-cut material (Mamalis et al., 2004). Concerted research efforts have been directed towards the development of fabrications technologies for micro-electrodes using micro-EDM. Among all these methods, wire electro-discharge grinding (WEDG) method, mesh method, EDM block method, LIGA and other micromechanical machining method are commonly practiced. The block EDM method has been extensively used due to its lower

investment cost and easy set up. More importantly, it makes possible on-machine fabrication of electrode, which reduces electrode installation cost and error (Nachiappan Ravi, 2002). In addition to this, with micro EDM technology, there is no direct contact between electrode and work piece, thus eliminating mechanical stress, chatter and vibration problems (Jung-Chou and et al., 2006). In our previous work, we have used block EDM method only for shaping circular tool using simple tungsten block (Perveen et al.). Different geometry of tool has not been tried and is not possible with that tungsten block even. Therefore, in this study modification of block EDM method for fabricating electrodes of various shapes has been chosen and with those on machine fabricated electrodes, micro-features of different types can be fabricated on glass. Although numerous researches have been conducted on grinding of glasses and silica using commercially available diamond grinding wheels (Gao et al., 2009; Sun et al., 2006; Takahashi and Funkenbusch, 2000), the application of micro PCD rod has not yet been studied extensively. A number of issues remain to be solved before the micro-grinding of glass using PCD tool becomes a well-accepted process, especially in industries. Moreover, extensive researches on the selection of optimum tool geometry for improved surface finish, reduced cutting forces, and less wear are still scarce. Hence, this chapter intends to investigate the possibility of fabricating PCD tools of different geometry using block-EDM process for glass micro grinding. Moreover, the effect of tool geometry on cutting forces, achieved surface finish and tool wear during the micro grinding of BK7 glass has also been studied.

5.2. Methodology

For the fabrication of different geometry tool, specially prepared fixture is required to use. The block containing three v-slots was designed and manufactured by wire EDM. Prior to using PCD tools for micro grinding, the tool was first fabricated with a two-step process using block micro-block EDM and scanning micro-EDM with a polished flat surface. The use of a specially designed conductive block as a tool electrode and the PCD

rod as a work piece in block-µEDM has been identified as a useful approach for producing microelectrodes of different shapes due to its low investment cost and quick set-up rather then WEDG. A tungsten block of higher wear resistance was used for this specially designed block fabrication, which is used for PCD tool fabrication later on. During the tool fabrication process, the tool was set in positive polarity and the tungsten block was used as negative polarity. When a voltage is applied between the rod and block, an intermittent spark occurs between the inter-electrodes gap. Subsequently, the spark caused a rise in the surface temperature of both the block and the rod to a point where the temperature exceeded the melting point of the materials. Consequently, a small amount of material is removed from both the electrodes and flushed away from the machine zone using side flushing. In this process, varying capacitance and voltage can control surface roughness. Side surface of tool was prepared using 1000pF and 100V, for bottom surface 100v and 100pF was used. After the fabrication of PCD tool with desired shape and surface finish using block-EDM, the tool was used for glass grinding on the same machine without changing the tool from collet. During glass micro-grinding, the specimen was mounted on top of a three–component force dynamometer (KISTLER type 9345) fixed on the machine table. The dynamometer was connected to a charge amplifier (KISTLER type 5007) from which the output voltage signals were fed into a digital data recorder and the signals were recorded at a sampling frequency of 180 KHz. Thereafter, average diameter and length of the microelectrodes were measured and examined using Keyence optical microscope and SEM.

5.3 Fabrication of Different Geometry of Micro tools in Single Setup

5.3.1 Design and Fabrication of Fixture

For the fabrication of square, circular, D-shape, triangular, conical shape tool of 60º, 90º and 120º, a fixture was manufactured which made possible the fabrication of all these shapes in single set up. For this purpose, Makino conventional horizontal wire EDM

machine was used, the ultra-high accuracy UPJ-2 automatically threads and machines with wire as small as 0.00078 inches (0.02 mm) in diameter. Wire EDM conditions were automatically fixed by the wire material and diameter and work piece material and thickness. In this case, brass wire of 200µm diameter and work piece material of WC (3mm cut thickness) was used. Angles of these V-shapes were determined to be 60º, 90º, and 120º respectively. Fabricated block is shown in Fig.5.1. Fig.5.2 illustrates the schematic of this fixture along with the tool for fabricating triangular, conical and square microelectrodes.

Fig.5. 1: Specifically designed block**.**

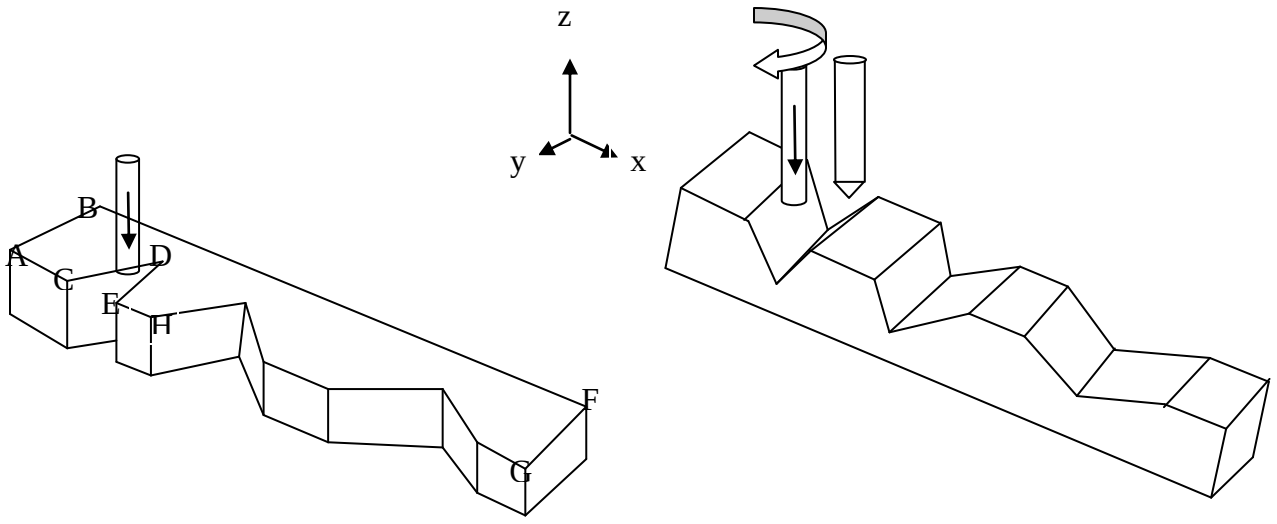

(a) (b)

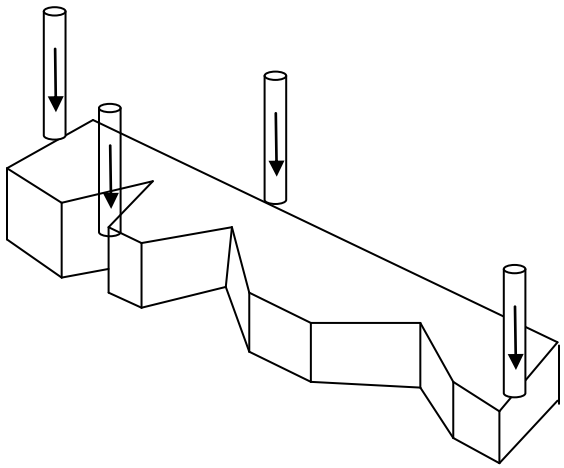

(c)

Fig.5. 2: Schematic diagram (a) Before machining PCD rod along with fixture prepared by wire EDM for triangular microelectrode (b) same fixture in different orientation for conical micro-electrode preparation(c) fixture orientation for square and D-shaped tool.

5.3.2 Fabrication of Microelectrode for Micro-grinding Glass

Microelectrodes of symmetrical and non-symmetrical sections can be fabricated using this specially designed block. Unlike conventional EDM machining, it is critical to carry out micro-machining in EDM system with a few machining passes, as a high volume of material removal in a single step may lead to electrode breakage, especially when required electrode size is of micron level. The above-mentioned technique has been used for fabricating symmetrical electrode using indexing attachment with transistor type circuit and with tungsten tool electrode (Nachiappan Ravi, 2002). The authors suggested setting the micromachining in Z direction rather than Y direction to reduce the machining contact area and electrode breakage. The basic of block micro-EDM will be the same here in this study; only change is to use one fixture of desired shape. Fig.5.2 shows the methodology of fabricating microelectrodes with different shapes and cross sections. As demonstrated in Fig.5.2 (a), the rod electrode was feed downward from CD edge to the required feed length in Z direction along the face of triangular slot without tool rotation.

Few passes was required to remove the material to have desired electrode shape. From mechanical drawing the number of passes was calculated and dimension of tool was checked using camera during machining. Once one face of the triangle was prepared, and then next DE edge of triangular slot was used to fabricate another face. Finally, BF edge was used to get the third face of triangular tool. Thus, using this method, fabrication of equilateral triangle and triangle with others angles too are possible.

Next for making conical tool, 3 slots of 60º 90º and 120º were already cut in the tungsten block. For conical tool, the same block was tilted to 90°. Slope of these triangular slots were used to fabricate different angle conical tool. In Fig.5.2 (b), PCD rod with rotation was feed along the slop in Z direction. After one pass was finished, tool was moved along Y-axis to have fresh place of cut and then next pass along Z-axis started. Hence, in this way, conical tools of 3 different angles were possible to fabricate. In addition to this, AB, EH, BF, and FG edge of the same block were used to fabricate square tool without tool rotation. Moreover, any of the edges like AB or BF can be used to fabricate circular tool with tool rotation. When tool was given feed along Z direction without rotation, D-shaped tool was possible to fabricate. Thus, using this same block, it is possible to fabricate triangular, square, conical, circular and D-shaped tool. Fig.5.3 showed the fabricated tools using this specifically designed block.

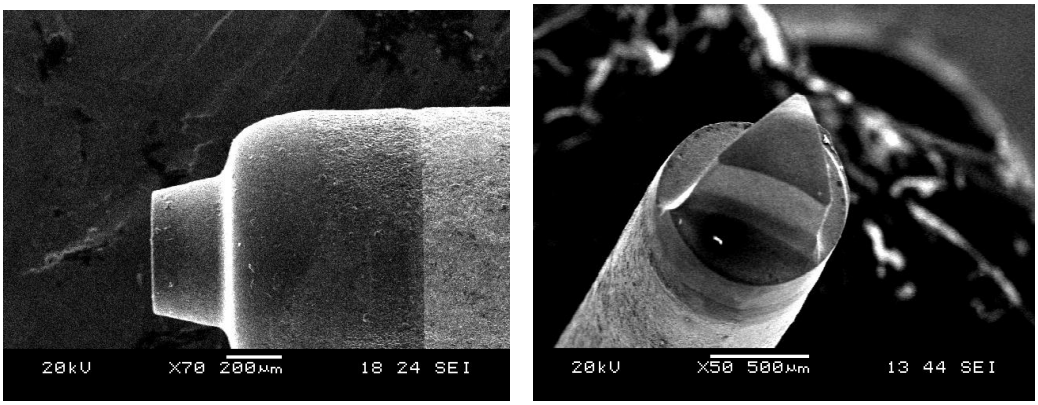

(a) (b)

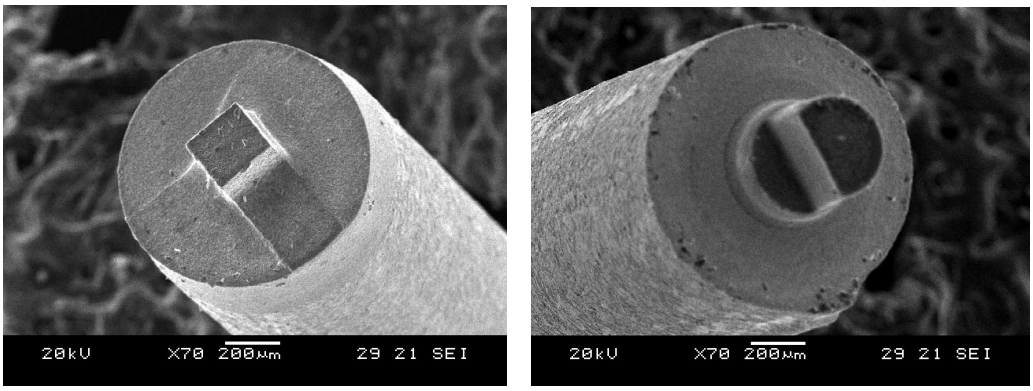

(a) (d)

Fig.5. 3: (a) Circular tool (b) triangular tool (c) square tool (d) D-shaped tool.

5.4. Comparison on Micro-grinding Performance of Different Shape Tool on BK7 Glass

5.4.1 Comparison of Cutting Forces

Brittle material like glass is very problematic to mechanically micro machine due to damage resulting from material removal by brittle fracture, cutting force induced tool deflection or breakage and tool wear. The forces arise from micromachining processes need important consideration as it can affect the material removal rate, surface finish and dimension of the microstructure. The following section will present a comparative analysis of cutting forces generated along all three axes during micro-grinding of BK7, glass using on-machine fabricated four different shaped PCD tool. The cutting conditions (depth of cut=2 µm, feed rate=25 µm/min, spindle speed=2000 rpm) remain same for all experiments. In addition, the effect of cutting geometry on the grinding forces and surface finish of the glass has been investigated. The analysis of cutting forces has been carried out for four different tools geometry like circular, triangular, square and D-shape tool. Fig.5.4(a), (b), (c), (d), (e), (f), (g), (h), (i), (j) (k), (l) showed the cutting force for the above mentioned tools.

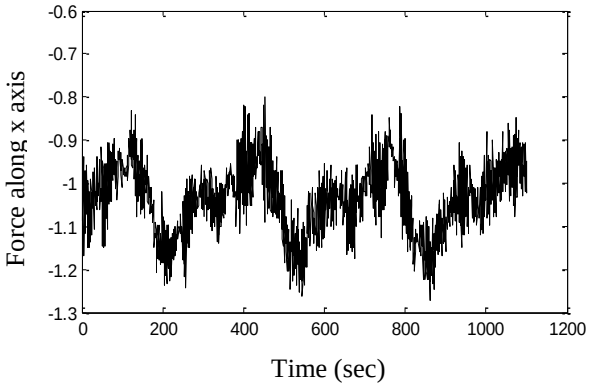
Force along x axis
Time (sec)

(a)

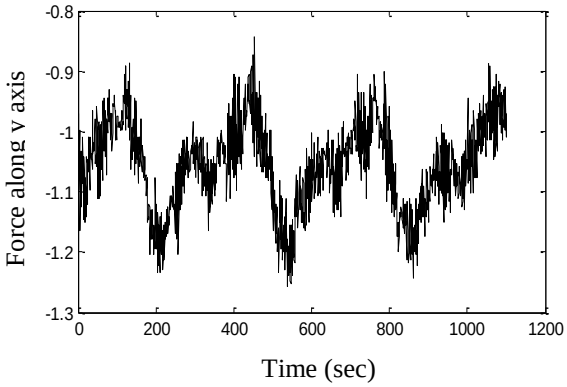
Force along v axis
Time (sec)

(b)

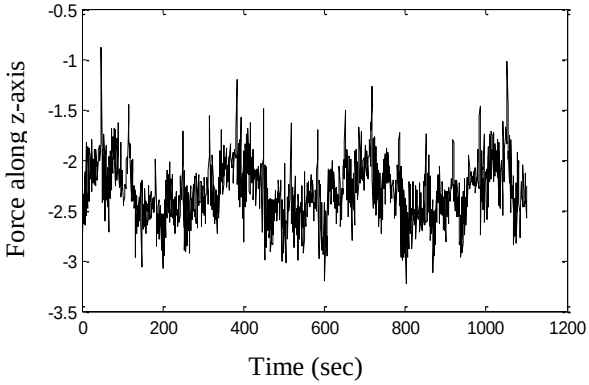
Force along z-axis
Time (sec)

(c)

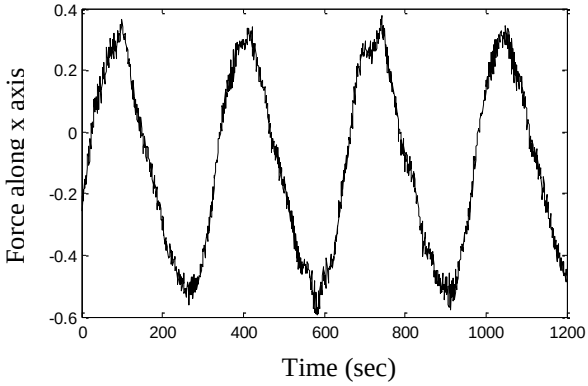
Force along x axis
Time (sec)

(d)

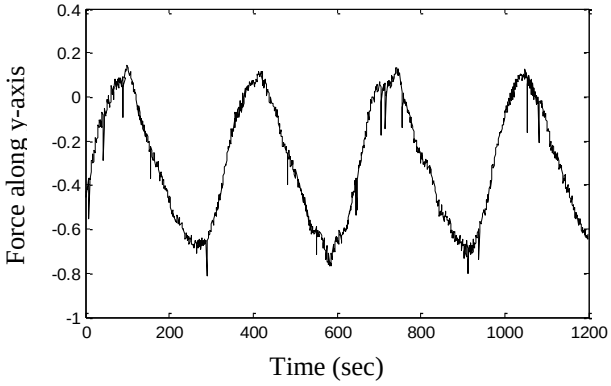
Force along y-axis
Time (sec)

(e)

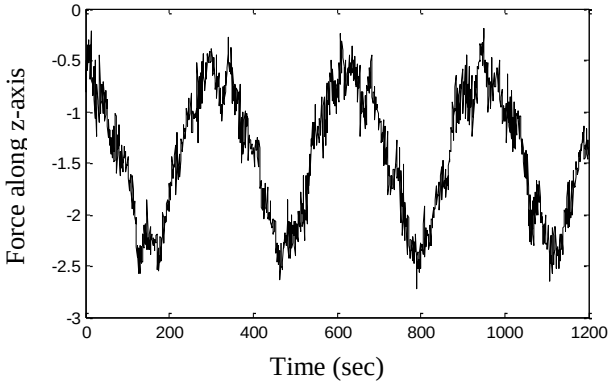
Force along z-axis
Time (sec)

(f)

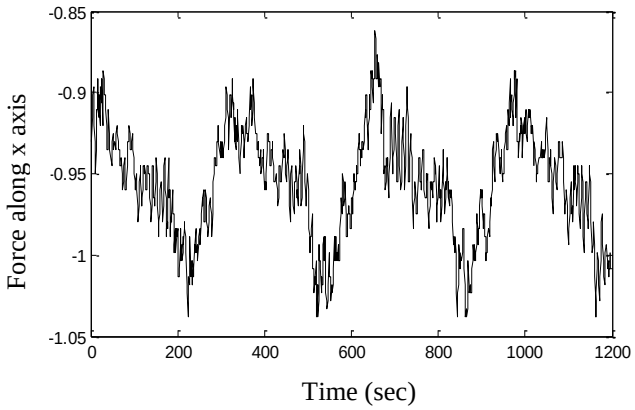
Force along x axis
Time (sec)

(g)

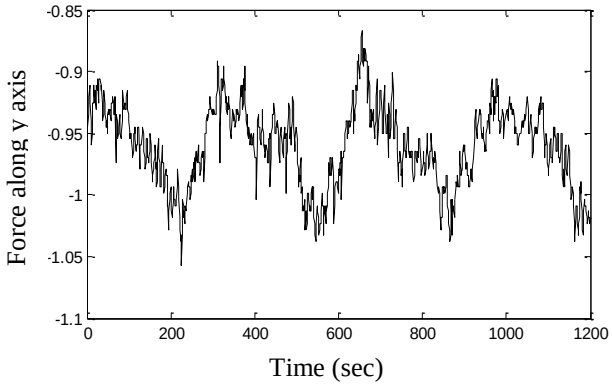
Force along y axis
Time (sec)

(h)

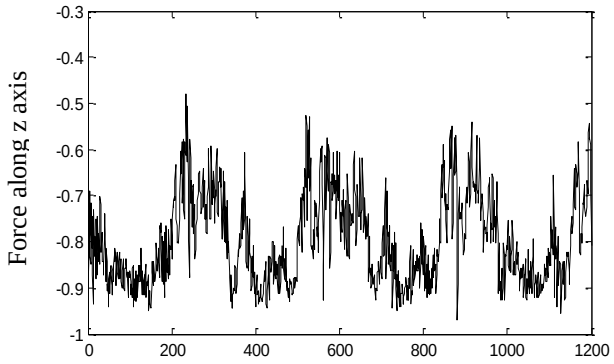
Force along z axis
Time (sec)

(i)

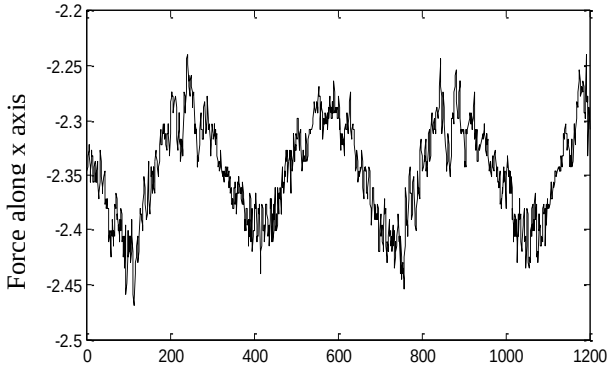
Force along x axis
Time (sec)

(j)

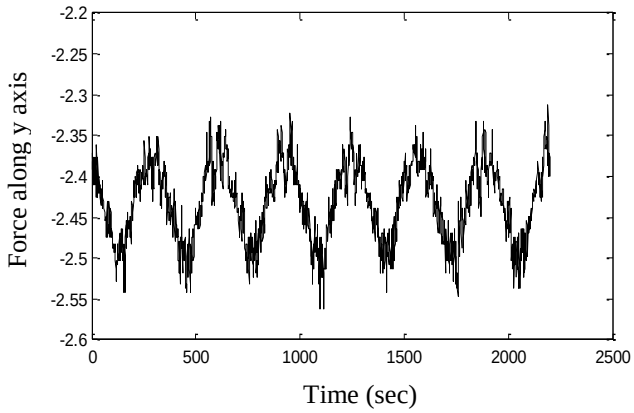
Force along y axis
Time (sec)

(k)

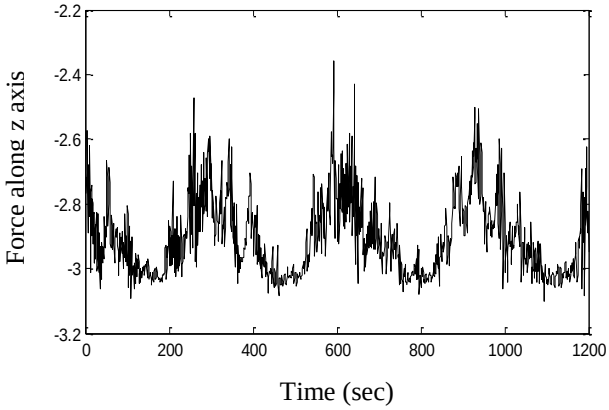
Force along z axis
Time (sec)

(l)

Fig.5. 4: (a),(b),(c) cutting force for circular tool(d)(f)(g) cutting force for d-shape tool (e)(h) (g) cutting force for triangular tool (i)(j)(k)(l) cutting force for square tool.

With the change of cutting tool shape, how the cutting force along three axes has changed can be seen from Fig.5.4. From the cutting force vs. time curves it has been found that cutting force for D-shape tool is quite different from other tools. Discontinuous cutting was observed for D-shape tool (throughout the whole cycle it does not remove material, when the D-shape is on the opposite to feed direction it does not remove any material at that time), which results zero point force in curve. For one full rotation, it removes material during half rotation and during rest half rotation removes chips. Hence, due to its shape chip removal becomes easier in case of D-shape tool. On the other hand, square tool cut with 2 or 3 edges at the same time and triangular tool cut using 1 or 2 cutting edges at the same time. In fact, the 3 and 4 edges of triangular and square tool work like single point cutting tool. So cutting process become intermittent for these two tools. In addition, circular tool exhibited continuous material cutting using its periphery consisted of diamond grains. All of the force curves are sinusoidal though they have some difference in their pattern, which indicates the difference in cutting process due to different geometry of tool. For example, in case of circular tool cutting force curve, every cyclic pattern consists of small small cycle due to the stochastic nature of cutting using infinite numbers of diamond cutting edge. That is why lots of peaks are observed on the curve. In fact, rake angle is changing from 0° at side surface to 90° at middle of the surface for circular tool but there is no clearance for chip removal. When the tool become machined to D-shape, force pattern become so sharp still possessing some peak. For D-shape tool, rake angle is varying like circular one, but clearance area for chip removal has been facilitated due to its shape. In case of square tool, crown like sinusoidal force curve along axes with lots of peak has been found. Along with material removal by the edge, side surface can sweep the chip away from the machined area.

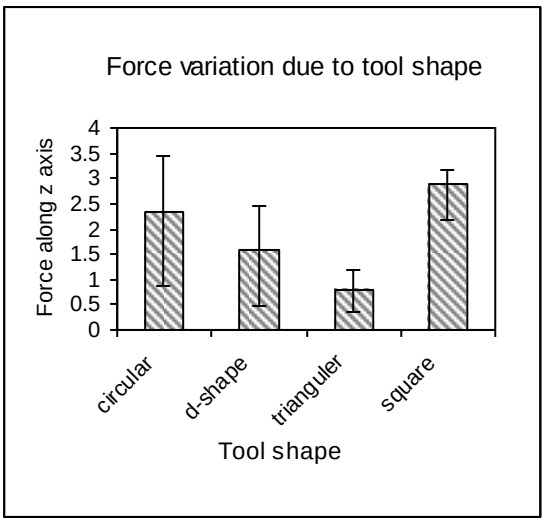

(a)

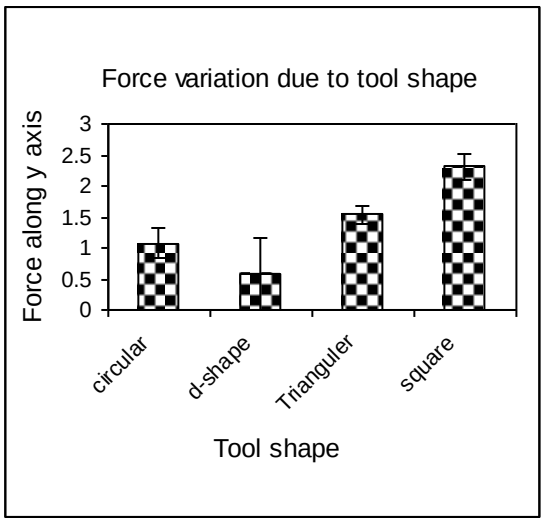

(b)

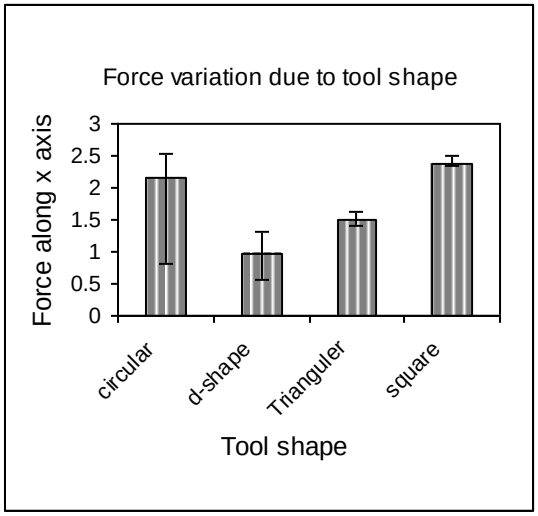

(c)

Fig.5. 5: Average, minimum, and maximum cutting force (a) along X axis (b) along Y axis (c) along Z axis for different geometry tool.

Fig.5.5 (a) (b) and (c) shows average, maximum, and minimum force data for same cutting condition for different shape tools. Error bar was used in the figure to indicate the minimum and maximum force experienced by these tools. From average force data, it was found that average forces along three axes for square tool were higher than other

shaped tools. To the contrary, D-shaped tool experienced lower force in all axes compared to others. In addition, force experienced by circular tool along Z and X-axis are also comparatively higher than other tools but little smaller than square tool. For the same cutting conditions, force along Z axis showed decreasing tendency form circular tool to D-shape tool and triangular tool and then increases again for square shape. On the other hand, force along X and Y-axis showed decreasing trend from circular to d-shaped tool and then increasing tendency from triangular to square tool. Higher cutting force along Z-axis resulted in the more bending effect for square tool then other tools. While observing force variation e.g. maximum and minimum force, it was found that circular and D-shape tool experienced variation higher than rest of the two tools. This is probably due to the stochastic nature of cutting in case of circular and d-shape tool. Triangular and square tool has defined geometry and therefore they only cut with their three or four edges. At the same time in case of triangular or square tool two or three edge are taking part in cutting process. These edges consist of diamond grains, which stand in straight line along edge. Moreover, chip removal is easier for these tools compared to circular tool. Hence, chip loading on these tools will be comparatively less then circular tool. As a result, variation of force for square and triangular is less than others. On the other hand, circular and D-shape tool surface consist of non-countable diamond grains. Circular tool removes material from the surface continuously whereas, D-shape tool remove material during half cycle. Hence chip removal is also easier for D-shape tool. Even that due to stochastic nature of cutting, variation of force is higher for these two tools. Significantly reduced amount of cutting force can be observed for the D shaped. Its chip clearance space is higher compared to circular, triangular and square tool. As the D shape tool removes material in half cycle while the other half cycle it clears the chip from the surface, the occurrence of additional force due to chip attachment on the surface is reduced. For circular tool, it removes material continuously throughout the whole cycle and does not have clearance for chip removal, so that some chip adheres on the machined surface. For triangular and square tool, they also cut intermittently and these tools also

have some clearance space for chip removal as well but not as good as that with the D shape tool.

5.4.2 Comparison of Surface Roughness

Surface roughness is a measure of texture of a surface. It is quantified by the vertical deviations of a real surface from its ideal form. If these deviations are large, the surface is rough; if they are small the surface is smooth. Surface roughness of the machined surface was measured using Atomic Force Microscopy (AFM), Taylor Hobson Profilometer. In addition, optical image of machined surface using different shape tool was also taken to compare the cutting mode (ductile or brittle). From optical images in Fig.5.8, it can be observed that ductile mode cutting was dominant for all four different type tools. Surface roughness has been improved much using D-shape, triangular and square tool rather than circular. Fig.5.6 shows a comparison of 3D surface topography of the machined surface using different shaped PCD tool. From AFM images of machined surface, it is clearly seen that how the surface has experienced transition with the change of the cutting edge shape. It has been observed that, except circular PCD tool, the surfaces generated by other tools are comparatively smoother. Surface machined by circular tool contains small small particle throughout the whole area, which are absent on the surface machined by others tools. Except circular tool, all the tools have some clearance space which facilities easy chips removal. Chips removed by the circular tool have the higher chance of being paste on the machined surface again due to continuous cutting. Hence, this might be due to easy chip removal for other tools rather than circular one, although the entire surfaces still have some scattered sudden peak here and there. Moreover, these peaks are prominent for the all the tool except circular one. During machining, materials adjacent to the tool edge are immediately compressed and displaced upward form the bulk work pieces. As the tool is further advanced more material along the cutting path is displaced on the tool edge with a change in direction according to the degree of curve radius.

Therefore, these high peaks are becoming noticeable in case of square triangular and D-shape tool (Soon, 2009).

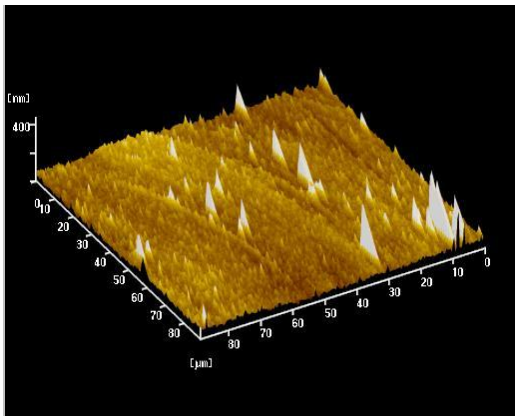

(a)

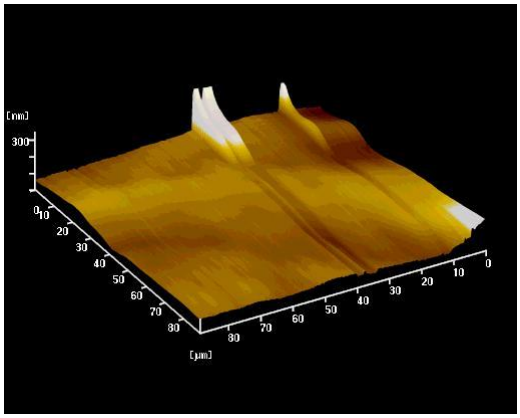

(b)

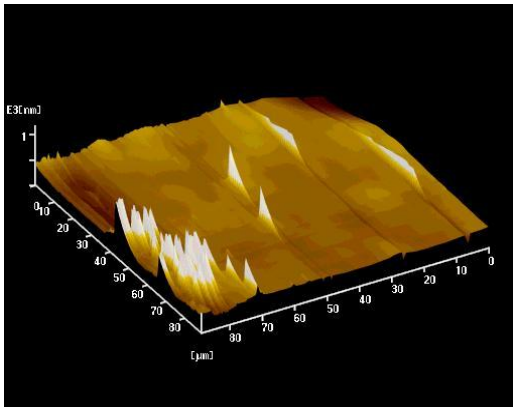

(c)

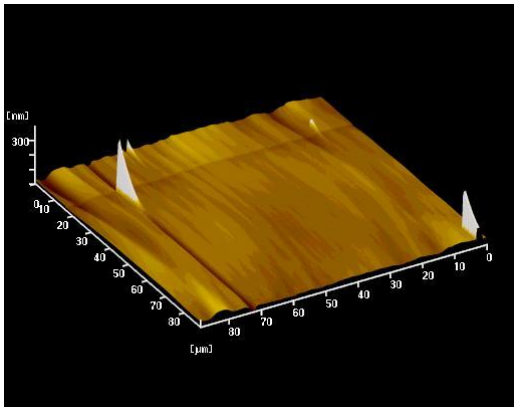

(d)

Fig.5. 6: AFM image of machined surface using (a) Circular shape (b) D-shape (c) Triangular tool (d) Square tool.

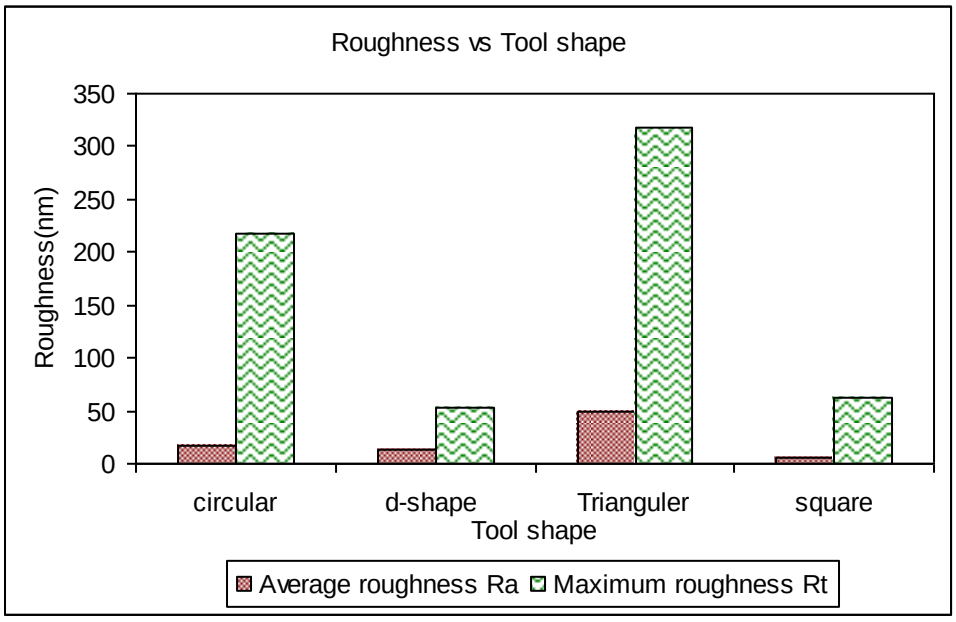

Fig.5. 7: Surface roughness value for different tool.

A comparison of average surface roughness and maximum roughness values of machined surface are shown in Fig.5.7. It was found that average roughness of the machined surface has been improved a little form circular tool to d- shape and square tool. Surface machined by triangular tool has higher average and maximum roughness than the rest. The reason behind this higher roughness is the sudden peak density, which is higher in case of surface machined by triangular tool.

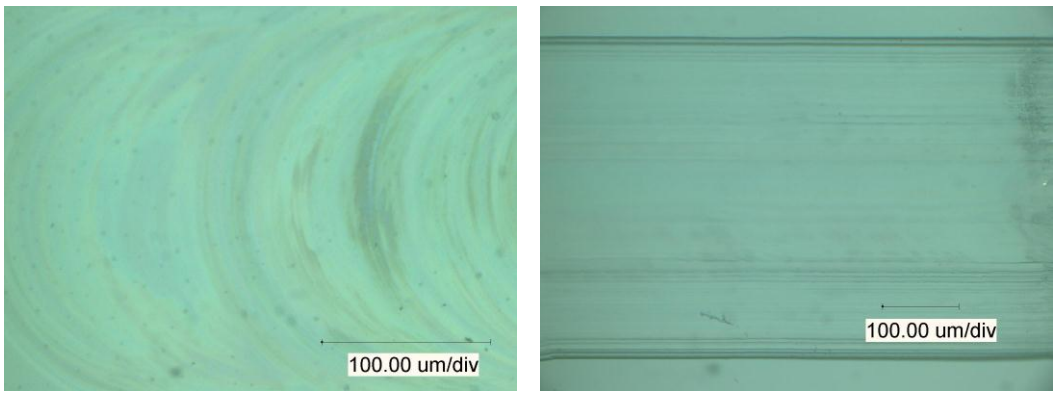

(a) (b)

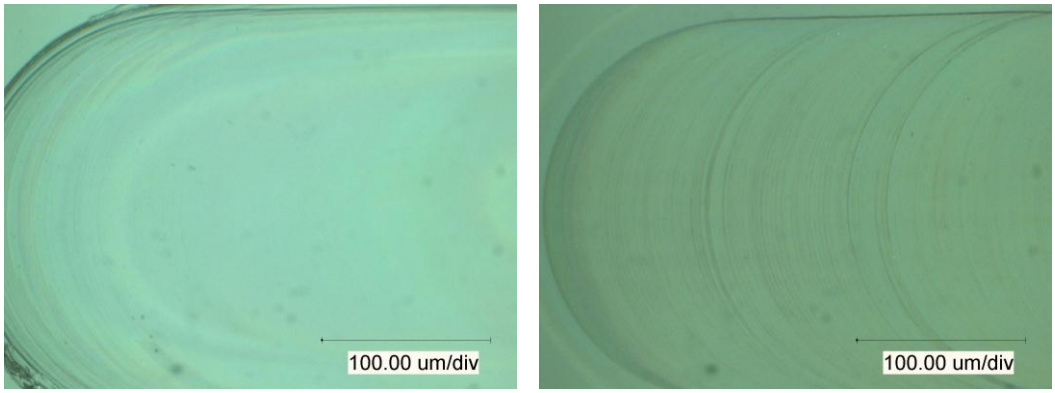

Fig.5. 8: Optical image of ground surface by (a) Circular (b) D-shape (c) Triangular (d) Square tool.

Fig.5.8 showed the optical images of ground surface for different tool geometry. It was observable from the optical images that all four tools produced ground surface with better roughness. Some grinding marks were also present on the surface as well. Magnified image of side of the grooves were also presented in Fig.5.9. For surface ground by circular tool side seemed reasonably straight even in higher magnification. For D-shape tool, the edge of the micro-slots became deteriorate at some position. Side flow of glass material has been found. The edge of micro slot machined by triangular tool was found to be worst among all. Usually, material around the cutting edge was subjected to high pressure which causes the material to flow to the side. The similar phenomenon can be observed in case of machining with blunt tool edge, which tries to remove more material from the side surface than a sharp edged tool. Comparatively larger radiuses of curvature at the edge of the slots are the typical proof of the phenomenon. In addition, the edge surface machined by square tool also had some waviness as well but with lower curvature than that of triangular tool. Moreover, this side surface phenomenon was not present throughout the whole groove rather it appeared suddenly on the machined grooves. Among all the surfaces, the ground surface with triangular shaped PCD tool suffered more rounding in edge of the micro-slots, thus providing inferior surface finish at the side

wall of the slots. Brittle and amorphous properties of glass material can also contribute to this side flow behavior (Liu and Melkote, 2006).

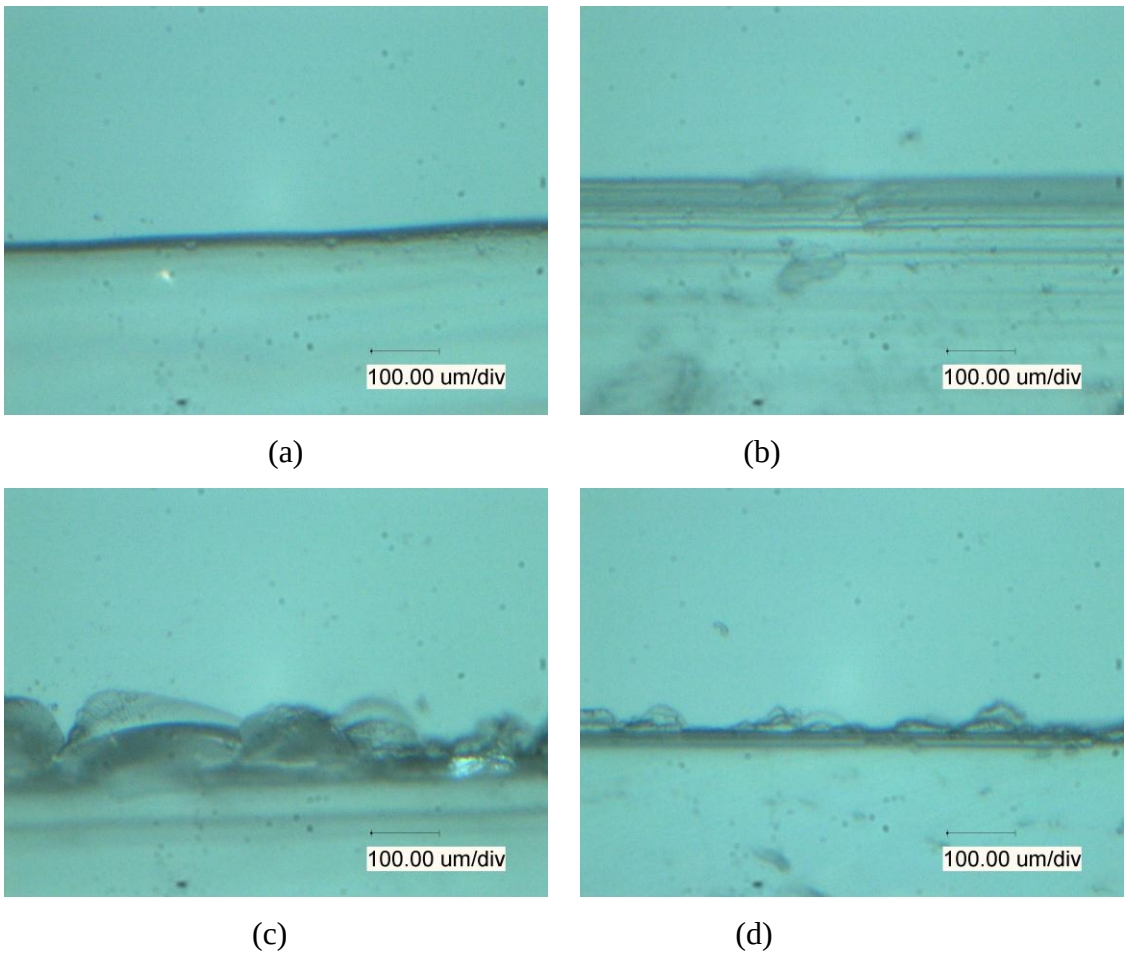

Fig.5. 9: Optical image of side surface of ground groove by (a) Circular (b) D-shape (c) Triangular (d) Square tool.

5.4.3 Comparison of Tool Wears

Fig.5.10 shows a comparison of different shaped PCD tool surface after grinding micro-slots in the glass material. From the SEM picture of tools in Fig.5.10 after machining, it was found that all shaped tool except circular one had the tendency of wearing more. This was basically due to the sharp edge of the tool suffered more wear and became round. When circular tool experienced wear or re-sharpening, it became smaller in diameter but

still become round. Hence, a worn out circular tool did not affect the machining performance significantly. On the other hand, when the edges of square or triangular tool experienced wear, wear is usually non-uniform as all the four or three edges cannot wear out at the same rate. For the shaped tool it was found that edge rounding or pull out of grain was the main wear mechanism. At the same time machining condition varied form sharp edge to round edge. In contrast to conventional sharp edge cutting model, chip shearing in micromachining occurs along the rounded tool edge. Therefore, this large edge radius affects the magnitude of ploughing and shearing forces. Higher plastic deformation resulted from larger cutting edge radius. As a result, surface roughness as well as cutting force kept changing with this wears of square and triangular tool(Kim and Kim, 1995).

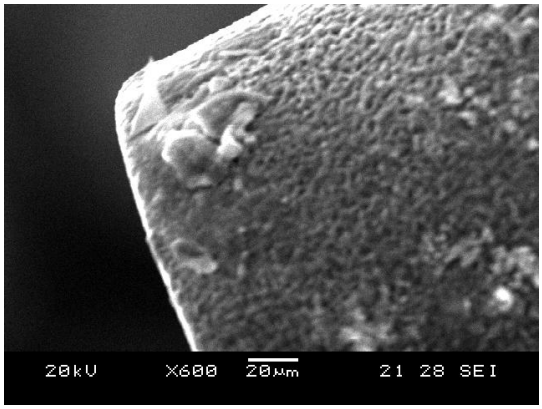

(a)

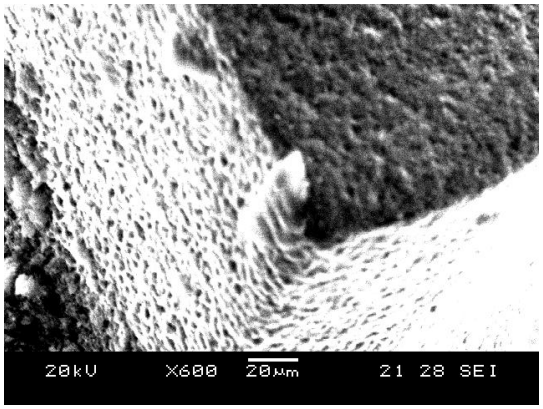

(b)

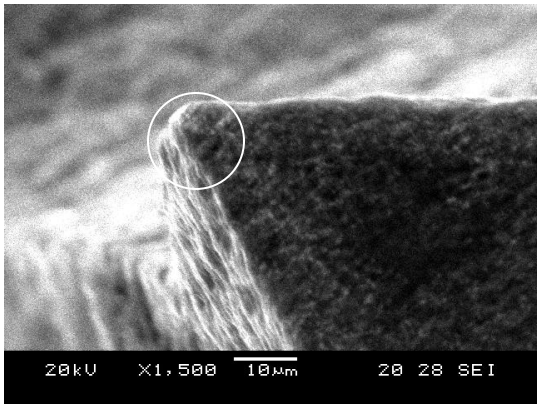

(b)

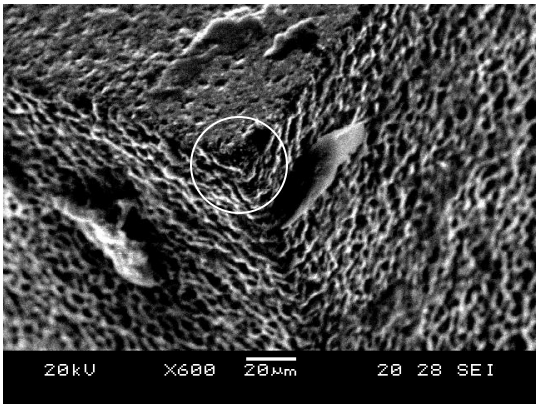

(d)

Fig.5. 10: SEM image of Tool after machining (a) Circular (b) D-shape (c) Triangular (d) Square tool.

5.5. Concluding Remarks

In this study a comparative analysis on the micro-machining performance of four different geometry PCD tools: circular, D-shaped, triangular, and square on BK- glass was carried out. In addition, the effect of tool geometry on the cutting forces surface roughness and tool wear were investigated during the glass micro-machining. Following conclusions can be drawn from this experimental investigation:

- With the aim of fabricating different shaped tool in a single setup, a specially designed block containing three 'v-slots' has been designed and fabricated using wire cut. With the concept of block micro-EDM and using this specifically designed block, microelectrodes of conical, triangular, square or rectangular, circular and D-shaped tool have been fabricated. Using this specifically designed block has been established to be a feasible method for the fabrication of microelectrodes of few tens micrometer.
- D-shaped tool experienced lowest cutting force along X and Y-axis, whereas triangular tool has experienced lowest force along Z-axes. Both square and circular tool had generated quite high cutting forces along Z and X-axis during micro-grinding, though along all axes square tool had experienced highest cutting force. Comparatively lower cutting force along Y-axis has been observed for triangular tool than square one.
- For the groove machined by micro-grinding using PCD tool, surface roughness showed considerable change from circular tool to others. Small small particles, which were present on the surface machined by circular tool, was almost absence in case of surface machined by other tools. Lowest average surface roughness has been achieved using square tool and little higher in case of d-shape tool. Due to

higher peak density on the machined surface by triangular tool resulted in higher average and maximum surface roughness. Moreover, side surface of machined groove using d-shape tool was much better than square or triangular tool, whereas circular tool demonstrated the best result.

- ❖ Square and triangular tool experienced more wear compared to circular and D-shaped tool due to the tendency of tool edge blunting
- ❖ Finally, D-shape tool demonstrated better performances among all the tools in terms of cutting force, roughness value, side surface and wear rate due to its geometry, which enhances the chip removal process form the machined surface.

Chapter 6

Analysis and Monitoring of Wear of PCD Micro-tool

6.1. Introduction

One major problem of glass micro grinding is the tool wear caused by the hardness of material. The tool wear process can be divided into three main wear mode, namely Attritions wear, grain fracture, and bond fracture. Attritions wear involves dulling of abrasive grains and the growth of wear flats by rubbing against the work pieces. Grain fracture refers to the removal of abrasive fragments by fracture within the grain and bond fracture occurs by dislodging the abrasive from the binder (Malkin and Guo, 2008).
Recent researches on micro-grinding have been mainly focused on assessing its tool life and wear mechanism, since the performance of the micro grinding wheel is more sensitive to the tool wear than those of conventional size. The tools wear of electroplated micro-grinding wheels in side grinding of porcelain and zirconia was investigated by Ohomori et al.(Yin et al., 2004).The wear mechanism of the metal bonded micro grinding wheel in end grinding of Zirconia was studied by Feng et al(Feng, 2007). Onikura et al. investigated its performance in end grinding of silicon suggesting that electroplated micro-grinding wheel wears too fast for the practical applications (Onikura, 2003). Luo et al. analyzed the wear of resin bond diamond wheel while grinding of tungsten carbide and found that interrupted cutting causes higher grinding ratio while continuous cutting causes poor grinding performance (Luo et al., 1997). Bai et al. (Bai et al., 2004) and Philbin et al. (Philbin and Gordon, 2005) has studied the wear mechanism of PCD cutter for laminated floor and wood based composites.

However in practice, ductile regime machining of glass material is often limited by rapid wear of diamond tools. Although a diamond tool can be used to cut nonferrous metals such as aluminum and copper for a distance up to a few hundreds of kilometers,(Hamada,

1985) when cutting glass an initially sharp tool will wear and become worn out rapidly. As the geometry of the contact zone between tool and the work pieces is extremely important for the attainment of perfect geometric shape, the wear of the diamond tool become a limiting factor in developing machining process for glass. Tool wear not only raises machining cost but also degrades product quality. The problem becomes particularly serious when machining large volume of components (C.K.Syn, April 1998). For this reason better understanding of the performance of the diamond tools in glass machining will result in significant production cost savings. Various researchers in the past have made their valuable contributions to the understanding of the process that take place when a diamond tool wears. However most of the work carried out has involved the wear of diamond tool in cutting metal materials. Up to date, there is very little literature available on the tool wear during glass micro-machining.

Therefore, this chapter describes some experimental results on the wear of diamond tools in during micro grinding test of BK7 glass. As a complete understanding of the wear of diamond tools can only follow understanding of the individual mechanism, this chapter is focused exclusively on the wear propagation of diamond tool during time consumed and their effect on the geometry of machined surface. The results involve the scanning electron process (SEM), white light interferometer image of machined surface and diamond tools as well as the measurement of surface roughness and cutting force. In addition to this, tool condition has been monitored using cutting force and AE signal to correlate these with tool wear.

6.2. Methodology

PCD tool was fabricated to 670 µm size using 100V and 100pF capacitance. During experiment, total 65 micro-channels of 1mm length were ground onto the Bk7 glass material using feed rate of 25 µm /mint, depth of cut 2 µm, spindle speed of 2000 rpm. Grinding forces and acoustic emission signal were recorded and optical images of tool

were taken in between the experiments. The goal of monitoring is to determine the patterns of process signals in monitoring the tool wear. The assessment of actual grinding tool wear was conducted by inspecting its topography and the channel geometry with FESEM and white light interferometer (Wyko NT2000). The white light interferometer has resolution of 0.1nm in vertical and 0.825µm in horizontal direction.

6.3. Results and Discussions

6.3.1. Tool wear pattern

In order to investigate the on machine fabricated PCD tool wear pattern during micro grinding of BK7 glass, several measurements are conducted to examine the tool geometry in the presence of tool wear. Firstly, average reduction in the tool diameter and length are measured which represent the change in the micro tool geometry caused by the tool wear. If the diameter of tool is difficult to measure, especially for online measurement, the width of the ground channel can be taken as a measure of the tool wear after the experiment. Here in this study, optical microscope (Motic Image) is used to measure the tool diameter and length in between the experiment. The diameter difference between subsequent channel grinding is assigned as radial tool wear. The major geometric change of tool is occurred due to the corner tool wear. Due to tool wear, both length and diameter reduction are found to take place. Fig.6.1 (a) and (b) have shown the actual diameter and length of tool decrement along with increasing number of channels. Basically during vertical micro-grinding, tool experiences corner wear which causes the rounding of tool at bottom portion also (Malkin and Guo, 2008). As a result, diameter of the tool starts to decrease. Interesting thing is observed that, when length reduction goes faster than diameter reduction, corner wear tends to reduce or almost diminishes sometimes. At the same time abrasive nature of glass material also contributes to the tool length wear as well as diameter reduction. As seen from Fig. 6.1(a), length wear of the tool has steeper slope initially then it becomes flattened a bit. This behavior indicates that initially tool

has suffered more wear and then it becomes lesser as the number of channels increase. It is also observed that the slope of radial tool wear curve is less steep than the slope of length wear curve. The reason might be the diminishing tendencies of radial wear along with the length wear increment. An illustration of typical radial PCD tool wear behavior is shown in Fig.6.1(c) as a plot of volumetric wear versus the accumulated metarial removal Vw. The wear behavior seen here is not so similar with other wear processes as seen in macro-grinding. Initially insginifacnt tool wear is followed by intermediate tool wear where wear rate increases steadyly. A third regime of accelerating wear as seen in Fig.6.1(c), usually indicates catestrophic wear situation and it requires the micro-tool redressing. Commonly used performance index to charecterize tool wear resistance is the grinding ratio, also reffered as G ratio or G, which is basically the volume of material removal per unit volume of wheel wear. This is usually expressed as follows.

$G = Vw/Vs$

Here the volume of radial wheel is measured using the formula $Vs = \prod d_s \Delta r b$, where Δr is the measured decrease in tool radius, ds is the mean of the tool diameter before and after wear has occured and b is the grinding width . In some cases, only for the steady state wear region , this value can be written as $G = \Delta Vw / \Delta Vs$. From Fig.6.1(c) this perticular value in this study is calculated to be nearly 904 in case of glass micro-grinding which is pretty good value according to those found in literature.

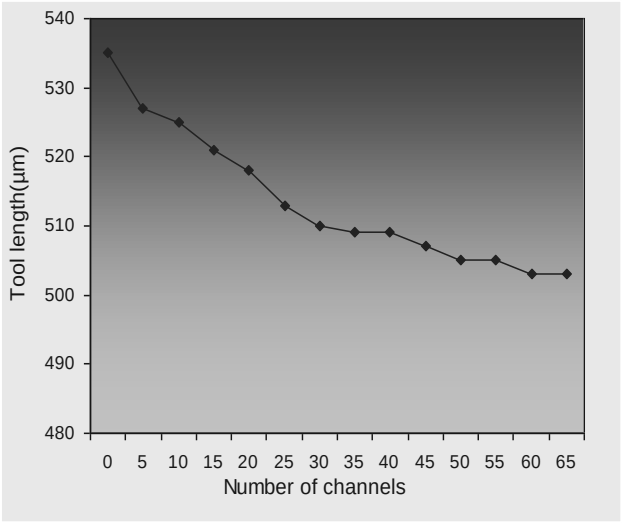
Tool length(µm)
540
530
520
510
500
490
480
0 5 10 15 20 25 30 35 40 45 50 55 60 65
Number of channels

(a)

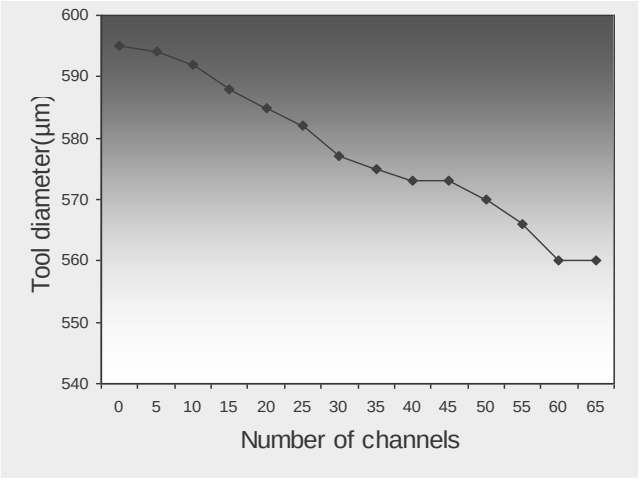
Tool diameter(µm)
600
590
580
570
560
550
540
0 5 10 15 20 25 30 35 40 45 50 55 60 65
Number of channels

(b)

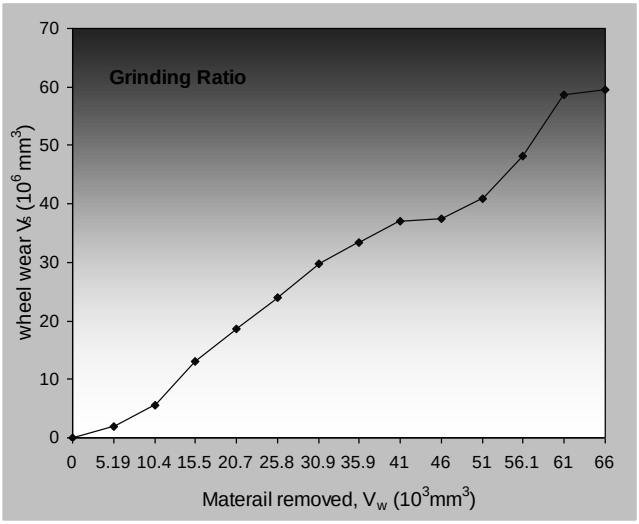

(c)

Fig.6. 1: (a) Tool length decrease (b) tool diameter decrease as the total number of slot no increase(c) Radial volumetric wear versus accumulated metarial removal.

Bottom of the tool before and after machining can be seen from Fig.6.2 (a) and (b) where grinding marks is found to be visible on the tool bottom after machining. Abrasion type of wear has been noticed to be dominating on the bottom of surface mainly. This wear is also the reason of radial wear and length reduction. Before machining the bottom of the tool does not contain any circular mark which is basically due to abrasive wear and circular motion of tool itself. Abrasive nature of glass also contributes to this wear. Hence, abrasive wear is the dominant PCD wear mode during micro-grinding of glass. While looking at higher magnification in Fig. 6.3, details of PCD tool morphology can be seen clearly. Arc pattern like wear land is found in Fig. 6.3(b) .This is being the typical abrasion wear. The cause of these appearances may be that the binder of the tool is abraded by silicon particles of the hard glass material, which leads PCD grains to be detached from the bond (Luo et al., 1999). Some hole is also found on the bottom of tool after grinding 30th and 65th channels due to the pull out of grain along with the bonding element. This void type of hole actually indicates the location where diamond grains were dislodged from the cutting edge. It is possible that diamond gain becomes weekend after abrasion of the cobalt binder around them, and then becomes dislodge from the tool edge when subjected to the intermittent cutting force while micro-grinding of glass. From Fig.

6.4(a) (b) and (c), it is found that with the increase of machining time tool side surface starts to become irregular in shape. Adhered chip is found on the surface linking bottom and side wall. As length reduction was taking place continuously during machining, and very small like 2 to 4 micron of tool length get involved while machining, this surface gives less information than bottom one regarding wear process.

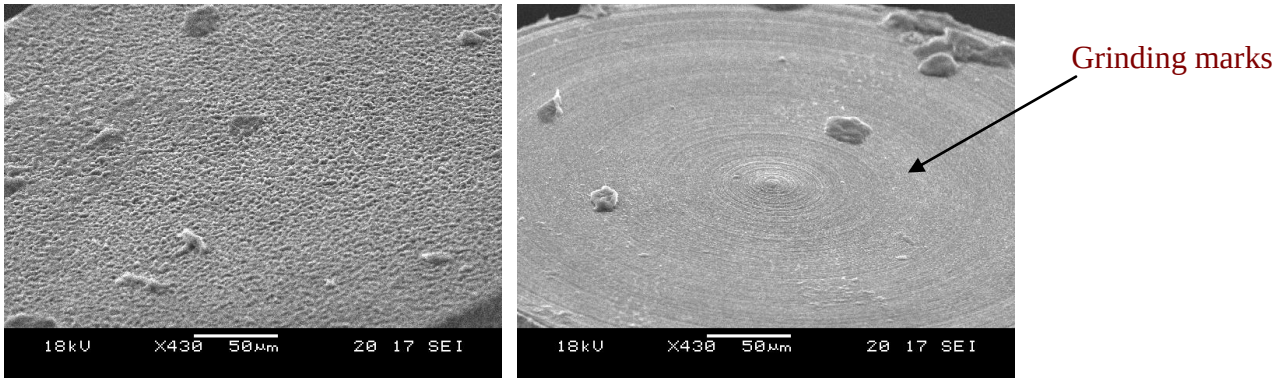

Fig.6. 2: Bottom surface of tool (a) before machining (b) after machining.

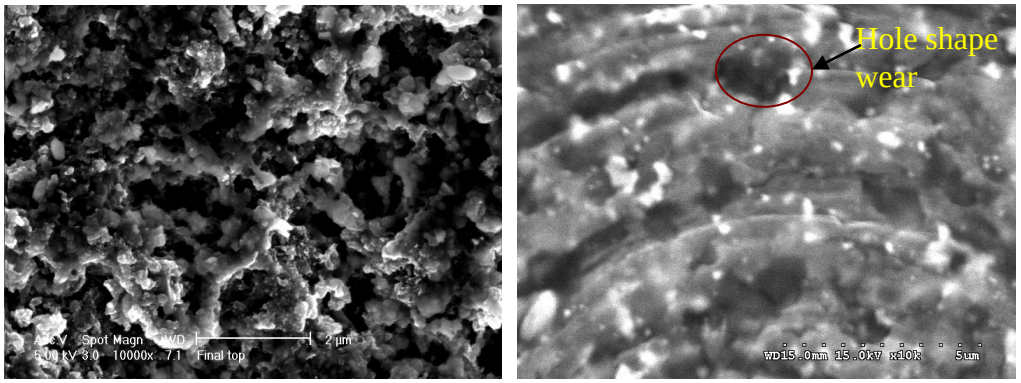

(a) (b)

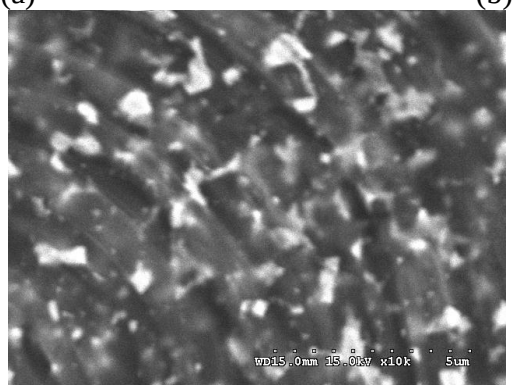

(c)

Fig.6. 3: Magnified view of bottom after machining (a) 0 slots (b) 30 slots(c) 60slots.

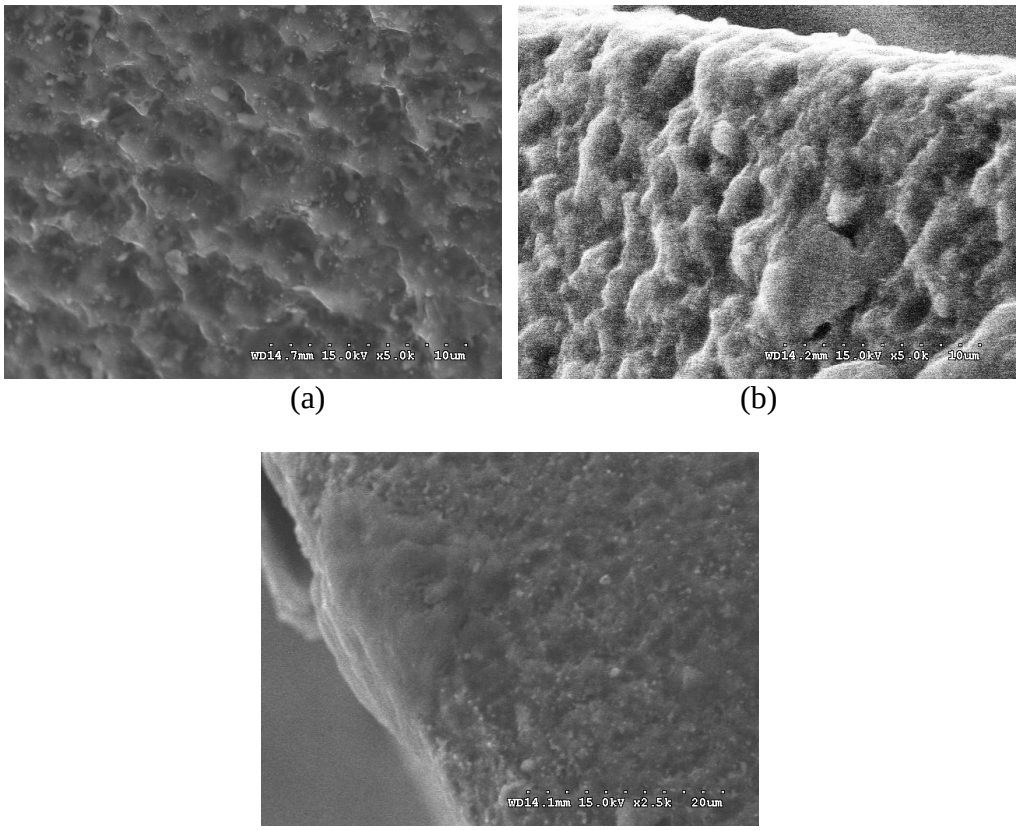

(a) (b)

(c)

Fig.6. 4: Magnified view of tool side surface after 0 slots (b) after 30 slots(c) 60 slots.

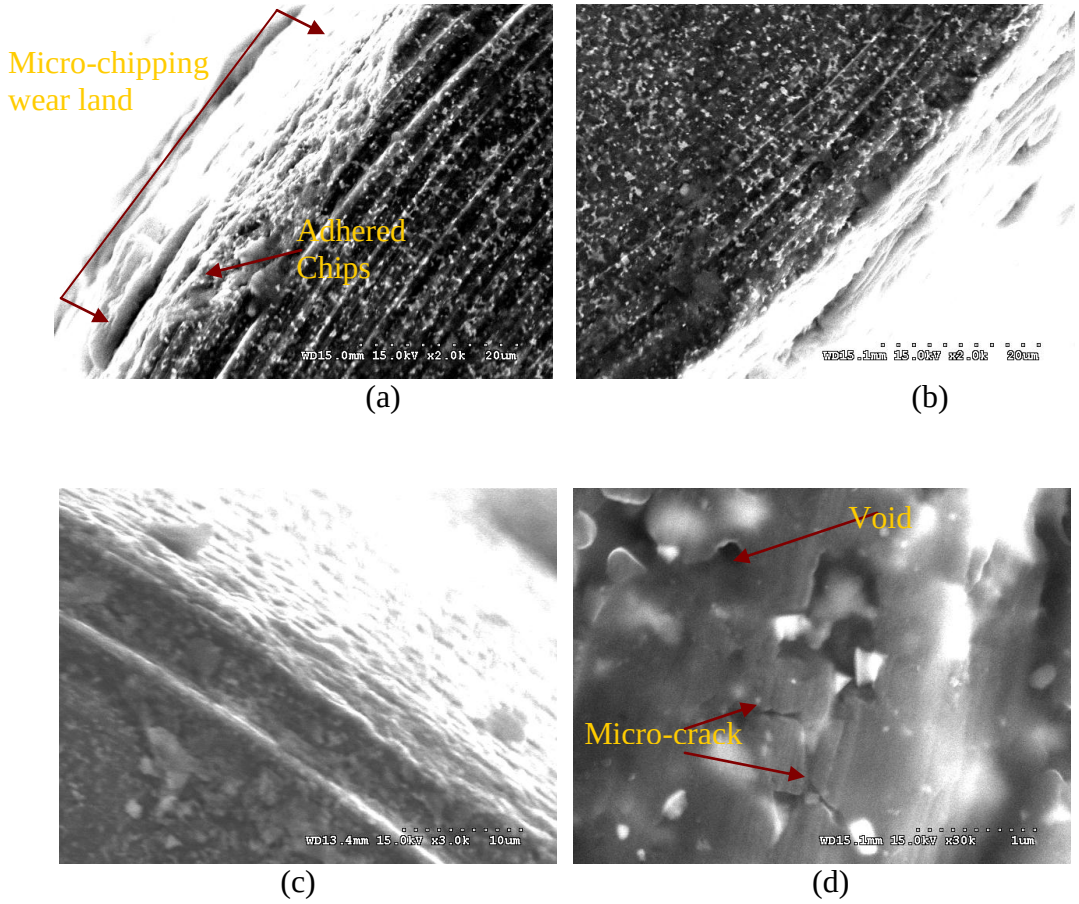

.

Fig.6. 5: Wear condition at the junction point of bottom and side surface after cutting 65 mm distance.

It is usually not the overall wear across the bottom of the wheel, but localized wear at corners and sharp protrusions on the profile which is likely to necessitate wheel redressing. Corner wear is especially problematic with vertical surface micro-grinding which also causes the radial wheel wear. Some edge chipping type of wear is found in Fig. 6.5(a) and (b).The length of this kind of wear is found to be nearly 30-50 µm. Repeated impact with the cutting edge are thought to generate a sufficient load at the cutting edge that could produce chipping wear (Philbin and Gordon, 2005). As the grinding wheel keeps rotating, accumulated chips at the wheel-work piece interface increases friction and heat. In such situation, the normal force is supported by the minutes asperities in contact with the chips trapped between diamond grains causing plastic deformation at the junction due to high normal stresses and heat. As the plastic

deformation develops gradually, the speed of the wheel reduces possibly due to the sticky conditions beneath the tool. This contact finally creates an adhesive bond between the work pieces surface, the chips and diamond grits. Therefore, the possibility of micro weld formed between chips and surface asperities similar to adhesive wear cannot be ruled out completed. However due to higher tangential cutting force, the wheel rotation overcomes the micro weld bond strength by breaking the minute asperities joints. The breaking action causes chips and few diamond grits to pull out from the wheel. As a result, this type of microchiping wear land can be seen on the tool(Zhou et al., 2006). The adhered chip near the micro-chipped zone proved this. These layers usually cover some of the abrasive cutting edges. Hence, these layers can be able to reduce the deterioration of cutting edge during cutting by acting as protective cover which usually reduce the tool wear and improve tool life. However, when this type of layer is removed by severe abrasive action, the tool wear has chance to accelerate rapidly (Luo et al., 1999). It is also noticed that the number of micro-chipping wear land increases along with the machining time. It is addressed that two nearby chipping layer superimpose and become a long chipping layer. And a time comes, when these micro-chipping layers get connected to each other along the periphery of the tool and becomes longer chipping layer. Fig. 6.5(c) also shows the double lining along the edge of tool due to wear. Again, Fig. 6.5(d) shows the remarkable micro cracks in the wear region of PCD tool using higher magnification and these cracks can be observed in the wear region of most PCD cutter as well. These cracks can propagate along a grain boundary or through a group of grains, under the variable impact loadings and form the wear regions. So it is envisaged that the wear process of PCD is basically this type of initiation and propagation of these cracks causing rupture and disintegration of the tool material (Bai et al., 2004). In addition, these cracks are thought to be the obvious reason for diamond spalling. It is also assumed that both the extrinsic loadings and the intrinsic structure and defects of PCD contribute to the initiation of these micro cracks (Miklaszewski et al.). From Fig. 6.5(c), grain pull out voids is also noticed. Grain pull out type of wear is basically the consequence of using

very fine grain as cutting edge which is also true (0.5 micron) in our case. Wear resistance becomes lower with PCD tool with fine grains and fine diamond grain is very easy to abrade. Micro-crack propagation also tends to contribute to the fraction, whole and group of grains pullout.

As relatively lower cutting speed and fine feed are used in this study, the heat generated due to the cutting speed in the cutting zone should not high enough to facilitate the diffusion or oxidation of the tool material, but some oxidation of the PCD tool already has taken place during tool fabrication which is also evident from the EDX (Fig.6.6 (a) and (b)) analysis of tool. Although, the bottom of tool is in contact with the machined surface consistently, the heat produced cannot be conducted to the surrounding which may soften the glass but rarely high enough to oxidized tool. The layer deposited on the tool surface can be also detected using EDX analysis which is mainly Si element from glass material.

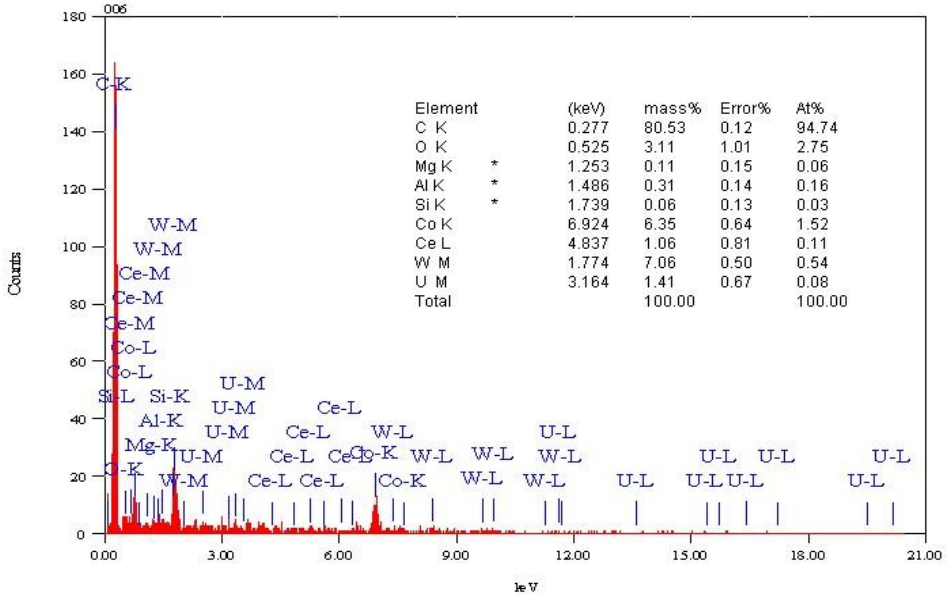

(a)

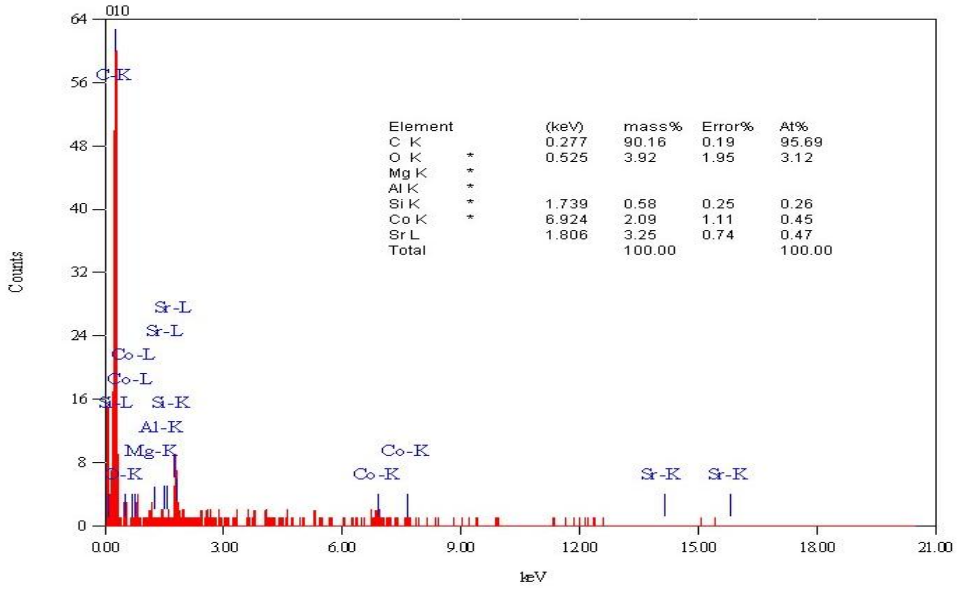

(b)

Fig.6. 6: (a) Before machining EDX of tool surface (b) after machining EDX of tool surface.

It is also observed (Fig.6.5 (a)) that severe wear occurred on the edge of the tool rather than on the bottom surface of tool. As diamonds cutting edge on the tool play principle role in material removing, they are likely to experience higher mechanical impact load. When these cutting edges on the tool start to wear, the performance of micro-grinding tool deteriorates. It is also found from the above discussion that worn tool has severe asymmetry. From the SEM view of the tool it can be said that tool wear is not even uniform along whole edge surface. This type of complicated tool wear may cause variation in the tool geometry and will in turn result in an increase or uneven surface roughness. Hence, in next section details study on ground surface due to tool wear will be given.

6.3.2. Effect of tool wear on micro-ground surfaces

Next the variation of cutting behavior with tool wear at a cutting condition of axial depth of cut 2 micron, feed rate of 25 micron/mint and rotational speed of 2000 rpm has been investigated. The assessment of actual micro grinding tool wear can be conducted by inspecting its topography and channel geometry by white light interferometer and Taylor Hobson Profilometer (cut off length (Lc) of 0.08 mm, (Ls) 0.0025mm, bandwidth 30:1 and evaluation length of 1mm). The sampled 3D surface profiles for the channel no 5th, 23rd, 45th and 63rd are shown in Fig. 6.7(a), (b), (c), and (d). From this Fig.s it is obvious that the surface quality changes greatly with tool wear progression. The Ra values for the floor surfaces are found to be 39.7nm, 65.3nm, 132.6nm, and 385.6nm respectively.

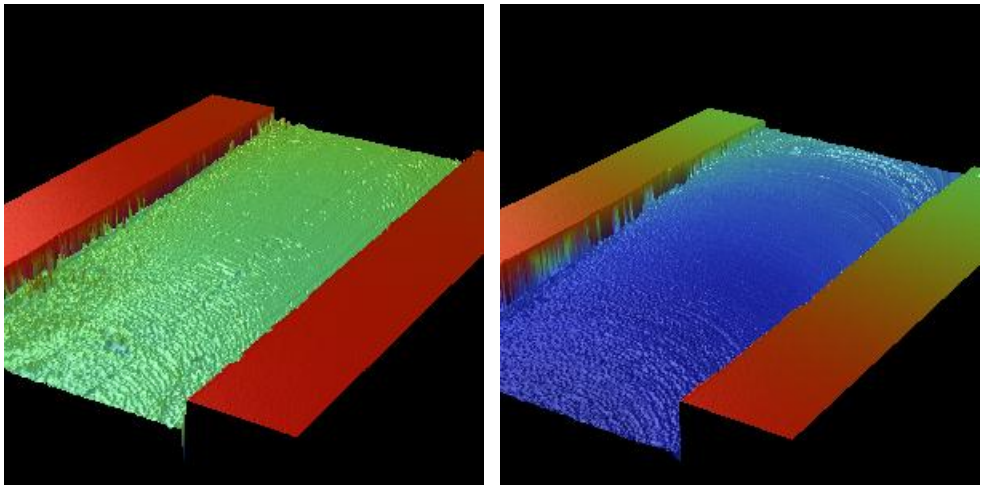

(a) (b)

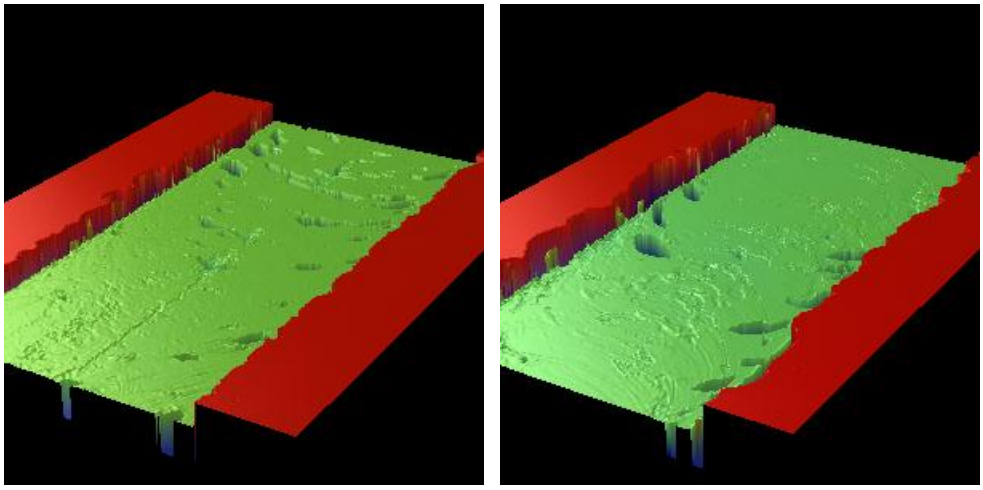

(c) (d)

Fig.6. 7: 3Dprofile of (a) 5th (b) 23rd(c) 45th and (d) 63rd micro-ground channel using interferometer.

Before the experimental analysis, the criterion for surface roughness evaluation needs to be determined due to the complicated surface characteristics when the tool wears. As for the conventional milling, the surface roughness along the center line of the channel surface is used to evaluate the surface quality since the feed rate is greatest when the tool passes the center line and lowest feed rate at the side of slot. As a result of this, largest roughness along this line is expected. In case of vertical grinding this phenomenon is still applicable too. Although this criterion is exclusively convincible as long as the tool is in good condition, the situations get totally unpredictable when the tool wear occurs. It is observed that the tool path is no longer clean any more when the tool wears. As long as the tool is in good state, remarkable grinding mark on the bottom surface of micro-ground slot, geometrically straight side wall and invisibility of center line are usually found as shown in Fig.6.7 (a) and (b). Reduction of channel depth is also found in Fig.6.7 (b) which indicates the tool length reduction. During the progressive wear process of tool, little edge chipping of tool and few welded chips were found in SEM picture previously (Fig.6.5). This entrapped chip might causes the introduction of center line on the bottom surface and edge chipping resulted the irregular geometric shape of side wall as found in Fig. 6.7(c) and (d). During the drastic tool wear, it experiences longer chipped surface at

the edge, double edge as well as welded chips. Huge pitting on the bottom surface, drastically chipped side wall, noticeably longer center line, and double side wall lining are found to be the major phenomena of tool wear during the machining of 45th and 63rd channel.

Fig. 6.8 (a) shows the variation of roughness with the increased number of ground channels. It can be seen that overall average roughness changed greatly from starting stage being nearly 50nm to the maximum of 350nm with the progression of tool. From the analysis of average surface roughness the variations of surface roughness along the time can be divided into three stages. In the first stage, Ra value generally does not change much, which means that the tool does not experience significant wear during this period.

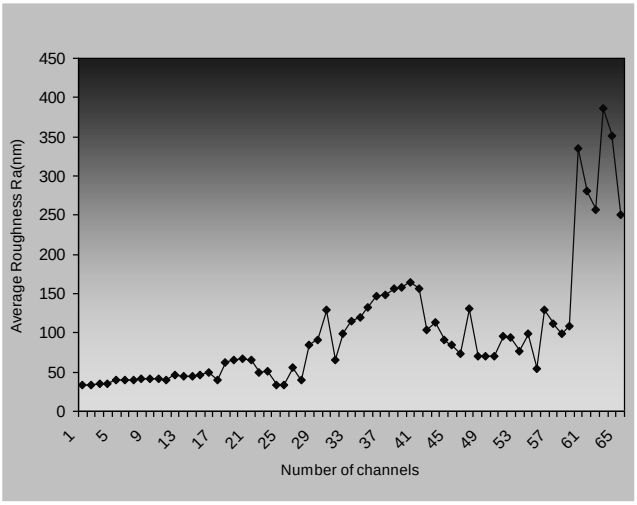

Fig.6. 8: Average surface roughness of ground surface.

It is observed that up to like 20 channels average roughness is less than 50nm.Then in the second stage; it suddenly increases to around 150nm. Then, again roughness gets decreased to 90 nm. After that roughness value shows irregular zigzag trends of increasing and decreasing. The reason behind this increasing trend can be explained with the irregular pattern of wear of micro-grinding wheel and wheel loading with the chip. The decreasing trend can be explained with the re-sharpening effect of tool due to the

abrasive nature of Bk7 glass. This trend of roughness illuminates how the tool wears starts and progress rapidly. After that in next step roughness value increases dramatically to higher peak value nearly 300nm from the 60th to 65th channel in the final stage which means tool wears very fast at that stage. Overall, it can be said that as the cutting time increases, surface roughness of the ground channel increased indicating the tool wear which is also clear from the progressive SEM image of tool surface. This also confirms the speculation of using surface roughness as the criterion to study tool wear in micro-grinding.

6.3.3. Analysis of Chips

Fig.6.9 shows the optical image of glass chips formed under the same cutting condition. Chips are collected in between the experimentations to understand the cutting behavior of PCD tool. Chips collected different time basically contains the combination of different type of chips. These chips are discontinues and can be classified into fragment type, saw tooth and filament type chips indicating the unsteadiness of the cutting process(Liu et al., 2005). It is observed that continuous chip may not be the only criteria to establish ductile machining as we obtained a very smooth machined surface with relatively shorter and discontinues chips even. Serrated chips (Figs.6.9 (b)) found during machining is basically semi continues chip with zone of low and high share strain. Usually, material with low thermal conductivity and strength that decreases sharply with temperature, such as titanium and glass exhibit this sort of behavior. This chip has saw tooth like appearance. Discontinuous chips are also found during machining which (Figs. 6.9(a) and (c)) consist of segments that may be firmly or loosely attached to each other. These types of chips usually formed under the condition like, brittle work pieces material as they do not have capacity to undergo the high shear strain developed in cutting or in case of very low or high cutting speed or lack of an effective cutting fluid.Hence, chips morphology is basically controlled by the machined material rathar then process condition like tool state keeping the other cutting condition same.

(a) (b) (c)

Fig.6. 9: Optical image of chips after cutting 65 mm of distance.

Because of the discontinuous nature of chip formation, forces continually vary during cutting. Consequently, the stiffness of the cutting tool holder and machine tool is important in cutting with discontinuous-chips as well as serrated chip formation. If not stiff enough machine tool may begin to vibrate and chatter. This in turn, adversely affects the surface finish and dimensional accuracy of the machined component and may damage or excessive wear of the cutting tool. Hence, morphology of chips formated during machining has effect on tool wear and surface roughness but analysis of chips morphology cannot actually tell us the actual tool wear condition.

6.3.4. Online monitoring of tool wear by using Normal force and AE signal

It has been also widely established that variation of cutting force can be also correlated to tool wear. This can largely be attributed that force becomes important in worn tools conditions as a result of the variation produced due to the friction between cutting tool and work pieces. Fig.6.10 shows the normal force variation along with grinding time. From Figure, it is found that initially force seems to be steady for certain period then it starts dropping to lower values. This tendency of dropping can be explained with reduction of tool length mentioned earlier which reduces the depth of cut as well. Next, step by step increment of force is also found in the Fig.6.10. This phenomenon can be explained as follow. Basically, localized high pressure on the glass surface is important to

create severe wear. The sharper the diamond abrasive, the higher the localized pressure and the faster the material removal rate as well as the smaller the grinding force. However, as the grit size decreases, the space for storing the chips becomes smaller and loading is easily encountered. Wheel loading occurs when chips fill the pores between active grits in surface of the wheel.

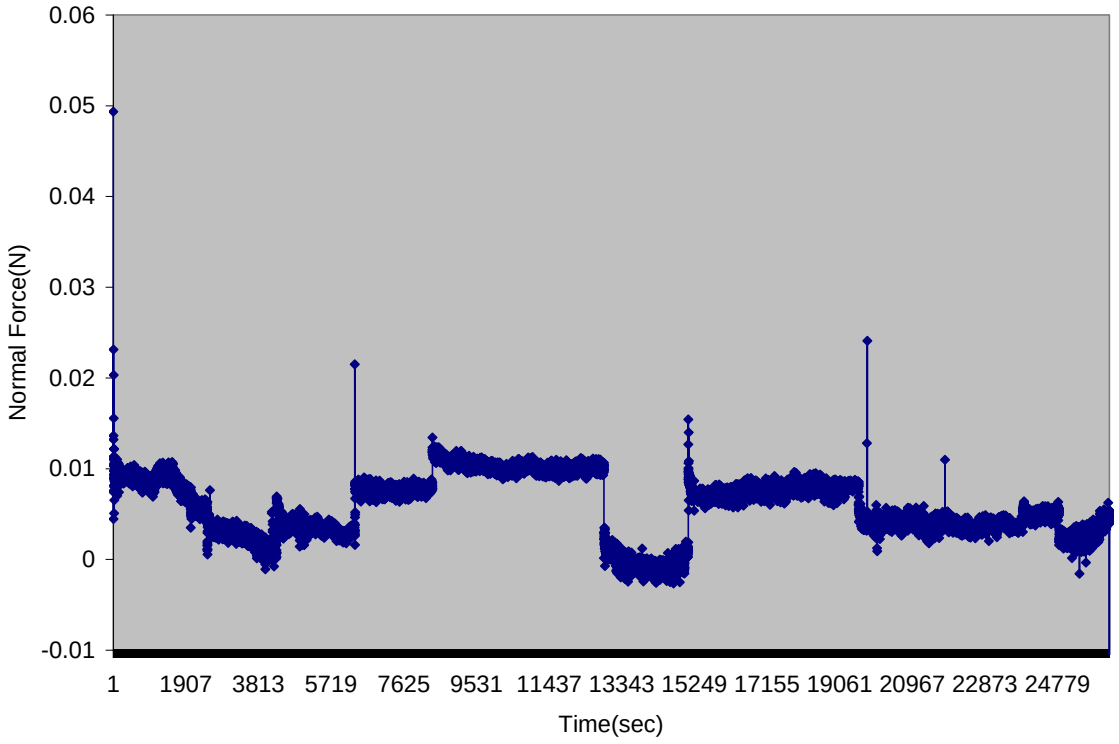

Fig.6. 10: Average normal force behavior during the micro-grinding process

When the removal rate exceeds the rate of chips storage available, chips will tend to become lodged in the chip storage space. During grinding process, when the wear of diamond wheel reaches a certain degree, the sharpness of diamond grits will become small. Grinding chips adhering to the tool surface reduce the level of grit protrusion and space for new chips resulting in dull rubbing action between tool work piece surfaces. This therefore makes it difficult to sustain a high grinding force for completing this grinding process. As a result, material removal rate will be decreased but friction force

will be increased due to rubbing. This force increment hence indicates the tool blunting which causes poor surface finish and sub-surface damage. After this increasing trend of force, there is one more decreasing trends as well. This decreasing trend is probably due to the re-sharpening effect of PCD tool by abrasive glass material which might also reduce the frictional force between tool and work piece. This increasing and decreasing trend keep going on during micro-grinding of BK7 glass due to PCD tool wear process. But this current trend cannot exactly tell us the severity or wear status of tool or exact timing of tool wear. Hence the observation of AE signal has been incorporated along with cutting force to get more accurate indication of tool wear.

During the metal cutting the work pieces undergoes considerable plastic deformation as the tool pushes through it. Within the deformation zone strain energy is released as the bonds between the metal atoms are disturbed. This released energy is commonly referred to as acoustic emission. Other sources of AE include phase transformations, friction mechanisms and crack formation or extension fracture. Apparently, the wheel work piece contact area largely influences the AE amplitude during grinding. With an increase in the amount of material removal or processing time, an grinding wheel becomes unable to perform proper cutting due to poor wheel topography. The average and root mean square values of dynamics signals are widely used in tool condition monitoring. As statistical parameters, they can reflect characteristics trends in the time domain signals, and they are much less computationally expensive than wavelet analysis and fast Fourier analysis. To determine the proper process signals for micro grinding tool wear monitoring, the RMS value of AE signals are analyzed as shown in Fig. 6.11 with time. It seems that initially AE signal gets decreased with time. This is due to the reduction of tool length and width as it was mentioned earlier. Then, again AE signal has increased a bit and remain same for some distance. This phenomenon can be explained as follows. As the grinding time increases, the number of cutting edges on PCD tool loses their sharpness and starts rubbing on the glass surface which is another potential source of AE signals. This will also increase the surface roughness as well which can be verified from Fig. 6.8. Again, if

significant bond wear can be induced during machining, damaged abrasive particles and other debris on the surface will be undermined and removed and fresh abrasive area is exposed. In other words the tool may be made to self-dress or self sharpening (Karow, 1993). Being abrasive material glass probably re-sharpenes the PCD tool, as a consequence of that the rubbing effect might be diminished after some time which can explain the further decreasing trend of AE signal. As grinding is multipoint cutting, this type of increasing and decreasing trends of AE signal keep going on instead of sudden devastating single pick of signal which is usually found in case of single point tool or defined geometric milling tool.

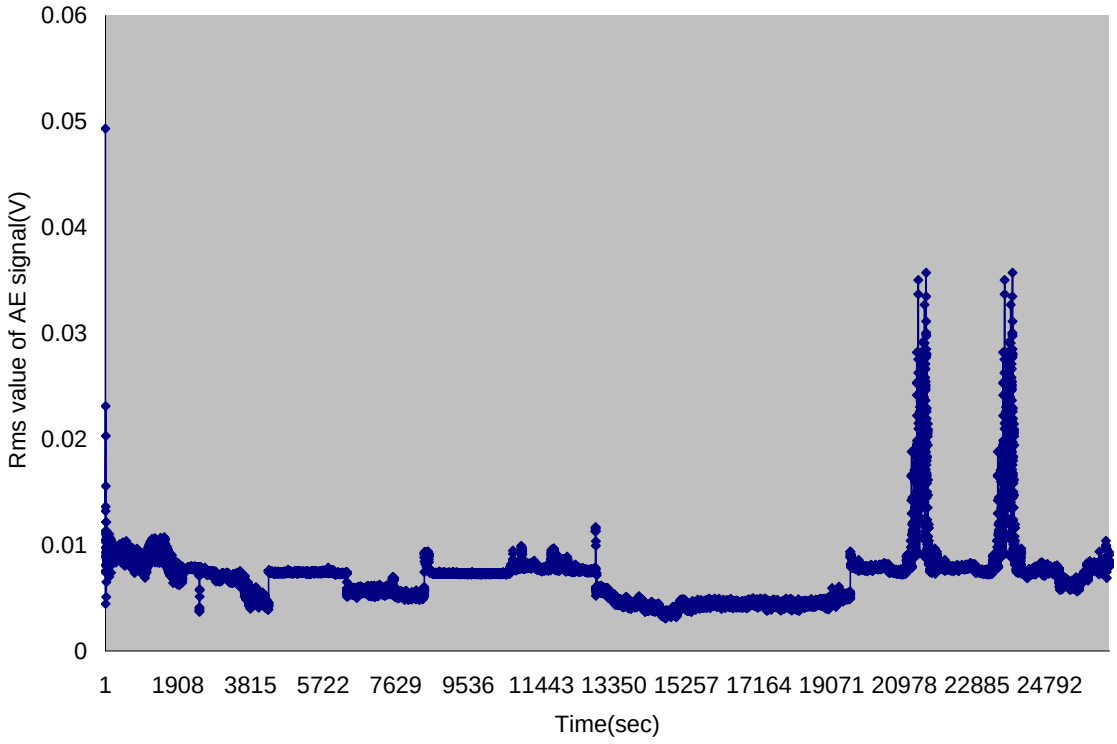

Fig.6. 11: Rms AE signal behavior during the micro-grinding process.

A time comes when sudden pick is also evident in Fig. 6.11. This sudden huge energy release can only be explained with the sudden fracture of tool which is totally different from previous signal. Fracture is also identified as one possible source, as the propagation

of micro cracks always releases elastic energy due to the generation of new surfaces. This type of micro-chipping (fractured) area is found in FESEM picture (Fig.6.5 (a)) of tool has explained this fact. The first small pick probably indicates the initiation of small chipping area on the PCD tool which is also evident in FESEM image and further two giant picks envisage the presence of several chipped area superimposing each other.

As a result of that, large chipped area is also evident in the FESEM image of PCD tool. From above discussion, it has been found that AE signal is capable of indicating the tool condition during micro-grinding of glass along with the severe chipping wear. So this RMS AE signal can be used as plausible tool condition monitoring method.

6.4. Concluding Remarks

Micro-grinding of BK7 glass has been performed using on machine fabricated PCD micro-tool in order to investigate the tool wear mechanism and tool condition monitoring under the same cutting conditions. From the results presented, the following conclusions can be drawn.

- It was found that the consequense of tool wear is the diameter reduction as well as length reduction and the G ratio for this PCD micro tool is found to be nearly 940. Basically, two type of tool wear has been detected. One is edge chipping at the tool rim which is actually responsible for radial reduction of tool as well. Chip accumulation at tool and work pieces interface causes built up edge formation and gradually this built up edge grow larger in size, become unstable then eventually breaks up. This process of built up edge is repeated continuously during the cutting process and the number of edge chipping is getting increase with the machining time. Nearby chipping edge get superimposed and create bigger area of chipping. Another is abrasive wear which occurs due to the faster weaker grain boundary break down and then creating some inter-granular crack. These cracks

propagate through the groups of grain or grain boundary causes the diamond grain spalling and form wear region.

- The effect of tool wear on the surface roughness is found to be significant through the micro-grinding experiments of BK7 glass using PCD micro-tool. In some conditions, the Ra value increases several times with the tool wear progress, which makes it necessary to consider tool wear along with other cutting conditions to contribute to surface roughness as well as cutting forces. Depending on the surface roughness value of ground channel, tool wear progress can be divided into 3 stages where, in initial stage tool suffers insignificant wear, then intermediate wear condition and finally severe worn out tool. Huge pitting on the bottom surface, drastically chipped side wall, noticeably longer center line, and double side wall lining are the major phenomena on the machined surface due to the severe tool wear.
- Generated chips has effect on tool wear and surface roughness but analysis of chips morphology during different time of machining cannot really tell us the actual tool wear condition.
- Observation of normal grinding force can give indication of the tool conditioning during grinding process only but it cannot tell us the severity of tool wear. Continuous monitoring of AE signal is found to give an indication of tool topographic condition, i.e. sharpness and bluntness of PCD cutting edge during micro-grinding. Moreover, this signal can also envisage minor and major tool chipping condition. Hence, monitoring the AE signal can be a plausible way of monitoring on machine fabricated PCD tool condition.

Chapter 7

Subsurface Damage Analysis of Glass

7.1. Introduction

Advanced engineering ceramics and glass have been extensively used in industrial applications in the past few decades due to their unique physical and mechanical properties. The advantages of ceramics and glass over other materials include high hardness and strength at elevated temperature, chemical stability, attractive high temperature wear resistance and low density. Because of these properties, they found their application in precision bearing for the use in nuclear industry, automotive component, biocompatible implant, refectories, lenses scientific testing devices and substrates etc. However, machining difficulties and high costs have been associated with the usage. This is mainly due to the poor machinablity of ceramics. As a result, great efforts have been given towards the development of machining, in particular grinding technology for advanced ceramics in an efficient mode (Inasaki, 1987; Li and Warren Liao, 1996; Malkin and Hwang, 1996; Marinescu et al., 2000; S. Jahanmir, 1999). Although, advances have been made in the near net shape technology, grinding with diamond wheel is still considered to be the most efficient and effective technique to finish these ceramics and glass work pieces. As quality of advanced glass and ceramics has dramatically improved with the modern manufacturing techniques, the bulk defects are significantly reduced in terms of their size and numbers. Hence, the primary source to introduce damage into glass and ceramics materials is grinding or other machining process. Due to low fracture toughness compared to metal and alloys, glass and ceramics are very sensitive to cracking and other damage. Hence, ground work pieces are always left with such damage as cracks pulverization layers, and a limited amount of plastic deformation which resulted from hard and brittle nature of work pieces (Conway and Kirchner, 1986; Kirchner, 1984; Koepke et al., 1969; Xu and Jahanmir, 1995; Zhang, 1993; Zhang and Howes, 1994). Grinding also induces surface residual stresses that may affect the strength and fatigue life. The residual surface and subsurface damage may

seriously alter the surface properties and cause strength degradation or even a catastrophic failure of the glass and ceramics components. The major form of machining damage usually occurs as surface and subsurface damage. The first type of damage is due to the radial cracks formed on the ground surface which is visible and the later damage is due the median and lateral cracks that are formed below the affected grinding zone which are not visible (Conway and Kirchner, 1986; Maksoud et al., 1999). The nature of grinding damage depends on the mechanism of material removal. The material removal mechanisms are usually classified into two categories: brittle fracture and plastic deformation (Conway and Kirchner, 1986). Brittle fracture similar to indentation of a brittle material by a hard indenter, involves two principle crack systems; lateral crack, which result material removal, and the median crack responsible for strength degradation. In the brittle fracture, material removal is accomplished through void and crack nucleation and propagation, chipping or crushing (Kirchner, 1984). Plastic deformation is similar to the chip formation in the grinding of metal, which involves scratching, plowing and chip formation. The material is removed in the form of severely sheared chips as obtained in machining of metals (T.G. Bifano, 1991).

Literature shows that damage induced by conventional grinding has been assessed and characterizes using large grinding wheel in case of ceramics material (silicon nitride, alumina, silicon carbide) mainly, for glass material using micro-grinding tool, the room is still left for further research. Hence, in the following study, subsurface damage is investigated on Bk7 glass with the help of bonded interface technique. This paper presents observation and measurement results of subsurface damage of the BK7 glass ground with micro-PCD tool which was prepared using micro block-electro discharge machining.

7.1.1. Subsurface Damage

Manufacturing process like grinding, lapping and polishing introduce different kinds of damages or defects, including fractures, scratches, sleeks, micro cracks and residual stresses. The cracked layer near the machined surface is known as subsurface damage (SSD) and may be explained by the hill model of plasticity (al., 1998). This damaged layer must be minimized and eliminated, in order to avoid failures in the final device

production like damaged coatings or unusable devices. Generally subsurface damages reduce the quality and life time of the work pieces because of the surfaces age faster and become dull. The single crystal characteristics are not given any longer and coatings may split. Therefore it must be guaranteed that these depth damages are removed for the final usage of the optical surface in order to avoid failures in the final device. Fig.7.1 indicates the layers after cold processing of advanced materials. The defect layer may be easily superficially smeared by simply polishing and a small polishing layer is generated on the leading surface. After that polished layer, the damages are not visible any more. Subsurface damages are contained in the defect layer, which is located under the surface and distinguishes from other regions in both composition and micro structure. The deformed layer, defect layer and polished layer overlapped successively in the defect free bulk material. Fig.71 (b) shows the classification of surface and subsurface damage on ground sample. It's typical subsurface damage can be generally described as a geometrical damage in terms of radial crack, both parallel and perpendicular to grinding direction. Median crack initiates at the bottom of pits pores and flaws and penetrate into subsurface region normal to surface plane. Cone crack initiate from side of pits pores and flaws and penetrate into subsurface region with an acute angle. Lateral crack are rarely seen in the subsurface region. In addition, there are also cavities beneath the ground surface with a similar depth to other kind of crack (Maksoud et al., 1999) .

The subsurface damage layer in optical glasses for example is unsymmetrical; every ion is not fully coordinated from the subsurface layer to the surface layer. Due to the high requirements in the optical field, the defect layers must be eliminated therefore the treatment and measurement of subsurface damages is a major topic.

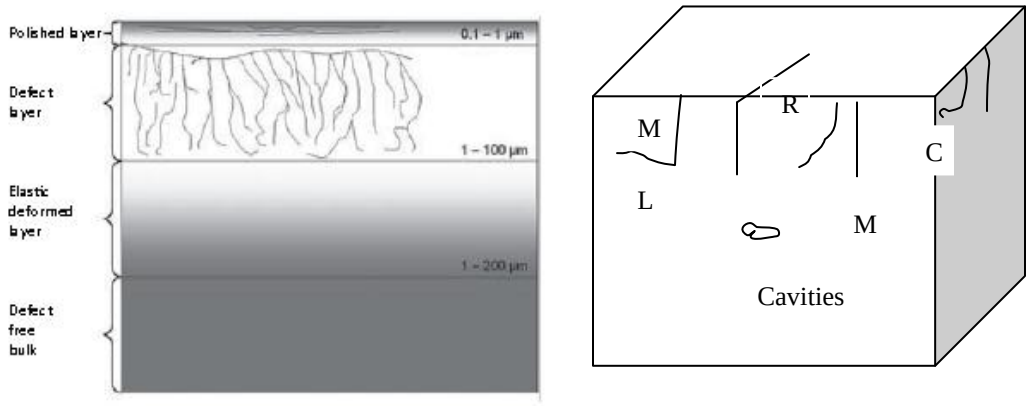

Fig.7. 1: (a) Schematic of subsurface damage (b) Classification of surface and subsurface damage forms of diamond ground glasses.

7.1.2. Subsurface Damage Evaluation Techniques

A wide variety of destructive and nondestructive methods for measuring the amount and depth of the SSD depth have been found in literature. Some of the direct SSD measurement techniques include the ball dimple method, taper polishing method and more recently a MRF spot method, where the ground or finished surface is partially removed to evaluate the depth of SSD. The most conventional ones consist in polishing a taper (taper method) (P. Hed, 1987; P. Hed, 1989) or a sphere (ball dimpling method)(Zhou et al., 1994) in the part to be measured with a depth deeper than the SSD depth. The latter form is then observed under a microscope after an optional diluted acid etching to open cracks and ease there observation. Carr also proposed to simply dilute the surface in a concentrated HF bath to reveal embedded cracks(Carr et al., 1999). Alternatively, the ball dimple can be replaced with an imprint done with a magnetorheological fluid (MRF) polishing machine. Since MRF apply very small normal stress to the surface during material removal compared to loose abrasive polishing processes, it can remove layers of material without inducing further damages(J. C. Lambropoulos, 1999; Joseph et al., 2002). This method was first proposed by Lambropoulos (J. C. Lambropoulos, 1999) and subsequently detailed by Randi (Randi et al., 2005) and is further referred to as MRF dimpling. Suratwala et al used also a MRF polishing machine to polish a taper on the sample to be measured (Miller et al., 2005; Suratwala et al., 2006). All these authors use a "last trace" criterion to evaluate the depth

of SSD. It means that this depth is obtained at the point after which no crack is observed in the dimple (or equivalent form depending in the technique) made on the part. There are several other techniques called flexural strength testing, fractography, and non-destructive testing, which are also considered to be useful for assessing subsurface damage. In addition to these, thermal wave measurement and ultrasonic techniques has also been used by some researcher to detect the subsurface lateral crack associated with indentation in glass and silicon nitride (Ahn et al., 1996). But the application of these nondestructive inspection techniques should be applied for small crack investigation. The damage differentiation resolution of the current non-destructive techniques is still too low to meet practical requirements. Incorporated with the flexural strength testing and fracture mechanics, the X ray diffraction techniques also allowed to determine the amount of machining damage in ceramics and glass. This technique is based on the information of the machining induced plastic deformation and residual stress. Unfortunately, the X ray diffraction technique neither differentiate subsurface damage form bulk structures , nor differentiate the effect of damage on the residual strength and surface tribolgical properties of a ground surface(W. Pfeiffer, 1993). Recently bonded interface sectioning technique was proposed to study subsurface damage modes and to identify mechanism of material removal. This technique has been effectively applied to grinding of a coarse grain alumina to identify the subsurface damage(H.K.Xu, 1995). This technique has been proved to be very effective and easily applied. Hence in our study, the bonded interface technique is used to examine the subsurface damage and details of this process are narrated in following section.

7.2. Experimental Details

The work material used for this investigation was Bk7 glass. The specimen has dimension of 25×25×10mm. micro-grinding was carried on 1 mm length . The spindle speed 2000 and 2500 rpm were used. The feed rate was taken as 25µm/min while performing the effect of depth of cut. The depth of cut was used 2 µm while observing the effect of feed rate. Experimental set up for this experimentation is given in Fig.2.1.

The ground surface was examined using a FESEM. Prior to examination, the ground surface were cleaned with acetone in an ultrasonic bath for at least 10 min and then gold coated for examination. The roughness of the ground surface was measured using a Taylor Hobson Profilometer(Talysurf-6 with cutoff value 0.8 mm).The roughness was the average value obtained by the scanning rectangular surfaces of the work pieces.

7.2.1. Work piece Preparation

A bonded interface sectioning technique was used to examine the grinding induced sub-surface damage. In this method, the two specimen of were ground with same dimension and one surface of each specimen was polished. The polished surface was subsequently bonded face with suitable adhesive. Clamping pressure was applied then to push the two specimens tightly together; leaving a thin layer of adhesive approximately 1 µm thick.Fig.7.2 shows the schematic illustration of the procedure used in preparation of SEM samples to study sub-surface damage. As shown in this, the two specimens bonded together at the xyx´y´ interface of the two polished surfaces. It is essential to clamp the two specimens tightly together during bonding, to make a bonded interface narrow. A wide interface between the two specimens could cause an artificial damage close to interface during grinding. When the interface is narrow, no extraneous damage will be observed along the interface xyx´y´ compared to the ground are away from the interface. Micro-grinding was performed on the plane ABCD passing symmetrically across the line xy. The specimens were separated after grinding by melting the glue and were cleaned with acetone in an ultrasonic bath. Then the specimens are etched with 10% weight HF solution in distilled water for 10 seconds. The polished surfaces were gold coated for FESEM examination.

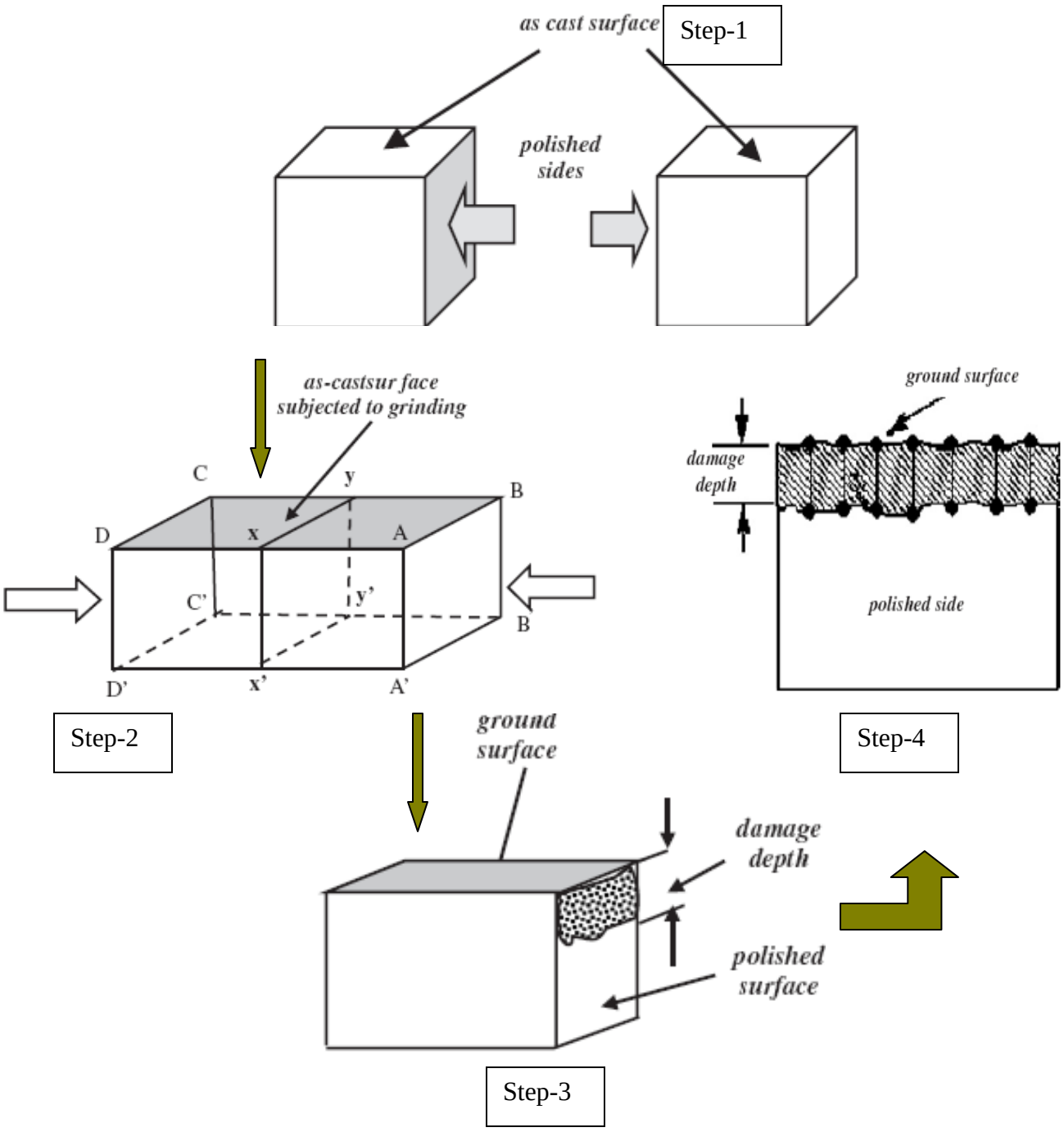

Fig.7. 2: Schematic illustration of procedure in the preparation of SEM samples to study subsurface damage.

7.2.2. Tool Preparation

PCD tools are increasingly used in the machining of brittle and hard material due to their superior tool life. PCD is synthesized, extremely tough inter grown mass of randomly oriented diamond crystals bonded to a tungsten carbide substrate. It is manufactured by sintering together with micron sized diamond grains at high pressure and temperature in the presence of a solvent/catalyst metal, usually cobalt or cobalt/nickel alloys (Buchmann, 1992). During the sintering process, the voids between PCD grains are filled with cobalt binder. Unlike cemented tungsten carbide however, individual grains actually bond to one another. The result is a tough, hard product that will retain its shape and strength if some of the metal matrix is removed even (D.J.Anthony, 1990). Commercially available polycrystalline diamond tool containing 0.5 micron grain size was used for micro grinding after shaping by micro-EDM. Diamond grains are exposed after block-EDM, which act as hard and tough cutting edge during micro grinding. The sacrificial electrode material used for PCD micro-rod shaping was pure tungsten (99.9% W) block of length 4.5 cm, width 1.3 cm and height 0.5 cm. In this study, the surface of PCD tool for micro grinding is prepared by means of dressing using block-EDM at a capacitance of 1000 pF and voltage of 100V. The cobalt binder is removed during micro-EDM as it is conductive, whether the PCD grain is exposed to surface that can work as cutting edge during micro-grinding. The bottom of PCD rod is also dressed by using 100pF and 100V. Flatness of bottom surface is very important to consider for maintaining the accurate depth of cut.

7.3. Results and Discussion

7.3.1. Ground Surface Characteristics

Typical FESEM micro-graphs of the ground BK7 glass are shown in Fig.7.34 and 7.4. Ground surface consists of four different areas (a) the smooth area; (b) the fracture area; (c) the smeared area; (d) the Ploughing striations. Debris is also found to be existed in some case. The smeared products and fine debris that cover the ground surface are

generated when the material removed from surface is trapped between the grinding tool and work pieces and is crushed against the surface. Ploughing or grinding marks can also be observed on the surfaces ground using small feed rate. Pores can be occasionally seen on the ground surface. The pores usually results from the pulling off the grain particles. This pull out is clearly associate with the surface cracking. The white areas found on the Fig.7.3(c) are cleavage facets parallel to the ground surface. When, small depth of cut is used, side wall looks so smooth and straight; on the other hand, higher depth of cut makes the side wall surface irregular and rough. At low rate of material removal, the cutting points on the tool remove and expel the material from the machined surface in an efficient manner. At high rates of material removal however debris is not expelled efficiently and the debris generated from the cut must pass between the tool and machined surface. The temperature generated during high material removal also account for the surface degradation. These are considered to be initiated by the tensile stress set up when the surface is quenched following the path of tool. Moreover, at larger depth of cut, lateral cracks developed radically from the groove and resulted in large scale of chipping and crushing.

Again, increasing feed rate causes some irregular marks on the ground surface due to this inefficient debris removal. At low rate of material removal, the cutting points on the tool surface remove and expel material from the machined surface in efficient manner and the mechanism of material is the combination of plastic flow, ductile and brittle cutting. At high rates of material removal however debris is not expelled efficiently and the void of tool surface load up. Fresh cutting surface on the tool are thus prevented from impacting the work piece and the material must be removed by plastic flow.

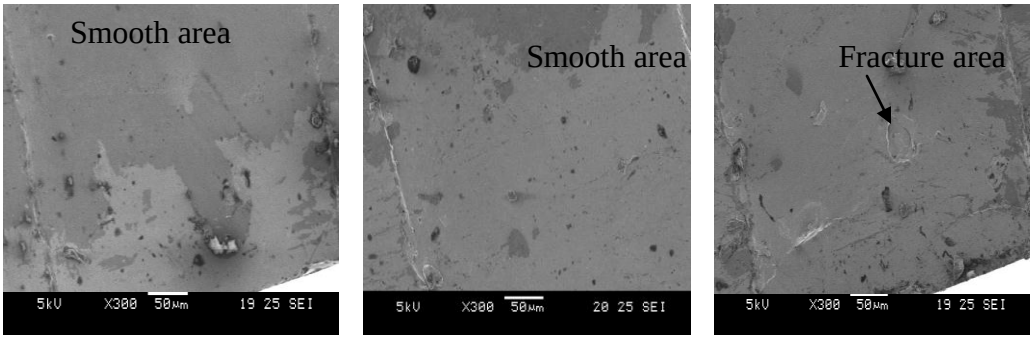

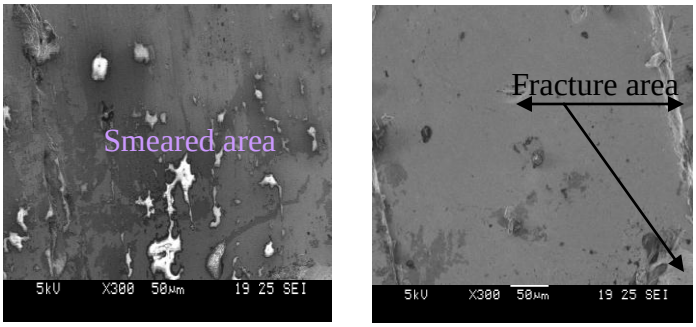

Fig.7. 3: Ground surface characteristics of BK7 glass for varying depth of cut.

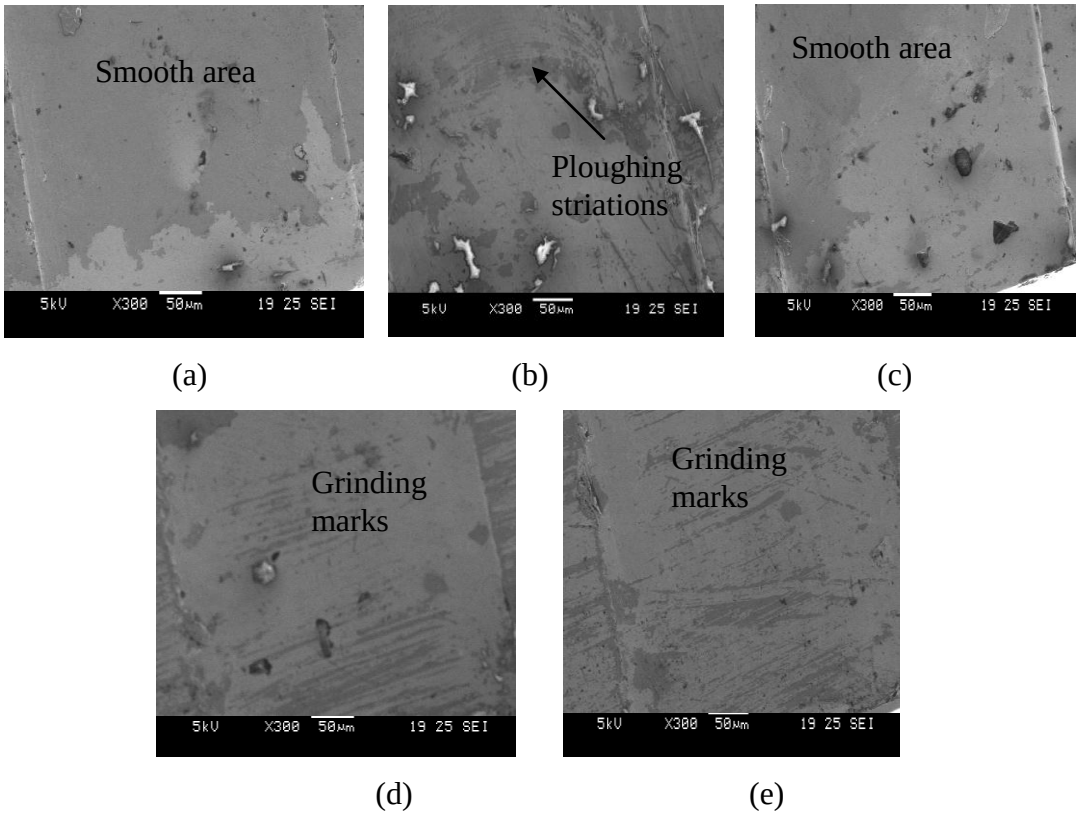

Fig.7. 4: Ground surface characteristics of BK7 glass for varying feed rate.

The plastic deformation involved in chip formation generates heat causing an increase in glass surface temperature. The high temperature generated during high rate of material removal also account for (Fig.7.4 (d), and (e)) the spaced surface marks. These are considered to be initiated by the tensile stresses set up when surface starts quenching following the passage of tool (Koepke et al., 1969). The FESEM images also reveal that

the surface generated by the removal modes of brittle and ductile. It is difficult to quantitatively identify the effect of the grinding conditions on the surface characteristics using FESEM.

7.3.2. Grinding Induced Subsurface Damage

Usually the observation of surface shows no chipping or cracking on the ground surface except some scratches sometime. This situation gives an indication that grinding did not originate any damage to the work piece. However, it's not the real fact. Due to pulverization in grinding, a layer of pulverized grains smeared over the work piece, which forms a makeup surface later on (Zhang et al., 2003). Subsurface damage of the ground specimens, which were prepared using the bonded interface sectioning technique, was examined using an FESEM**.** Fig.7.5 and 7.6 gives the FESEM images of ground surface and Fig.7.7 shows the numeric value of chipping damage and total damage under different grinding condition. As the damage value is not equally distributed throughout the surface, measurements have been taken at five different places and average of which is used as data point in Fig.8. It is noticed that chipping damage grows with the increase of depth of cut. With the further increase of depth of cut it shows jig jag trend of decreasing and increasing afterward. Chipping damage for higher depth of cut seems to more overwhelming and it might cover the total damage layer too. This fact can be explained as follows. As the depth of cut increases during grinding, the local contact force also increases and the number of contacting particles would also increase which leads to the possible removal of a segment of material containing a number of individual grains, rather than dislodgements of individual grain only. While removing this segment material, chipping damage no more depends on the depth of cut, which might be the reason of further reduction of chipping damage layer even with the increasing depth of cut (Agarwal and Rao, 2008).

From Fig.7.5 and Fig.7.6, the effect of depth of cut on the subsurface damage can be revealed. Chipping damage or pulverization is found to exist on the ground surface as found from figures. This chipping layer is an outcome of either intergranular or

transgranular micro-cracking due to localized stress field or shear stresses superimposed by hydrostatic compressive stresses induced by the abrasive grain. Usually when the fracture resistance in the grain boundary and in the grain has same level; the crack would always prefer to follow the shortest way and the fracture path would always be transgranular. The occurrence of intergranular fracture indicates that the fracture toughness of the grain boundary is lower than that of the grain and that it is energetically favorable for the crack to prefer the longer way around the grain. Lower loading rate usually promotes the intergranular fracture while the contribution of transgranular fracture increases at higher loading rates. In chipping damage, micron-sized glass grains are crushed into finer one (Collin and Rowcliffe, 2002). Although, it is not clearly seen in this lower magnification, later on higher magnification image reveal the crack path through the grain and along the grain boundary. It is also found that SSD of ground surface using lower spindle speed are much larger from Fig.7.5 and 76. This might be due to the fact that, the abrasive particles have certain mechanical load strength; they might be smashed under a certain wallop. Higher spindle speed will have usually higher probability to produce higher wallop. Under lower spindle speed the abrasives have a lower tendency to crash into further smaller pieces. As a result, larger size abrasives take part in the grinding and consequently produce larger sub-surface damage.

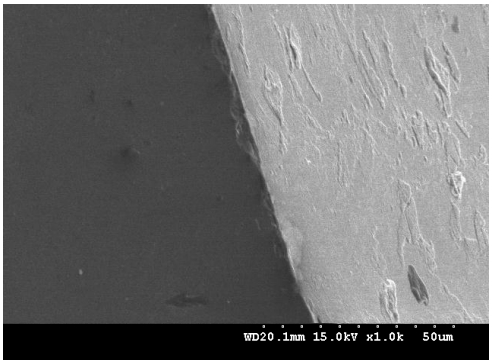

(a)Depth of cut=2µm

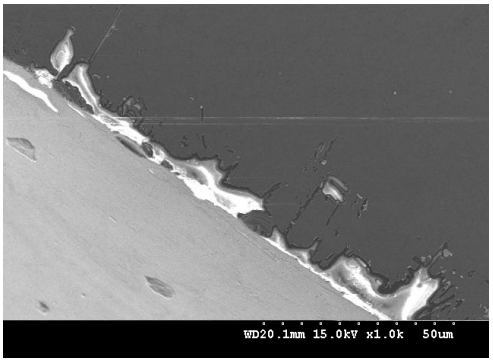

(b) Depth of cut=5 µm

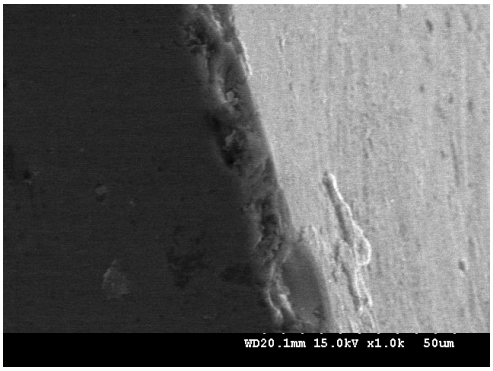

(c)Depth of cut =10µm

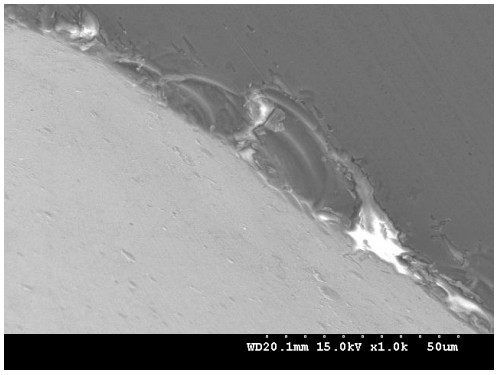

(d) Depth of cut =15 µm

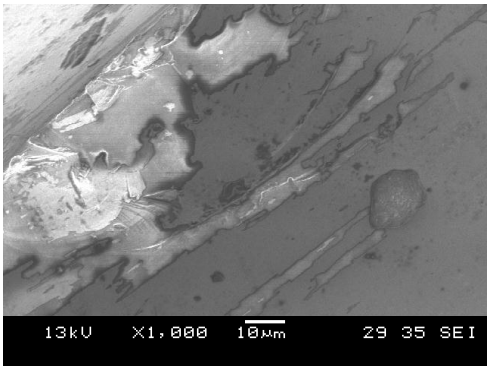

(e)Depth of cut =20µm

Fig.7. 5: Sub-surface damage of Bk7 glass during micro-grinding varying depth of cut using spindle speed of 2500 rpm.

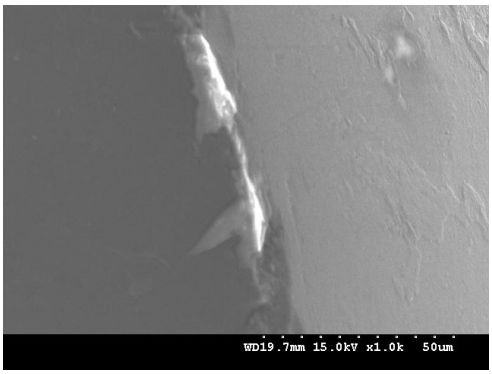

(a)Depth of cut =2µm

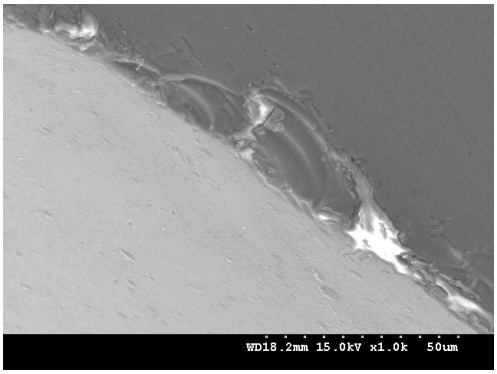

(b) Depth of cut =5 µm

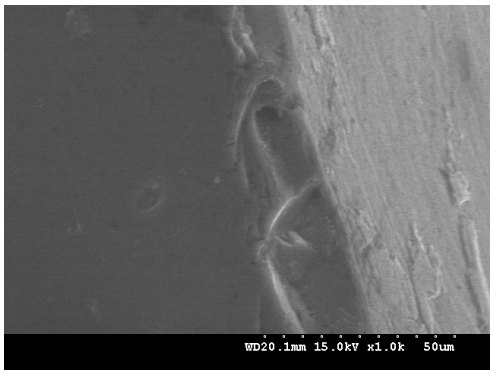

(c)Depth of cut=10µm

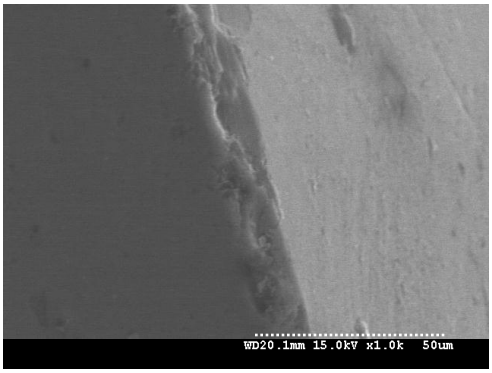

(d) Depth of cut=15 µm

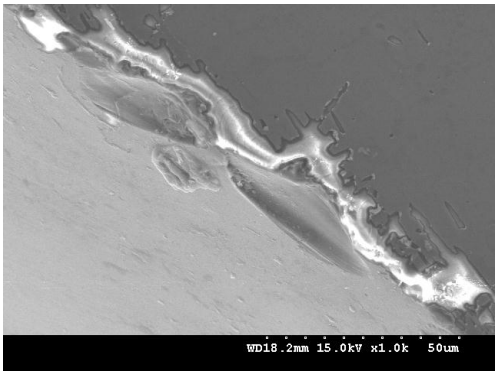

(e)Depth of cur=20µm

.

Fig.7. 6: Sub-surface damage of Bk7 glass during micro-grinding varying depth of cut using spindle speed of 2000 rpm**.**

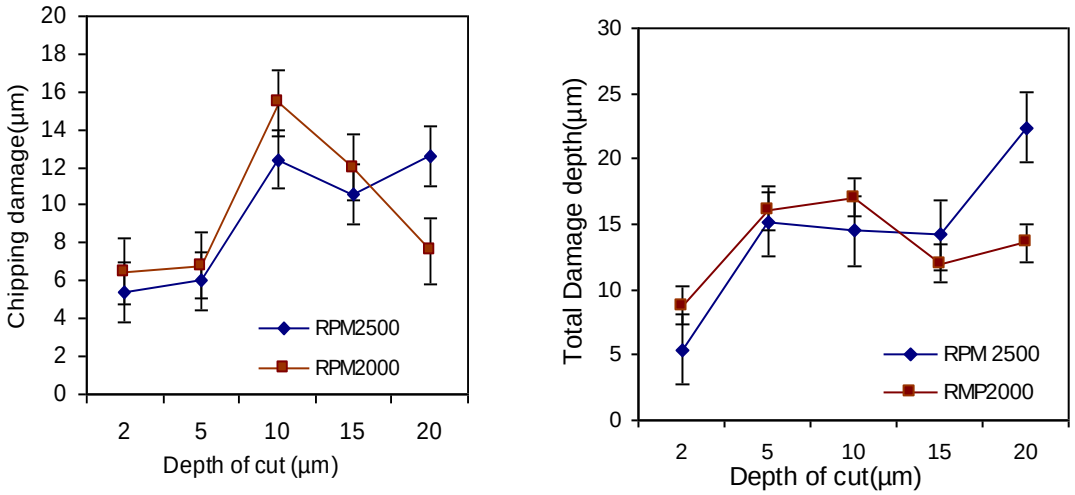

(a) (b)

Fig.7. 7: Effect of depth of cut on the chipping layer thickness and total damage depth.

The damaged layer found right underneath the machined surfaces seems likely to be generated by means of chipping manner. As shown in Fig.7.5 and 7.6, grain dislodgement seems to be contributing largely to the induction of this type of chipping layer. During micro-grinding process, the contact of an individual diamond particle with the glass work piece might produce this damage zone which contains distributed grain-boundary micro-cracks. The dislodgement of individual grains resulting from the grain-boundary micro fractures consequently contributes to this damage layer. This fact might reveal that the chipping layers might be introduced by this grain dislodgements phenomenon. Apart from this, micro-cracks are also found to be existed while taken higher magnification view (as indicated by arrows) as shown later in Fig. 7.10 in the subsurface layer of the ground surface, usually under the chipping layer.

In order to determine the total damage, it would be interesting to club together both the modes of damage known as total damage which contains both chipping and cracking layer. The depths of total damage layer measured from the FESEM images were plotted in Fig.7.7. It is found from the graph that with the increasing value of depth of cut the total damage depth also increasing initially. Then further increment of depth results in a dropping of total damage layer then finally again tends to increase. This trend is similar for both the spindle speed. As like chipping layer it is also noticed that the lower spindle contributes to higher depth of damage than higher one.

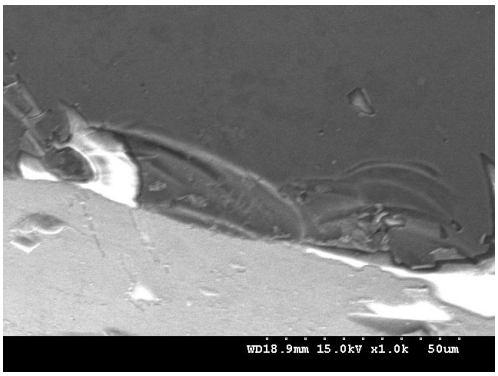

(a)Feed=1 µm/min

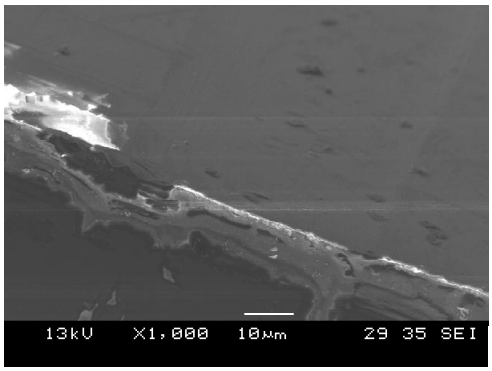

(b) Feed=10 µm/min

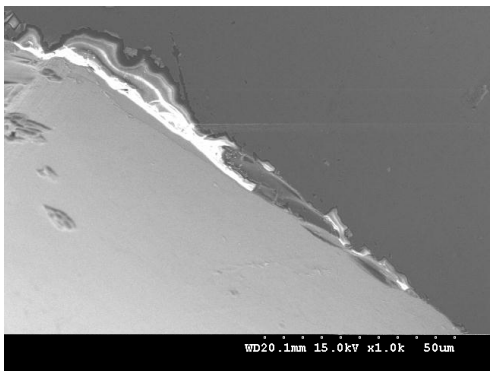

(c)Feed=25µm/min

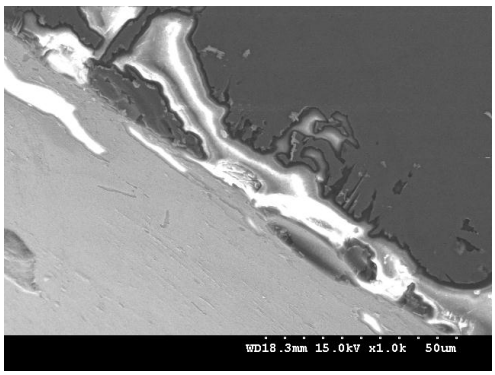

(d) Feed=50 µm/min

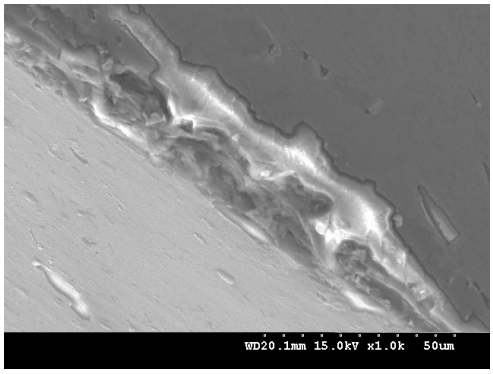

(e)Feed=100 µm/min

Fig.7. 8: Sub-surface damage of Bk7 glass during micro-grinding varying feed rate using spindle speed of 2500 rpm.

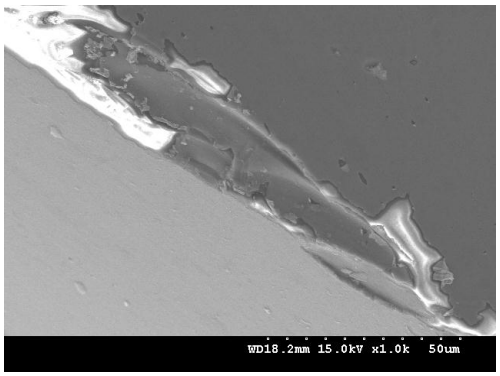

(a)Feed=1 µm/min

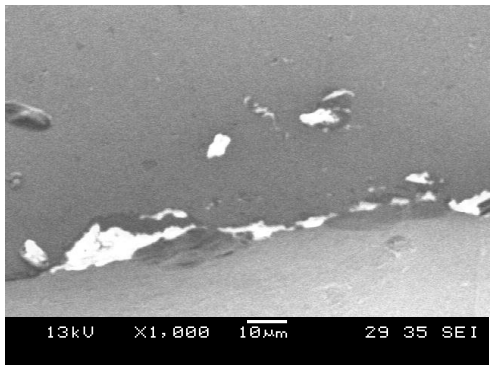

(b) Feed=10 µm/min

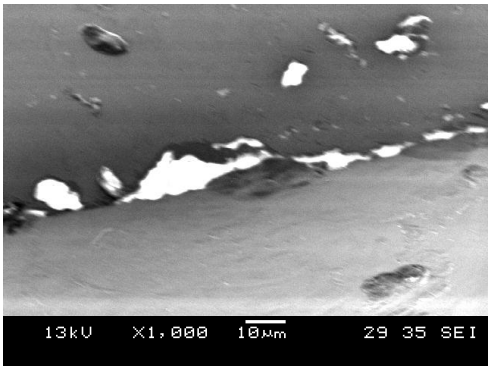

(c)Feed=25µm/min

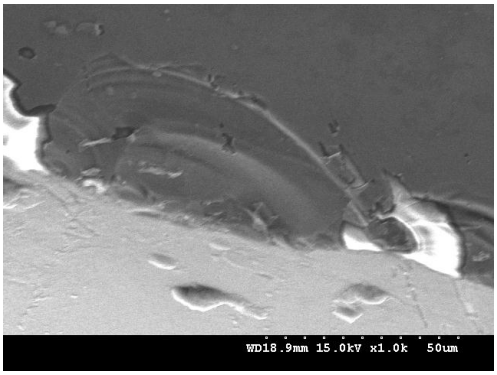

(d) Feed=50 µm/min

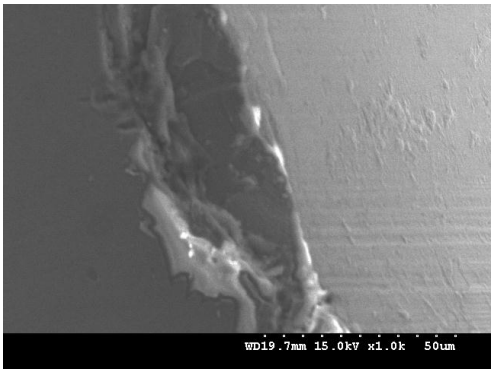

(e)Feed=100 µm/min

Fig.7. 9: Sub-surface damage of Bk7 glass during micro-grinding varying feed rate using spindle speed of 2000 rpm

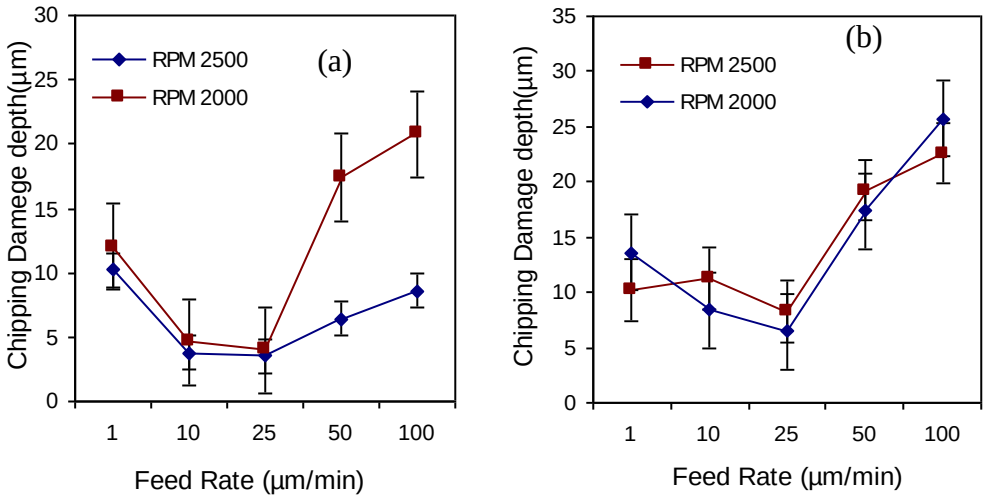

Fig.7. 10: Effect of feed rate on the chipping damage depth and total damage layer thickness.

The effect of feed rate on the sub-surface damages is found in Fig.7.8, 7.9, and 7.10. It is seen that the depth of damage decrease initially with the increasing feed rate. After this

initial reduction, this damage starts to grow again with the increase of feed rate. This trend is true for both chipping and total damage in case of different spindle speed also. This reduction of depth of damage can be explain with the fact that using very low feed rate causes the generation of lower thickness of chip, consequently introduce ploughing phenomenon and the contact time of PCD tool with the surface also higher, which might cause the increased damage layer depth. As the feed rate increase, this contact time will reduce and rubbing of surface also decrease which cause this initial reduction of damage layer depth. It is found from Fig.7.10 that until 25µm/min, the damage layer has decreasing trends, after that it again starts to increase along with the increment of feed rate. This increasing tendency of damage layer is probably due to higher feed rate which causes the deeper penetration depth and deeper crack depth consequently it results the brittle mode cutting. As this is the case of glass grinding, slightly higher feed rate even can initiate cracking or damage layer (Gu et al., 2011).

7.3.3. Subsurface Crack Configuration

The amorphous structure of glass makes it brittle. Because glass doesn't contain planes of atoms that can slip past each other, there is no way to relieve stress. Excessive stress therefore forms a crack that starts at a point where there is a surface flaw. Particles on the surface of the crack become separated. The stress that formed the crack is now borne by particles that have fewer neighbors over which the stress can be distributed. As the crack grows; the intensity of the stress at its tip increases. This allows more bonds to break, and the crack widens until the glass breaks. Slip is the predominant mechanism of plastic deformation. The limited dislocation movement does not allow glass material to accommodate a large scale plastic deformation as what happens in metallic material before fracture. The very nature of grinding process can cause a continual introduction of fresh dislocations due to the shear stress. There should be a link between the introduction of new dislocations and crack nucleation (Zhang et al., 2003).

Sub-surface cracks have been observed in the cross sectional view of the ground glass specimen (Fig.7.11) using higher magnification. Median, lateral and hertzian cone cracks have been reported as the major crack types when machining brittle materials. In the

cross section image shown in Fig. 7.11(a) the median and lateral cracks are found to be exist. These median cracks are perpendicular to the glass surface largely contribute to deeper the subsurface damage and potentially to some material removal thorough the interaction with the other cracks. The size of the median crack found from the FESEM image is nearly o.5 µm to 1.0 µm. The subsurface median cracks were found to be in deeper depth when the depth of cut increases. Lateral cracks were initiated and propagated by the residual stresses only close to the plastic deformation. By their geometry it is clear that the formation of lateral cracks will largely lead to the material removal and will contribute significantly to the observed surface roughness. The size of the lateral crack was found to be nearly 1 µm. Hertzian cracks are cone crack that will also contribute largely to the deeper sub surface damage and also the removal of some material through the interaction of some others cracks as well. From Fig.7.11 (e), the size of this category crack has been found to be nearly more than 2 µm. Hertzan crack arising at the edge of the compressed region followed by a conical propagation of the crack in material. Increasing the loading further generated the second third and additional similar cracks. It was demonstrated by Hertz that there was considerable scatter in the loads needed to cause such cracking with the fixed experimental geometry.

Combined with the grain dislodgment evidence obtained from Fig.7.5, 7.6, 7.8, and 7.9, it is inferred that material removal of this glass is dominated by brittle fracture either by dislodgement or lateral cracking. As seen from Fig.7.11 (a), the pores are apparently visible because of the pulling off of the glass particles. These pores can be a reason of crack expansion and deepen the damage layer.

A tortuous crack observed in the Fig.7.11 (h) was about to cleave several grains into pieces. The connection of median and lateral crack was arrested at the grain boundaries that hinder any further propagation of the crack in surroundings grains. The grain boundaries served a crucial role to confine the propagation of micro-crack and also pulverization process at local level. Because of unloading, lateral crack was produced before the median crack reached to its full depth. This lateral crack evident at the bottom of median crack tells that this median crack will not extends below it, which also suggests

that shielding has occurred. When considering grinding processes, sliding must be taken into account and friction between the tool grain and glass surface becomes important. This type of movement leads to a change in the stress distribution such that pick tensile stress is at the trailing edge of the particle. Fracture at the surface will then have the shape of ar which is also known as cone crack. Fig.7.11 (f) has shown the trailing indent crack.

(a)

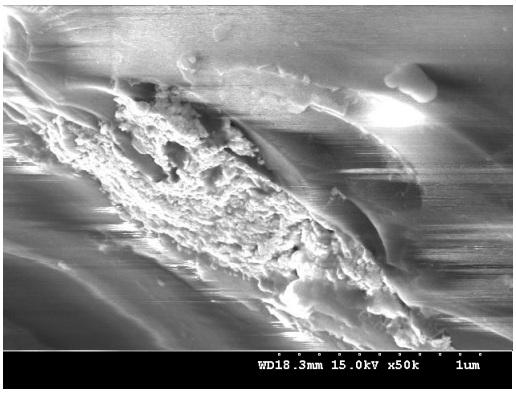

(b)

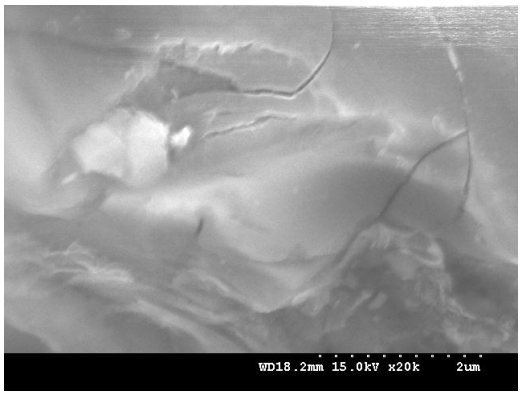

(c)

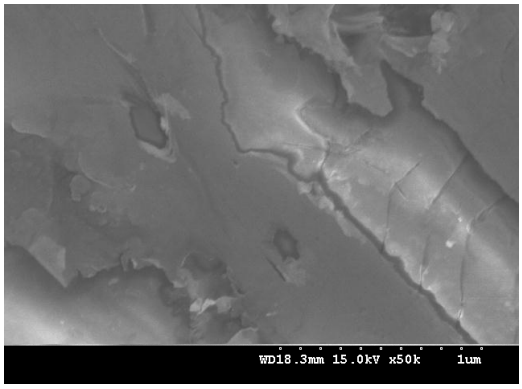

(d)

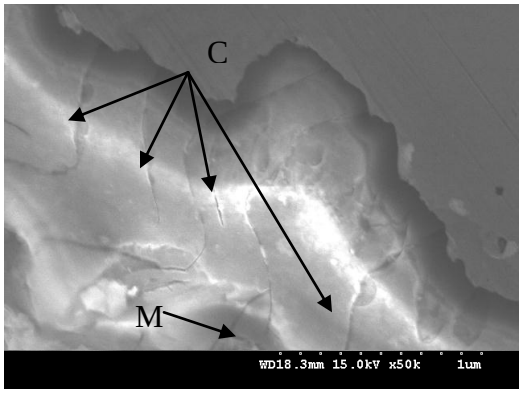

(e)

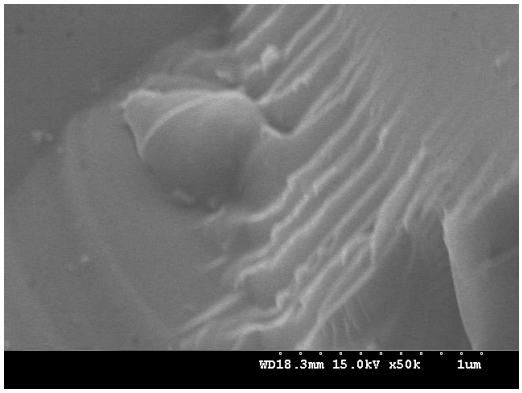

(f)

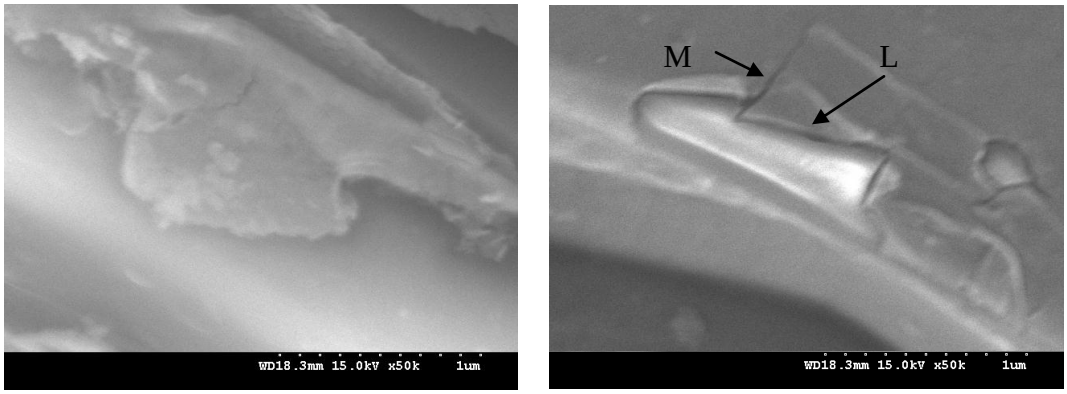

(g) **(h)**

Fig.7. 11: Micro-crack observed from the subsurface layer of BK7 glass. (G.D=grain dislodgement, P=Pulverization, M=Median crack, C=Cone, L=lateral)

Observation has also been done on the ground surface. These surfaces look fracture free or ductile mostly. However, cross sectional microscopy still reveal subsurface cracks. This is very important observation. It leads to the fact that when machining brittle material likes glass, whether the machining is in ductile regime cannot be assured by only observing the machined surface.

7.3.4. Analysis of Surface Roughness

In addition to the SEM image observation of damage layer surface roughness also act as an indicator of characterize the material removal process during grinding. Although the quality of surface generated during grinding largely dependent on the material properties rather than cutting condition during grinding of brittle material, still it can work as parameter to identify the sub-surface damage(Perveen et al.). The surface roughness data has been plotted in Fig.13 (a) and (b) with respect to depth of cut and feed rate. Each data point is an average of five measurements and the error bar indicated the maximum and minimum values of surface roughness.

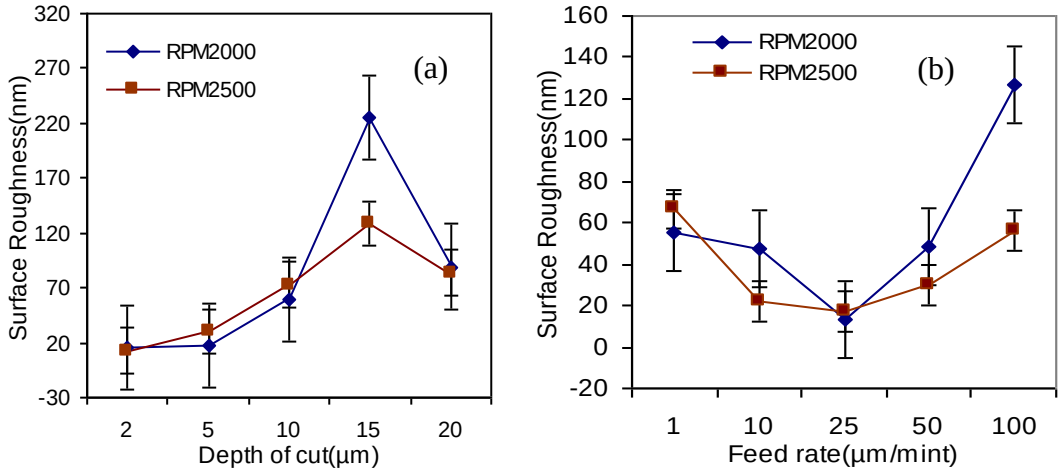

Fig.7. 12: (a) Effect of depth of cut on surface roughness (b) effect of feed rate on surface roughness.

It can be seen from the Fig.7.12 (a) that surface roughness increases initially with the increase of depth of cut and the decreases with the increases of depth of cut. This increased depth of cut would normally lead to the greater grinding force and thus worsen the surface finish. In other words, surface roughness value was supposed to be increased. The elevated temperature in grinding zone due to the increased depth of cut might explain the contradictory result of surface roughness. The increase of depth of cut makes the coolant penetration difficult into grinding zone and thus reduces the cooling effects. Thus might cause a local temperature elevation in the grinding zone, consequently soften the work pieces surface and thus promoting ductile mode cutting or reduce the brittle mode cutting. As a result a slightly improved surface finish is evident in the Fig.7.12 (a) even with the further increment of depth of cut (H. Huang, 2003). Obviously more effect is needed to take into account thermal aspects in the mechanism of material removal and damage generation. It can also be noticed that higher level of spindle speed also improved the surface roughness slightly. This surface roughness value shows the significant agreement with the grinding damage value for different value of depth of cut.

Fig.7.12 (b) shows the effect of feed rate on surface roughness. It is found that with the increase of feed rate surface roughness initially get decrease and then finally starts to increase. Initial reduction can be explained with the rubbing effect due to the very low feed rate. With the increase of feed rate this rubbing effect is eliminated. Further increase

of the feed rate will cause the generation of higher chip thickness and brittle mode cutting initiate consequently resulting increment of surface roughness again. Again, using higher spindle speed can improve surface roughness a little also. This trend of surface roughness also shows good agreement with sub–surface damage, although this surface roughness cannot reveal the morphology of sub-surface damage.

7.4. Concluding Remarks

In order to develop an individual process, it is very important to know the subsurface damage induced by each machining process. Such knowledge for surface grinding of BK7 glass by on machine fabricated PCD tool has been provided by this study.

The following conclusion can be drawn from the above studies.

- Ground surface consists of four different areas (a) the smooth area; (b) the fracture area; (c) the smeared area; (d) the ploughing striations.
- At low rate of material removal, the cutting points on the tool remove and expel the material from the machined surface in an efficient manner. At high rates of material removal however debris is not expelled efficiently and the debris generated from the cut must pass between the tool and machined surface and hence influence the machined surface and as well as sub-surface.
- It is noticed that chipping damage grows with the increase of depth of cut. With the further increase of depth of cut it shows jig jag trend of decreasing and increasing afterward. Total damage also shows the same trends along with the change of depth of cut
- It is also found that SSD of ground surface using lower spindle speed are quite larger. This might be due to the fact that, the abrasive have certain mechanical load intensity, hence they might be smashed under a certain wallop. Higher spindle speed will have usually higher probability to produce higher wallop. Under lower spindle speed the abrasives have a lower tendency to crash into further smaller pieces. As a result, larger size abrasives take part in the grinding and consequently produce larger sub-surface damage.

- It is found from the graph that with the increasing value of depth of cut the total damage depth also increasing initially. Then further increment of depth results in a dropping of total damage layer then finally again tends to increase.
- It is seen that the depth of damage decrease initially with the increasing feed rate. After this initial reduction, this damage starts to grow again with the increase of feed rate. This trend is true for both chipping and total damage in case of different spindle speed also.
- During micro-grinding process, the contact of an individual diamond particle with the glass work piece might produce this damage zone which contains distributed grain-boundary micro-cracks. The dislodgement of individual grains resulting from the grain-boundary micro fractures consequently contributes to this damage layer. This chipping layer is an outcome of either intergranular or transgranular micro-cracking due to localized stress field or shear stresses superimposed by hydrostatic compressive stresses induced by the abrasive grain. Usually when the fracture resistance in the grain boundary and in the grain has same level; the crack would always prefer to follow the shortest way and the fracture path would always be transgranular.
- Grinding induced subsurface crack exhibit different configuration likely median lateral, branch, and cone. These crack size is found to be nearly 1µm. Subsurface crack may exist under those ground surface which look even fracture or damage free by the microscopic observation.
- It can be seen that surface roughness increases initially with the increase of depth of cut and the decreases with the increases of depth of cut. It is found that with the increase of feed rate surface roughness initially get decrease and then finally starts to increase. This trend of surface roughness also shows good agreement with sub–surface damage, although this surface roughness cannot reveal the morphology of sub-surface damage.

Chapter 8

Modeling of Vertical Micro Grinding

8.1 Introduction

Although there has been a lot of research on conventional grinding, very little knowledge has been accumulated on micro scale grinding due to the fact that it is an emerging field of research. This micro scale grinding is sharing some aspects with the conventional grinding. Grinding process is a complex process due to its multi-cutting points and also because it is influenced by numerous parameters as well. The early grinding models developed are based on the parameters such as wheel and work piece velocity, depth of cut and grit size of the grinding wheel. Those early models showed that the grits penetrate and cut the material from the work piece surface and the generated grinding forces are proportional to the material removal. However those models are not suitable for micro grinding because of mode of material removal and the method of contact between surfaces are different from the macro scale method. Due to the small feed rate used in glass machining, ploughing force needs to be considered in addition to the chip formation force.

Micro scale grinding process apparently resembles the conventional grinding in terms of its stochastic nature. It is distinctive in view of size effect on the interaction between a single grit and work piece. So the analytical model considering individual grit interaction is a critical factor in micro grinding process. This single grit interaction can be characterized by micro cutting with a high negative rake angle at high strain rate. The size effect can be applied through the coupling of micro cutting and ploughing mechanism with the associated friction effects within the single grit interaction for the micro grinding process(Kopalinsky and Oxley, 1984; Oxford; UK; 9-12 Apr.; Shaw, 2003).

The normal force generated during grinding is related to the actual area of contact between surfaces, grit density and force generated per grit. Hence, the model development can be subdivided into several steps as follows.

- Modeling of chip formation
- Modeling of chip formation force for individual grain
- Modeling of ploughing force for individual grain
- Modeling of Grinding force

8.2 Modeling of chip formation

Grinding tool topography plays an important role in the interaction between tool and work piece during chip formation. The most relevant tool surface parameter that governs the chip formation process is the number of dynamic cutting edges engaged in work pieces during machining process. The number of cutting edge is the base to estimate the whole tool surface performance based on the understanding of the local grain effects. For instance, the total grinding force can be deduced from the total number of active grains multiplied by the average grain force.

Again the number of dynamic cutting edges not only depends on the distribution of static cutting edge but also depends on the kinematics grinding conditions and dynamic grinding effects. The static number of cutting edges depends on the grain size, wheel porosity and dressing condition.
The static cutting edge density function is depicted as following(Hecker et al., 2003).

$C_{s(z)} = A\, Z^{k}$ …… (1)

Where $C_{s(z)}$= Static cutting density(mm^{-2})

A= Empirical constant

Z=Radial distant measured into the wheel (µm)

The static density of Eqn.(1) is modified due to the inward deflection δ, as the normal force developed by the grain engagement. This deflection is considered to be a local effect for every grain. Hence, the original coefficients A and K are not considered to be affected, while the new inputs to the static grain distribution function can be evolved in order to take care of this deflection is as follows(Shaw, 1996).

$Z' = Z + \delta$

Hence, Eqn.(1) can be written as follows.

$C_{s(z')} = A\,(Z')^{k}$ ..... (2)

As because every active cutting edge removes a space of material and those grains behind and near the active one could not get any material to remove, reduction of cutting edges takes place. It is considered that each active grain produces a 3-D shadow that reduces the active zone volume on the wheel periphery, where active grains are found. Hence, the active cutting edge density deduced by Heckar et al.(Hecker et al., 2003) is as follows.

$C_{d(z')} = C_{s(z')}(1-V_{sh}/V_t)$ …….. (3)

V_t= total volume on the periphery of the wheel engaged in the work piece

V_{sh}= total kinematic shadow volume generated by active cutting edge

V_{sh}/V_t represents a reduction in the possibilities for each cutting edge to find material to remove in its path and consequently considered as active.

Grits on the wheel active surface becomes either active or inactive depending on the contact between the wheel-work asperities. Increasing the area of contact increases the number of grits in action. Moreover, the benefit of micro-grinding is that the grain density per unit area remains constant throughout the process which can produce more uniform material removal from the work piece.

After dressing the PCD tool using Block EDM process, the cutting edges on the grain can be considered as equivalent to a spherical edge based on another assumption that one grain only acts as one cutting edge. The diameter of equivalent spherical grain can be determined from the geometrical interaction between tool and work piece which can be deduced later on. Firstly, the diameter of the grain contact circle d_c can be deduced as follows(Verkerk and Peters, 1977).

$d_c = \sqrt{a_c}\, b_c$ ..... … (4)

Where, a_c is the maximum contact length of grain in the cutting direction and b_c is the cutting width of the grain, d_c = diameter of contact grain circle.

When the cutting depth of grain *t* is available, the diameter of the equivalent grain d_{geq} can be determined from the geometry as follows.

$$d_{geq} = (t^2 + (d_c/2)^2)/t \quad \ldots\ldots (5)$$

Usually the size of the dressed grain will be smaller than the original one, but this equivalent grain diameter of the cutting edge can be smaller or larger than the original diameter of the grain. The equivalent grain diameter depends on the shape of the grain and depth of cut of the grain (Hecker et al., 2003).

Vertical surface micro-grinding can be compared to the face milling operation, wherein the cutter rotates in the horizontal plane with the work piece being fed into it. Fig. 8.1 shows the schematic diagram of the vertical micro-grinding process where the pattern of chip formation with a continuous tool has been given as well.

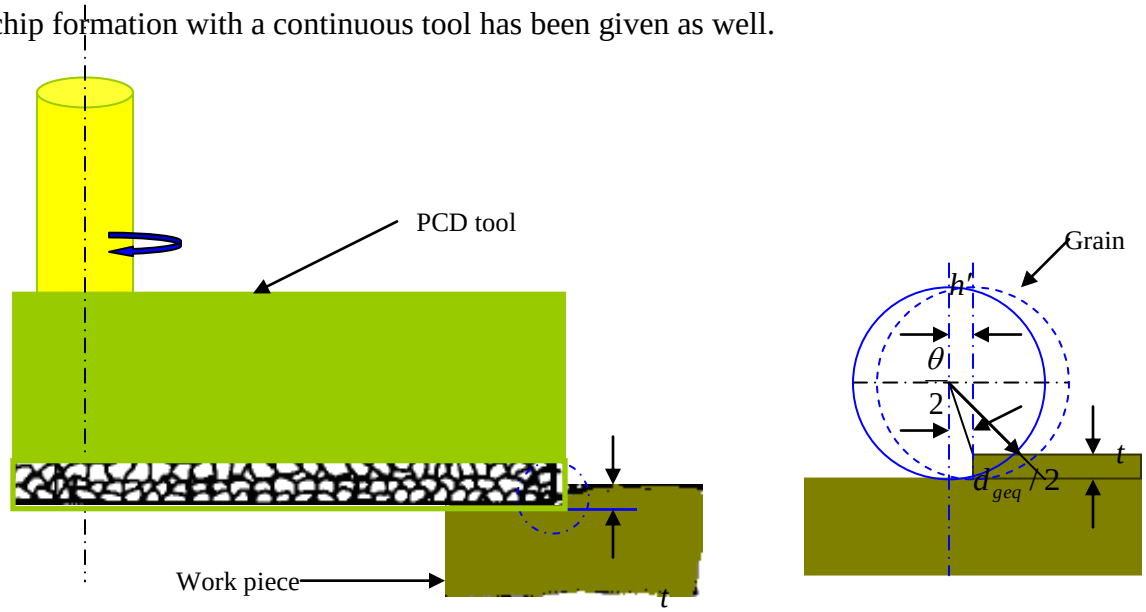

(a) (b)

Fig.8. 1.Vertical surface grinding (a) schematic diagram (b) Chip formation.

The unreformed chip thickness h increases from zero to a maximum value as a grain takes an approximate circular path. The feed per grain s is calculated to be $(v/C_{d(z')}V)$ where, v is the table feed and V is the PCD tool rotational speed and $C_{d(z')}$ is the linear dynamic grain density. From Fig.1 (b), the arc length l' can be written as follows.

$$l' = d_{geq}\,\theta/2 \approx \sqrt{d_{geq}\,t} \quad \text{..... (6)}$$

Where, t is the depth of cut. Now, putting the value of d_{geq} from Eqn. (5) in Eqn.(6).

$$l' = \sqrt{(t^2 + (d_c/2)^2)} \quad \text{..... (7)}$$

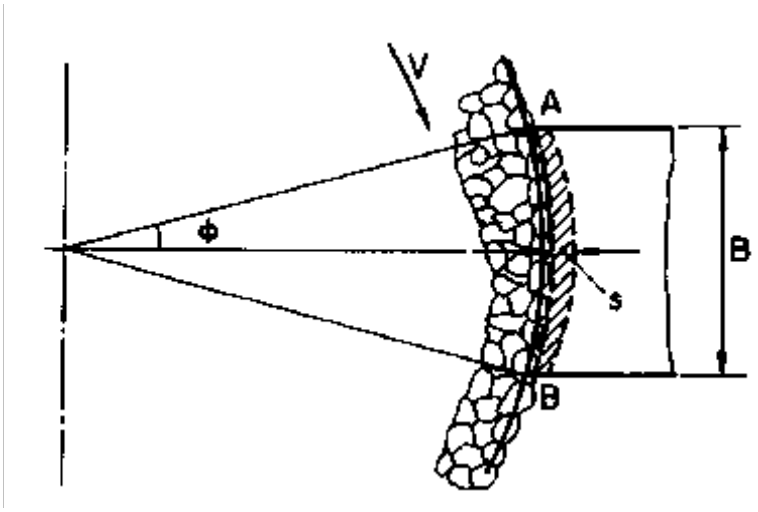

(a)

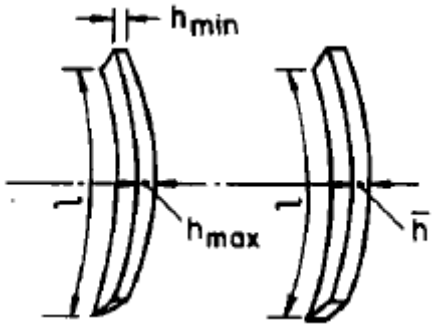

(b)

Fig.8. 2.(a) Schematic diagram of the vertical micro grinding (b) actual chip shape (c) idealized chip shape.

Now the length of the chip *l* during the micro-grinding of work pieces of width equal to the tool diameter *D* can be evaluated from the Eqn. below.

$$l = D\varphi \quad \text{..... (8)}$$

$$\varphi = \cos^{-1}\left[1-(B/D)^2\right]^{1/2} \approx B/D\left[1+(B/2D)^2\right]^{1/2} \quad \text{..... (9)}$$

From the Eqns. (8) and (9), value of *l* can be deduced as follows.

$$l = B\left[1+(B/2D)^2\right]^{1/2} \quad \text{..... (10)}$$

The cross sectional area of the chip A_m can be deduced from the Fig. 2(b) as follows.

$$A_m = (\pi d^2{}_{geq}\ \frac{\theta}{2\pi} + d_{geq}\bar{h}) - (\pi d_{geq}{}^2\ \frac{\theta}{2\pi} + d_{geq}\bar{h}\ \frac{d_{geq}-t}{d_{geq}}) = \bar{h}t \quad \text{..... (11)}$$

And now the volume of chip V_{chip} can be calculated from the cross sectional area A_m and the length of chip *l*.

$$V_{chip} = A_m l = \bar{h}tB\left[1+(\frac{B}{2D})^2\right]^{\frac{1}{2}} \quad \text{..... (12)}$$

Therefore the volume of chip material Vol_{chip} removed in time τ can be expressed as follows.

$$Vol_{chip} = C_{d(z')}V\tau\bar{h}tB\left[1+(\frac{B}{2D})^2\right]^{\frac{1}{2}} \quad \text{..... (13)}$$

Again, the volume of the material removed from the work piece V_{wp} during the same machining time τ can be expressed as follows.

$$V_{wp} = vtB\tau \quad \text{..... (14)}$$

A different approach to calculating the undeformed chip thickness is based on making material balance between of the chips produced at the cutting points and the overall removal rate. Hence, equating the volume expression from the Eqns. 13 and 14 gives the mean undeformed chip thickness(Srihari and Lal, 1994).

$$\bar{h} = \frac{v}{VC_{d(z')}\left[1+(\frac{B}{2D})^2\right]^{\frac{1}{2}}} \quad \text{..... (15)}$$

where $\bar{h}$ = undeformed thickness, v =Feed rate, V= spindle speed, B= work piece width, D= tool diameter, $C_{d(z')}$ =dynamic cutting edge density.

From this undeformed thickness $\bar{h}$ the line spacing, *L*, between successive cutting points can also be determined. Now, if the average effective cutting width for each cutting point can be denoted as $\bar{b}_c$, the number of cutting points N_g around any line on the PCD tool periphery is equal to $C_{d(z')}$ times the area given by the tool circumference multiplied by the effective cutting width (Malkin, 1989).

$$N_g = C_{d(z')}(\pi D\bar{b}_c) \quad \text{.....(16)}$$

As $N_g = \frac{\pi d_{geq}}{L}$ ..... (17)

The line spacing can also be derived as follows.

$$L = \frac{1}{C_{d(z')}\bar{b}_c} \quad \text{..... (18)}$$

Hence, the expression for chip thickness $\bar{h}$ and number of cutting edge N_g can be deduced from this section.

8.3. Modeling of chip formation force for individual grain

Basuray et al have related the transition point from the ploughing to microchip formation to a critical rake angle. According to the geometrical relationship, the critical rake angle can be expressed by the minimum undeformed chip thickness and the cutting edge radius as follows (Basuray et al., 1977).

$$\alpha_{cr} = \sin^{-1}(\frac{d_{geq} - 2\bar{h}}{d_{geq}}) \quad \text{..... (19)}$$

Where α_{cr} is critical rake angle, $\bar{h}$ is minimum chip thickness, d_{geq} is the equivalent grain diameter.

In the micro grinding, the instantaneous rake angle is obtained from a geometrical relationship as follows.

$$\alpha_s = \sin^{-1}\frac{(d_{geq} - 2h)}{d_{geq}} \quad \text{.....(20)}$$

Where h is the undeformed chip thickness

Above the minimum uncut chip thickness, the micro-cutting mechanism can be represented by using Merchant's model to each of the infinitesimal elements. let us consider an element of undeformed chip thickness, $d\bar{h}$, being cut at a position corresponding to the associated local rake angle, a pair of chip formation and thrust forces can be related with the friction and rake angle as shown in Fig. 3. Therefore, the incremental micro-cutting force df_{cgx} in the two dimensional simplified configuration can be expressed as the following Eqn.(Liu and Li, 2001; Son et al., 2005).

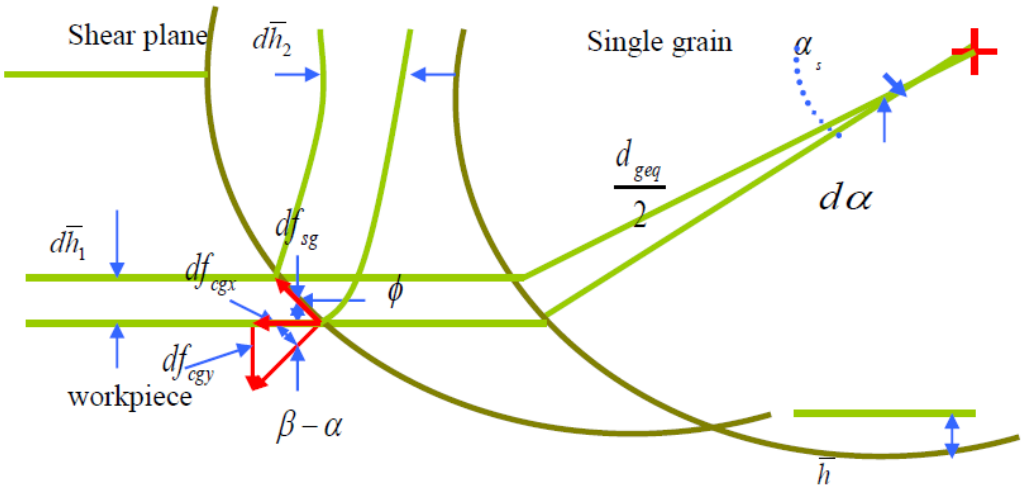

Fig.8. 3.The relationship between infinitesimal cutting and tangential force.

$$df_{cgx} = -\frac{\sigma_s \cos(\beta - \alpha)}{\sin\phi \cos(\phi + \beta - \alpha)} d\bar{h}_1 \text{ .... (21)}$$

Here, df_{cgx} is the incremental cutting force, σ_s is the shear strength of the material, β is the friction angle, and ϕ is the shear angle. The grain shape is assumed to be approximately spherical shape in order to model the single grit interaction. The cross section area of an ideal spherical shape grain dA between the increment of depth of cut and rake angle is given as follows:

$$dA = 2(d_{geq}/2)^2 \cos^2\alpha . d\alpha = \frac{d^2{}_{geq} \cos^2\alpha . d\alpha}{2} \text{ .... (22)}$$

Hence the total chip formation force per grain f_{cgx} can be deduced as follows.

$$f_{cgx} = \int_{\alpha_{cr}}^{\alpha_s} \frac{\sigma_s \cos(\beta - \alpha)}{2\sin\phi \cos(\phi + \beta - \alpha)} d_{geq}{}^2 \cos^2\alpha . d\alpha \text{ .... (23)}$$

The incremental normal force df_{cgy} can be expressed in term of f_{cgx} as follows.

$$df_{cgy} = df_{cgx} \tan(\beta - \alpha) \text{ ....(24)}$$

Finally, the overall expression for normal force per grain can be expressed as follows.

$$f_{cgy} = \int_{\alpha_{cr}}^{\alpha_s} \frac{\sigma_s \sin(\beta - \alpha)}{2\sin\phi \cos(\phi + \beta - \alpha)} d_{geq}{}^2 \cos^2\alpha . d\alpha \text{ .... (25)}$$

8.4. Modeling of ploughing force for individual grain

The work piece material below the minimum undeformed chip thickness experiences a different phenomenon in the micro scale grinding process. In this region, the material is plastically deformed in the front of the grit without formation of chips. The plastic deformation is known as ploughing force and this force developed during single grain interaction can be formulated by the association of this process with the Brinell hardness test. The Brinell hardness number, HB, is defined as the ratio of the load f_{brnl} to the curved area of indentation(Shaw, 1972).

$$HB = \frac{2 f_{brnl}}{\pi d(d - \sqrt{d^2 - b^2})} \quad \text{..... (26)}$$

Where d is the diameter and b is the diameter of impression.

In our analysis, the indentation force acting in the direction of α_{cr} with respect to the normal direction is attributed to the ploughing force. The total tangential and normal ploughing force per grain can be calculated by combining the indentation effect with the friction reaction as follows.

$$f_{pgy} = f_{brnl}(\sin\alpha + \mu_p \cos\alpha) \quad \text{..... (27)}$$

$$f_{pgx} = f_{brnl}(\cos\alpha - \mu_p \sin\alpha) \quad \text{..... (28)}$$

Here μ_p is the ploughing friction coefficient.

This ploughing friction coefficient μ_p can be estimated using extended predictive model of Goddard and Wilman and Sin and Suh as follows(Goddard and Wilman, ; Sin et al., 1979).

$$\mu_p = \frac{2}{\pi}\left[\left(\frac{w}{d_{geq}}\right)^{-2}\sin^{-1}\left(\frac{w}{d_{geq}}\right) - \left\{\left(\frac{w}{d_{geq}}\right)^{-2} - 1\right\}^{\frac{1}{2}}\right] \quad \text{..... (29)}$$

Where, w is the width of indentation and d_{geq} is equivalent grain diameter.

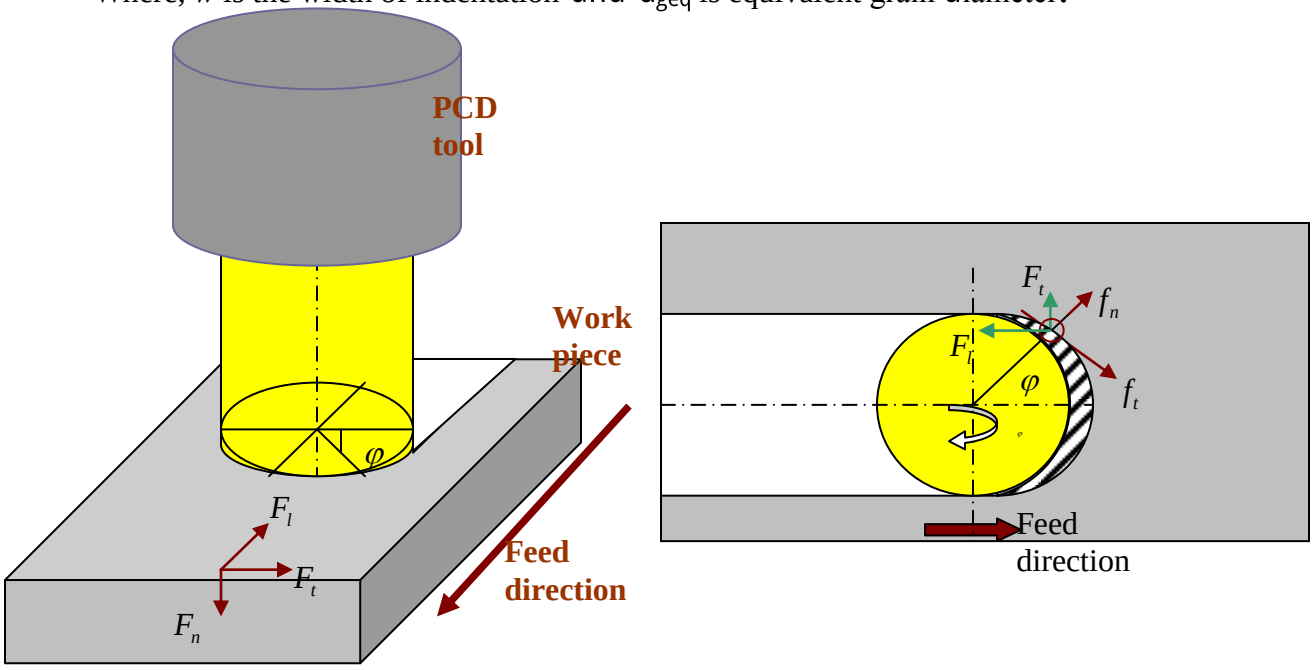

(a) (b)

Fig.8. 4: Micro-scale grinding force

8.5. Modeling of grinding Force

Total grinding force per grain can be calculated by combining the cutting force and ploughing force together.

$$f_n = f_{cgy} + f_{pgy}.$$

$$f_n = \int_{\alpha_{cr}}^{\alpha_s} \frac{\sigma_s \sin(\beta-\alpha)}{2\sin\phi\cos(\phi+\beta-\alpha)} {d_{geq}}^2 \cos^2\alpha.d\alpha + f_{brnl}(\sin\alpha + \mu_p \cos\alpha) \text{ …….. (30)}$$

$$f_t = f_{cgx} + f_{pgx}$$

$$f_t = \int_{\alpha_{cr}}^{\alpha_s} \frac{\sigma_s \cos(\beta-\alpha)}{2\sin\phi\cos(\phi+\beta-\alpha)} {d_{geq}}^2 \cos^2\alpha.d\alpha + f_{brnl}(\cos\alpha - \mu_p \sin\alpha) \text{ …… … (31)}$$

Traditionally, the shear angle solution from Ernst and Merchant model has been widely used. In this model we have also used that expression of Ernst and Merchant model as follows(Merchant, 1945).

$$\phi = \frac{\pi}{4} - \frac{1}{2}(\beta-\alpha) \text{ …… (32)}$$

The resulting force F_{res} in vertical grinding can be resolved into three components, the normal force F_n, the longitudinal force F_l and the transverse force F_t as shown in Fig.8.4. These forces can also be thought of as the sum of the individual grain force along the PCD tool and work piece interface and can be written as follows.

$$F_n = \sum_{i=1}^{N_g} (f_n)_i \cos\frac{\theta}{2} \text{ …… (33)}$$

$$F_t = \sum_{i=1}^{N_g} (f_t)_i \cos(\phi)_i + (f_n)_i \sin(\frac{\theta}{2}).\sin(\phi)_i \text{ …… (34)}$$

$$F_l = \sum_{i=1}^{N_g} (f_t)_i \sin(\phi)_i + (f_n)_i \sin\frac{\theta}{2}.\cos(\phi)_i \text{ …… (35)}$$

Here N_g is the number of active cutting edge, f_n and f_t are the normal and tangential forces on a single grain.

It is clear from the Fig.8.4 that second term on the right hand side of the Eqn. 34 and the first term on the right hand side of Eqn. 35, are zero when integrated over the path AB. Hence become reduced to the following format.

$$F_t = \sum_{i=1}^{N_g} (f_t)_i \cos(\phi)_i \quad \text{..... (36)}$$

$$F_l = \sum_{i=1}^{N_g} (f_t)_i \sin(\phi)_i \quad \text{..... (37)}$$

Alternatively, these three Eqns. can be written in following way.

$$F_n = f_n N_g \frac{B}{D} \sqrt{1 - \frac{t}{d_{geq}}} \quad \text{..... (38)}$$

$$F_t = f_t N_g \frac{B}{D} \quad \text{..... (39)}$$

$$F_l = f_n N_g \frac{B}{D} \sqrt{\frac{t}{d_{geq}}} \quad \text{..... (40)}$$

8.6. Simulation and verification of the model

This newly developed analytical model considering the grain interaction for micro-grinding has been simulated and compared with the experimental results.

Typical average values of grit size for the grinding tool have been deduced by using the formula derived by previous researchers. In this study, the dynamic grain density has been taken from the literature value (Li and Liao, 1997). The values of grain length and width involved in cutting have been assumed to calculate the average grain diameter. Then, the values of grain depth have been used to calculate the equivalent grain diameter d_{geq}. Again, using the spindle speed, dynamic cutting edge density value and feed date, undeformed chip thickness values have been calculated. For different feed rate values,

there will be several undeformed chip thicknesses, the lowest one has been chosen as minimum undeformed chip thickness.

Now, as we know both the chip thickness value, and equivalent grain diameter, rake angle can be deduced using these two parameters from Eqn.20. In addition, chip formation force for each grain has been calculated from Eqns. 23, 24, and 25 using MAT LAB simulation where properties of BK7 have been used. As, the rake angle is already known, ploughing force for each grain can also be calculated using Eqns. 27 and 28. The cumulative value of chip formation and ploughing force will give the total force per grain. Total grain on the tool periphery has been calculated using Eqn. 16. Finally, using Eqns.38, 39 and 40, it has been possible to calculate the predicted force value for different depth of cut and different feed rate.

The predictions of micro grinding forces were obtained on the basis of the above equations derived and micro grinder tool specifications. Then the model verification was conducted on the basis of comparing overall micro grinding components for PCD tool of diameter 670μm. In case of experiment, to measure the micro scale grinding forces during surface micro-grinding the Kistler dynamometer is used.
The comparison of predicted force value and experimental force value are given in Fig.8.5 and Fig.8. 6.

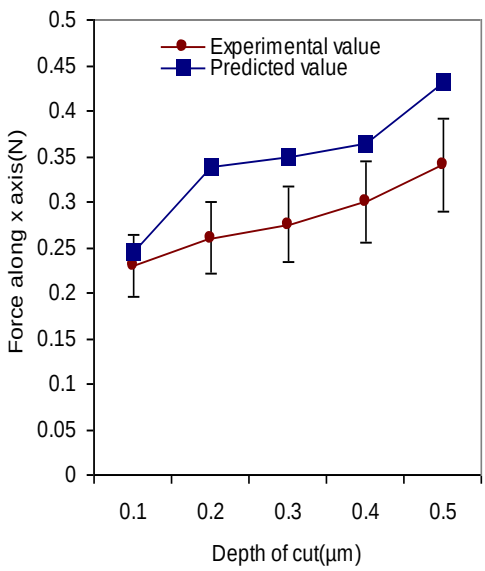

(a)

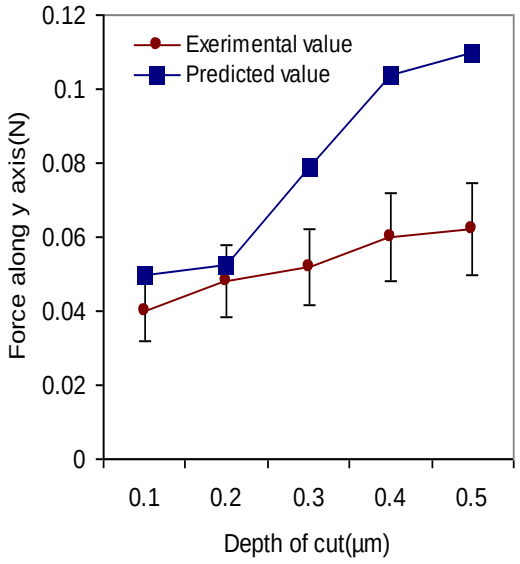

(b)

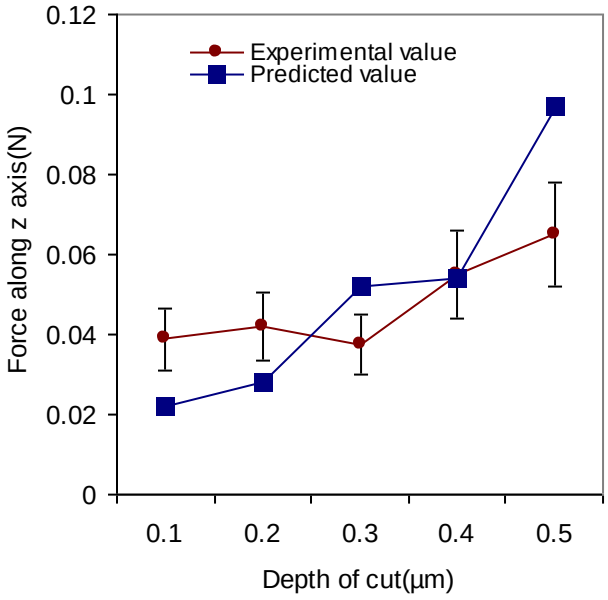

(c)

Fig.8. 5.Effect of depth of cut on the micro grinding force

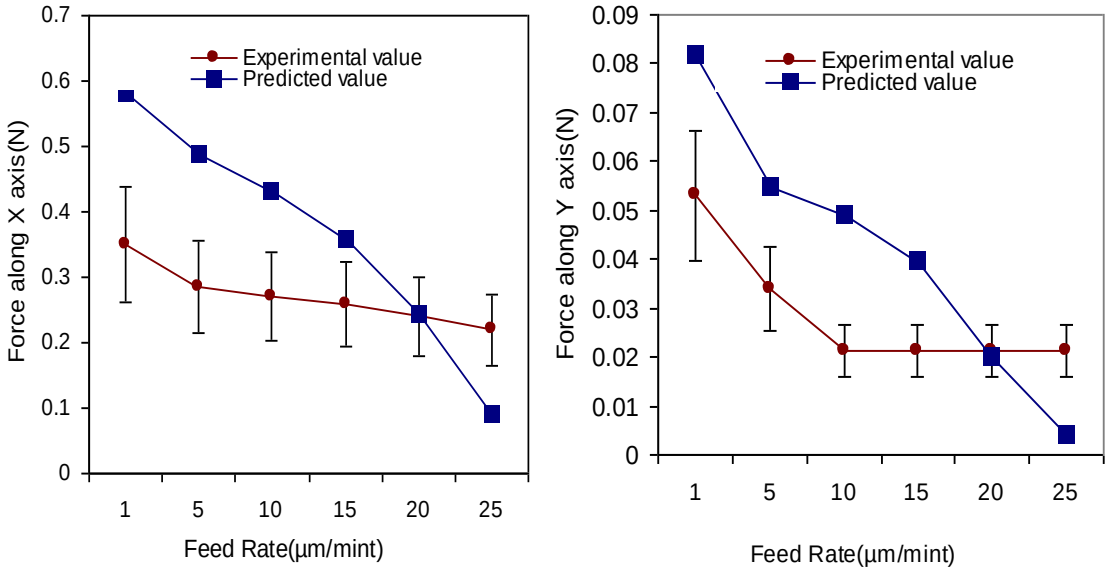

(a) (b)

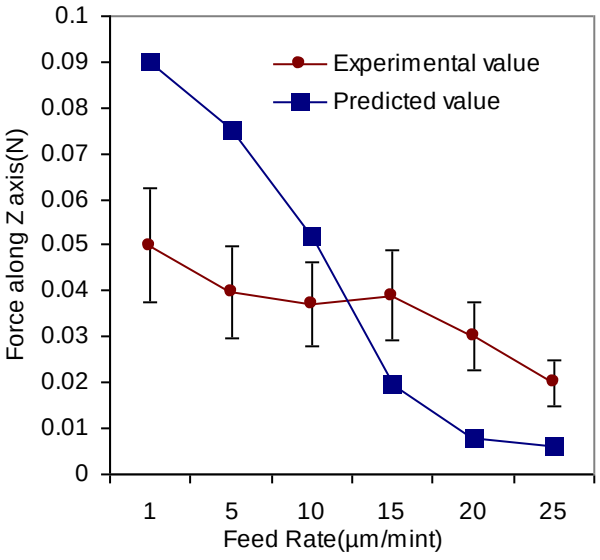

(c)

Fig.8. 6.Effect of feed rate on the micro grinding force.

From the figure 8.5 and 8.6, it can be observed that the trends of predicted force is quiet similar with the experimental data set. In case of varying depth of cut, predicted force along x and z axis show quite good agreement with the experimental values, though force in y axis show larger difference with the experimental data for higher depth of cut value. It is also found that, for lower depth of cut, predicted and experimental value shows

better agreement than that of higher depth of cut value. In case of varying feed rate, the predicted values also show good agreement with the experimental one. In addition, it is found that difference between experimental data and predicted data is larger in case of lower feed rate.

Reasons of discrepancy can be considered as follows.

- The effects of trapped chips

  During micro grinding, some of chips generated are paste on the machined surface and then trapped between the tool and machined surface. These chips prevents the engagement of the cutting edge with the uncut surface thus reducing the active cutting grain amount. Therefore the dynamic cutting edge might vary from the actual one.

- The rigidity of micro-grinding wheel

  Another source of error might arise from the tool stiffness. Usually the micro-grinding tool has low value of stiffness which may cause the elastic deflection during machining process. Due to this deflection, micro grinding process can be affected.

- Lower force value

  The force value is less than 1 N. Hence the percentage of errors is high as fraction of force even counts here.

- Non-conductivity of work piece

  As the W/p is non-conductive, temperature rise may be significant here which is not considered in the model.

8.7 Statistical analysis

In order to understand the variation between predicted and experimental data, Paired T-test has been performed considering 95% significance level, using both sets of data using the following hypothesis.

- Null hypothesis- if the difference between data set=0
- Alternative hypothesis- if difference between data set $\neq 0$
  - Now if P value <0.05, null hypothesis is rejected
  - if P value> 0.05; null hypothesis is accepted

Table 8. 1: T test value for force along different axis.

Force	Along x axiz	Along y axis	Along Z axis
P value(varying depth of cut)	0.1090	0.1002	0.84271
P value (varying feed rate)	0.249	0.3315	0.7148

Test result showed the P value is always greater than 0.05 proving that there is not much statically difference between experimental and predicted data set. Hence the predicted value seems well accepted.

8.8. Concluding Remarks

- This study presented a predictive method for quantification of micro scale grinding process based on physical analysis of the process.
- In this model, forces are expressed as function of the process configuration, work piece material properties, and micro-grinding tool topography.
- This model includes single grain interaction approach considering both chip formation and ploughing force.
- The model was validated by comparing predicted and experimental values. The comparison suggests that the prediction driven by the model captures the main trends of experimental data although there is some discrepancy still exist which can be attributed to the effect of microstructure on the material properties and temperature effect.
- Statistical analysis was performed to evaluate the model discrepancy which shows the model is significantly accepted.

Chapter 9

Conclusions, Contributions and Recommendations

This chapter includes the conclusions derived from the fundamental analysis of the micro-grinding of glass using on machine fabricated PCD tool, the contributions of the thesis in the field of precision finishing and future recommendations.

9.1 Conclusions

The conclusions obtained from the fundamental analysis of micro-grinding of glass using on-machine fabricated PCD tool are grouped under the following categories:

1. Parametric studies of PCD tool fabrications and selection of optimum parameters for micro-grinding of glass.
2. Fabrication of different possible and useful shape of tool in a single set up and comparison of the performance of these tools.
3. Analysis of tool wear
4. Analysis of sub-surface damage generated

9.1.1 Experimental Studies of Micro-Grinding of Glass

A comparative analysis on the micro-grinding performance of three commonly used glass materials: Lithosil, BK7 and N-SF14 glass was carried out using an on-machine fabricated PCD tool. The effect of micro-EDM conditions on tool fabrication, and its performance during microgrinding was studied. In addition, the effects of grinding parameters on cutting forces and surface roughness were investigated. Following conclusions can be drawn from this experimental investigation:

- The micro-EDM parameters have significant influence on the surface roughness and performance of the fabricated PCD tool during glass micro-grinding. Considering the machining time, optimum parameters for micro-EDM was found

to be 120 V, 1000 pF and 30 µm feed length. Nevertheless, better surface roughness required the consideration of lower energy level. During the fabrication of PCD tool using micro-EDM, lower discharge energy produces smoother surface on the PCD tool, which generates smaller chips on the glass surface during microgrinding and eventually generates better surface finish.

- The increase of axial depth of cut and feed rate results in increase of cutting forces along all axes, though some variations of forces are observed. Surface roughness was found to increase with the increase of axial depth of cut and feed rate. An axial depth of cut of 2 µm and feed rate of 1 µm/min were found to be optimum in terms of cutting forces and achieved surface finish.
- The cutting force is higher in case of Lithosil glass followed by BK7 compared to N-SF14. The BK7 glass showed intermediate behaviour by generating moderately lower cutting forces and causing lesser adhesion of glass chips at the bottom of PCD tool.
- For the slots machined by microgrinding using PCD tool, surface roughness is lowest at the middle of the slot with an increasing trend along the corners of the slots. In addition, some traces of scratching and dragging track were observed at the middle portion of the machined slot, especially in N-SF14 glass materials, as brittle mode cutting regime was found to dominate in this region.
- BK7 glass has better machinability during microgrinding with on-machine fabricated PCD tool based on cutting force and surface roughness analysis. Finally, smooth and defect-free surface with lowest average surface roughness of 12.79 nm has been achieved in the microgrinding of BK7 glass using micro-EDM-fabricated PCD tool.

9.1.2. Effects of Cutting Tool Geometry on the Glass Micro-grinding Process

In this study a comparative analysis on the micro-machining performance of four different geometry PCD tools: circular, D-shaped, triangular, and square on BK7 glass was carried out. In addition, the effect of tool geometry on the cutting forces surface roughness and tool wear were investigated during the glass micro-machining. Following conclusions can be drawn from this experimental investigation:

- With the concept of block micro-EDM and using the specifically designed block, microelectrodes of conical, triangular, square or rectangular, circular and D-shaped tool have been fabricated successfully in single set up. Using this specifically designed block has been established to be a feasible method for the fabrication of microelectrodes of few tens micrometer.
- D-shaped tool experienced lowest cutting force along X and Y-axis, whereas triangular tool has experienced lowest force along Z-axes. Both square and circular tool generated quite high cutting forces along Z and X-axis during micro-grinding, though along all axes square tool experienced highest cutting force. Comparatively lower cutting force along Y-axis has been observed for triangular tool than square one.
- For the groove machined by micro-grinding using PCD tool, surface roughness showed considerable change from circular tool to others. Small particles, which were present on the surface machined by circular tool, were almost absent in case of surface machined by other tools. Lowest average surface roughness has been achieved using square tool and little higher in case of d-shape tool. Due to higher peak density on the machined surface by triangular tool resulted in higher average and maximum surface roughness. Moreover, side surface of machined groove using d-shape tool was much better than square or triangular tool, whereas circular tool demonstrated the best result.
- Square and triangular tools experienced more wear compared to circular and D-shaped tools due to the tendency of tool edge blunting.

- ❖ Finally, D-shape tool demonstrated better performances among all the tools in terms of cutting force, roughness value, side surface and wear rate.

9.1.3. Analysis and Monitoring of Wear of PCD Micro-tool

Micro-grinding of BK7 glass has been performed using on-machine fabricated PCD micro-tool in order to investigate the tool wear mechanism and tool condition monitoring under the same cutting conditions. From the results presented, the following conclusions can be drawn.

- ❖ It was found that the consequences of the tool wear are the diameter reduction as well as length reduction. Again, the G ratio for this PCD micro tool was found to be nearly 940. Basically, two types of tool wear have been detected. One is edge chipping at the tool rim which is actually responsible for radial reduction of tool as well. Chip accumulation at tool and work pieces interface causes built up edge formation and gradually this built up edge grows larger in size, becomes unstable then eventually breaks up. This process of built up edge is repeated continuously during the cutting process and the number of edge chipping is getting increase with the machining time. Nearby chipping edge gets superimposed and create bigger area of chipping. In addition, abrasive wear which occurs due to the faster and weaker grain boundary break down and then creating some inter-granular crack. These cracks propagate through the groups of grain or grain boundary causing the diamond grain spalling and form wear region.
- ❖ The effect of tool wear on the surface roughness is found to be significant through the micro-grinding experiments of BK7 glass using PCD micro-tool. In some conditions, the Ra value increases several times with the tool wear progress, which makes it necessary to consider tool wear along with other cutting conditions to contribute to surface roughness as well as cutting forces. Depending on the surface roughness value of ground channel, tool wear progress can be divided into 3 stages where, in initial stage tool suffers insignificant wear, then intermediate wear condition and finally severe worn out tool. Huge pitting on the

bottom surface, drastically chipped side wall, noticeably longer center line, and double side wall lining are the major phenomena on the machined surface due to the severe tool wear.

- ❖ Generated chips have effect on tool wear and surface roughness but analysis of chips morphology during different time of machining cannot be related to the actual tool wear condition.
- ❖ Observation of normal grinding force can give indication of the tool conditioning during grinding process only but it cannot be perfectly related to the severity of tool wear. Continuous monitoring of AE signal is found to give an indication of tool topographic condition, i.e. sharpness and bluntness of PCD cutting edge during micro-grinding. Moreover, this signal can also envisage minor and major tool chipping conditions. Hence, monitoring the AE signal can be a plausible way of monitoring on-machine fabricated PCD tool condition.

9.1.4. Analysis of Sub-surface Damage (SSD) Generated

In order to develop an individual process, it is very important to know the subsurface damage induced by each machining process. Such knowledge for surface grinding of BK7 glass by on-machine fabricated PCD tools has been provided by this study.

The following conclusion can be drawn from the above studies.

- ❖ Ground surface consists of four different areas (a) the smooth area; (b) the fracture area; (c) the smeared area; and (d) the ploughing striations.
- ❖ At low rate of material removal, the cutting points on the tool remove and expel the material from the machined surface in an efficient manner. At high rates of material removal however debris is not expelled efficiently and the debris generated from the cut must pass between the tool and machined surface and hence influence the machined surface and as well as the sub-surface.

- ❖ It is noticed that chipping damage grows with the increase of depth of cut. With the further increase of depth of cut it shows jig jag trend of decreasing and increasing afterward. Total damage also shows the same trends along with the change of depth of cut
- ❖ It is also found that SSD of ground surface using lower spindle speed are quite large. This might be due to the fact that, the abrasives have certain mechanical load intensity; hence they might be smashed under a certain wallop. Higher spindle speed will have usually higher probability to produce higher wallop. Under lower spindle speed the abrasives have a lower tendency to crash into further smaller pieces. As a result, larger size abrasives take part in the grinding and consequently produce larger sub-surface damage.
- ❖ It is found from the graph that with the increasing value of depth of cut the total damage depth also increasing initially. Then further increment of depth results in a dropping of total damage layer then finally again tends to increase.
- ❖ It is seen that the depth of damage decrease initially with the increasing feed rate. After this initial reduction, this damage starts to grow again with the increase of feed rate. This trend is true for both chipping and total damage in case of different spindle speeds also.
- ❖ During micro-grinding process, the contact of an individual diamond particle with the glass work piece might produce the damage zone which contains distributed grain-boundary micro-cracks. The chipping layer is an outcome of either intergranular or transgranular micro-cracking. Usually when the fracture resistance in the grain boundary and in the grain has same level; the crack would always prefer to follow the shortest way and the fracture path would always be transgranular.
- ❖ Grinding induced subsurface crack exhibit different configurations like median lateral, branch, and cone. The crack size is nearly 1µm. Sub-surface crack may exist under those ground surface which look even fracture or damage free by the microscopic observation.

- ❖ It can be seen that surface roughness increases initially with the increase of depth of cut and the decreases with the increases of depth of cut. It is found that with the increase of feed rate surface roughness initially decreases and then finally starts to increase. This trend of surface roughness also shows good agreement with sub–surface damage, although this surface roughness cannot reveal the morphology of sub-surface damage.

9.1.5. Modeling of vertical micro-grinding

- ❖ This study presents a predictive method for quantification of micro scale grinding process based on physical analysis of process.
- ❖ In this model, forces are expressed as functions of the process configuration, work piece material properties, and micro-grinding tool topography.
- ❖ This model includes single grain interaction approach considering both chip formation and ploughing force.
- ❖ The model has been validated by comparing predicted and experimental values. The comparison suggests that the prediction driven by the model captures the main trends of experimental data.
- ❖ Statistical analysis confirms the validity of the model.

9.2 The Research Contribution

The contributions of the thesis in the field of the precision grinding have been classified and discussed in the following categories.

9.2.1 The Approaches and Analysis on this New type of Micro-grinding

- ➢ The approaches used in this thesis for the prediction of effectiveness of micro-grinding of glass techniques have never been reported earlier. The investigation conducted in this thesis will be certainly helpful for the PCD

users to understand the importance of choosing fabrication parameters that works in better associations with the microgrinding parameters and to utilize the full effectiveness of the PCD tool for precision finishing of brittle material like glass.

- In this thesis, block EDM process has been approached as microgrinder fabrication method and dressing method as well which can facilitate fabrication of different shapes and sizes tools in single set up. To the best knowledge of author, no or few studies conducted elsewhere on the microgrinding of glass using PCD tool fabricated by block EDM.

- The investigation conducted in this thesis on the wear progression and mechanism, wear rate of PCD tool while glass micro-grinding have never been done before. The relation among tool wear, cutting force and AE signal are entirely new and useful analysis, which are more essential to necessitate offline dressing for tool wear compensation.

- The investigation conducted on the sub-surface damage revels the behavior of PCD tool during micro-grinding. This knowledge of damage generation promotes the importance of selecting optimum parameters for machining of a particular work pieces.

- An modified analytical model for the prediction of cutting force for the microgrinding of glass using this PCD tool with extreme fine grain size has been established considering various process parameters. So far, very few studies have been reported on the modeling of micro-grinding process. Therefore, this modeling can have significant contribution in the area of microgrindging.

9.3 Recommendations for Future Research

This micro-grinding of glass using on-machine fabricated PCD tool is a new technique which needs to be analyzed and improved further. Some of the future directions are proposed as follows.

- Tool wears monitoring and wear compensation

  Tool wear is responsible for achieving profile accuracy of ground components. Profile accuracy of ground components has much more room for improvement and so there are many possibilities for development from this research .Hence, online tool wear monitoring and compensation are essential steps to perform in order to maintain the geometrical accuracy of machined parts. This way the desired profile can be achieved with less error.

- Vibrations assisted micro-grinding

  Till now combined effect of ultrasonic vibration with grinding of metal has proven to improve machining results. Even, combined with grinding process the ultrasonic vibration was found to improve the machining force for ceramics now a day. It was found to reduce the normal force component along with slightly increase tool wear. Hence for glass materials, vibration assisted micro-grinding using on-machine fabricated PCD has room for further improvement. This ultrasonic assisted grinding can be applied as an efficient production technology in the current process condition.

- Grinding of Si wafer using PCD tool

  As silicon is semiconductor which cannot be machined using micro-EDM properly, grinding of silicon wafer using PCD tool can be a good idea to look into. The exploration of silicon wafer grinding using on-machined fabricated PCD tool will be very interesting area to be explored.

- Temperature aspect of Grinding

One of the influential considerations in ductile mode grinding process is the effect of temperature. In ductile mode cutting energy consumed in plastically deforming and removing the material is eventually converted into heat energy. This heat content can be significant and may influence material properties in the cutting zone. The future works may consider this temperature effect of grinding using this on machine fabricated PCD tool.

- Modification of the Force model

  Temperature aspect has not been considered in the force model, which can be incorporated in the model as a part of future work. For making the model less complex, single row of grain are considered to be involved in the cutting which can be extended further for the more than one row of grain involvement in future work.

Bibliography

A.G.Mamalis, 2004. Two stage electro-discharge machining fabricating superhard cutting tools. Journal of Material Processing Technology 146, 318-325.

Agarwal, S. and Rao, P.V., 2008. Experimental investigation of surface/subsurface damage formation and material removal mechanisms in SiC grinding. International Journal of Machine Tools and Manufacture 48, 698-710.

Ahn, H.-S., Wei, L. and Jahanmir, S., 1996. Nondestructive Detection of Damage Produced by a Sharp Indenter in Ceramics. Journal of Engineering Materials and Technology 118, 402-409.

al., L.J.C.e., 1998. Subsurface Damage in Microgrinding Optical Glasses. Advances in Fusion and Processing of Glass 82, 469-474.

Allen, D.M. and Lecheheb, A., 1996. Micro electro-discharge machining of ink jet nozzles: optimum selection of material and machining parameters. Journal of Materials Processing Technology 58, 53-66.

B. Zhang, X.L.Z., H. Tokura, M. Yoshikawa, 2003. Grinding induced damage in ceramics. Journal of Materials Processing Technology 132 (1–3), 353–364.

Bai, Q.S., Yao, Y.X., Bex, P. and Zhang, G., 2004. Study on wear mechanisms and grain effects of PCD tool in machining laminated flooring. International Journal of Refractory Metals and Hard Materials 22, 111-115.

Basuray, P.K., Misra, B.K. and Lal, G.K., 1977. Transition from ploughing to cutting during machining with blunt tools. Wear 43, 341-349.

Beilby, G., 1921. Aggregation and Flow of Solids Macmillan and Co., London, .

Belloy, E., Thurre, S., Walckiers, E., Sayah, A. and Gijs, M.A.M., 2000. The introduction of powder blasting for sensor and microsystem applications. Sensors and Actuators a-Physical 84, 330-337.

Bu, M., Melvin, T., Ensell, G.J., Wilkinson, J.S. and Evans, A.G.R., 2004. A new masking technology for deep glass etching and its microfluidic application. Sensors and Actuators A: Physical 115, 476-482.

Buchmann, P.K., 1992. Properties and Applications of Diamond, by J. Wilks und E. Wilks, Butterworth-Heinemann, Oxford 1991 525 pp., hardcover, ISBN 0-7506-1067-0. Advanced Materials 4, 307-307.

C.K.Syn, D.A.K., P.J. davis, M.R. McClellan, P.C DuPuy, M. A. Wall, K.L. Blaedel, April 1998. An empirical survey on the influences of machining parameters in diamond turning of large single crystal silicon optics. ,p. Proceedings of the ASPE Spring Topical Meeting on Silicon Machining, California.

Cai, M.B., Li, X.P. and Rahman, M., 2007. Study of the mechanism of nanoscale ductile mode cutting of silicon using molecular dynamics simulation. International Journal of Machine Tools and Manufacture 47, 75-80.

Cao, G., Zhao, W., Wang, Z. and Guo, Y., 2005. Instantaneous fabrication of tungsten microelectrode based on single electrical discharge. Journal of Materials Processing Technology 168, 83-88.
Carr, J.W., Fearon, E., Hutcheon, I.D. and Summers, L.J., 1999. Subsurface damage assessment with atomic force microscopy.
Choi, D., Kwon, W.T. and Chu, C.N., 1999. Realâ€ • Time Monitoring of Tool Fracture in Turning Using Sensor Fusion. The International Journal of Advanced Manufacturing Technology 15, 305-310.
Chris, J.M. and et al., 2004. Micro machining glass with polycrystalline diamond tools shaped by micro electro discharge machining. Journal of Micromechanics and Microengineering 14, 1687.
Collin, M. and Rowcliffe, D., 2002. The morphology of thermal cracks in brittle materials. Journal of the European Ceramic Society 22, 435-445.
Conway, J.C. and Kirchner, H.P., 1986. Crack Branching as a Mechanism of Crushing During Grinding. Journal of the American Ceramic Society 69, 603-607.
Corman T, E.P., Stemme G,, 1998. Deep wet etching of borosilicate glass using an anodically bonded silicon substrate. J Micromech Microeng, 8, 84-87.
D.J.Anthony, 1990. Concepts of Polycrystalline diamond tooling for the woodworking industry. proceedings of the first international Symposium on Tooling for the Wood Industry, Raleigh, NC.
Daniels, W.H., 1989. Super abrasives for ceramic grinding and finishing. SME Technical Paper EM89-125.
Daridon, A., Fascio, V., Lichtenberg, J., Wütrich, R., Langen, H., Verpoorte, E. and de Rooij, N., 2001. Multi-layer microfluidic glass chips for microanalytical applications. Fresenius' Journal of Analytical Chemistry 371, 261-269.
Dietrich, T.R., Ehrfeld, W., Lacher, M., Krämer, M. and Speit, B., 1996. Fabrication technologies for microsystems utilizing photoetchable glass. Microelectronic Engineering 30, 497-504.
Egashira, K. and Mizutani, K., 2002. Micro-drilling of monocrystalline silicon using a cutting tool. Precision Engineering 26, 263-268.
Etoh, S., Fujimura, T., Hattori, R. and Kuroki, Y., 2003. Fabrication of on-chip microcapillary using photosensitive glass. Microsystem Technologies 9, 541-545.
F. Klocke, E.B., C. Evans, T. Howes, I. Inasaki, E. Minke, 1997. High speed grinding—fundamental and state of art in Europe, Japan and USA. Annals of CIRP 46 (2), 715–724.
F. Klocke, E.V., C. Schippers, 1999. High-speed grinding of ceramics. S. Jahanmir, M. Ramulu, P. Koshy (Eds.)Machining of Ceramics and Composites, Marcel Dekker, New York, 119–138.
Feng, J., Kim, B.S., Shih, A. and Ni, J., 2009. Tool wear monitoring for micro-end grinding of ceramic materials. Journal of Materials Processing Technology 209, 5110-5116.
Feng, j., Kim, G. y., Shih, A. J., Ni, J., 2007. Investigation of the micro-end grinding of ceramics using a sintered metal bonded micro grinding wheel International Symposium on Advance Abrasive Technology, 413-420.

Fielder, K.H., 1988. Precision grinding of brittle materials. Ultra precision in manufacturing engineering, Springer- Verlag, Berlin, 72–77.
Foy, K., Wei, Z., Matsumura, T. and Huang, Y., 2009. Effect of tilt angle on cutting regime transition in glass micromilling. International Journal of Machine Tools and Manufacture 49, 315-324.
Freitag, A., Vogel, D., Scholz, R. and Dietrich, T.R., 2001. Microfluidic Devices Made of Glass. 6, 45-49.
Friedrich, C.R., Coane, P.J. and Vasile, M.J., 1997. Micromilling development and applications for microfabrication. Microelectronic Engineering 35, 367-372.
Gao, G.F., Zhao, B., Xiang, D.H. and Kong, Q.H., 2009. Research on the surface characteristics in ultrasonic grinding nano-zirconia ceramics. Journal of Materials Processing Technology 209, 32-37.
Goddard, J. and Wilman, H., A theory of friction and wear during the abrasion of metals. Wear 5, 114-135.
Gretillat, M.A., Paoletti, F., Thiebaud, P., Roth, S., KoudelkaHep, M. and deRooij, N.F., 1997. A new fabrication method for borosilicate glass capillary tubes with lateral inlets and outlets. Sensors and Actuators a-Physical 60, 219-222.
Gu, W., Yao, Z. and Li, H., 2011. Investigation of grinding modes in horizontal surface grinding of optical glass BK7. Journal of Materials Processing Technology 211, 1629-1636.
Guitrau, E.B., 1997. The EDM handbook. Hanser Gardner Publications.
H. Huang, L.Y., 18–20 July, 2001. High speed grinding performance and material removal mechanism of silicon nitride. Proceedings of 10th International Conference on Precision Engineering, Yokohama, Japan, . 416–420.
H. Huang, Y.C.L., 2003. Experimental investigations of machining characteristics and removal mechanisms of advanced ceramics in high speed deep grinding. International Journal of Machine Tools & Manufacture 43, 811–823.
H. Huang, Y.C.L., T.L. Teo, 26–30 May, 2002. High speed deep grinding of yttria stabilized tetragonal Zirconia. Proceedings of Euspen Third International Conference, Eindhoven, The Netherlands, 201–204.
H.K.Xu, S.J., 1995. Microfracture and material removal in scratching of alumina. Journal of Materials Science 30, 2235-2247.
Hamada, H., 1985. Diamond tools for ultra precision machining. J. Jpn. Soc, Precis. Eng. 51(9), 9-13.
Hecker, R.L., Ramoneda, I.M. and Liang, S.Y., 2003. Analysis of Wheel Topography and Grit Force for Grinding Process Modeling. Journal of Manufacturing Processes 5, 13-23.
Hyung Wook Park, 2008. Development of Micro-grinding mechanics and machine tools.
I.Hutchings, 1992. Tribology: Friction and Wear of Engineering Materials. Butterworth/Heinmann.
J. C. Lambropoulos, Y.L., P. Funkenbusch, and J. Ruckman, 1999. Non-contact estimate of grinding subsurface damage. Proceedings of Optical, manufacturing and testing conference,P. Stahl, ed, Proc. SPIE 3782, 41–50.

J.A. Kovach, M.A.L., S. Malkin, S. Srinivasan, B. Bandyopadhyay, K.R. Ziegler, 1993. A feasibility investigation of high-speed, low damage grinding for advanced ceramics. SME Fifth International Grinding Conference 1, SME.

Jahan, M.P., Rahman, M., Wong, Y.S. and Fuhua, L., On-machine fabrication of high-aspect-ratio micro-electrodes and application in vibration-assisted micro-electrodischarge drilling of tungsten carbide. Proceedings of the Institution of Mechanical Engineers, Part B: Journal of Engineering Manufacture 224, 795-814.

Jahan MP, R.M., Wong YS, Fuhua, L, 2009. On-machine fabrication of high-aspect-ratio micro-electrodes and application in vibration-assisted micro-electro discharge machining drilling of tungsten carbide. Proc IMechE Part B: J Eng Manuf DOI: 10.1243/09544054JEM1718.

Jahan, M.P., Wong, Y.S. and Rahman, M., 2009a. A study on the fine-finish die-sinking micro-EDM of tungsten carbide using different electrode materials. Journal of Materials Processing Technology 209, 3956-3967.

Jahan, M.P., Wong, Y.S. and Rahman, M., 2009b. A study on the quality micro-hole machining of tungsten carbide by micro-EDM process using transistor and RC-type pulse generator. Journal of Materials Processing Technology 209, 1706-1716.

Jemielniak, K. and Otman, O., 1998. Tool failure detection based on analysis of acoustic emission signals. Journal of Materials Processing Technology 76, 192-197.

Joseph, M., Bernie, P., Phil, M., Tom, P., Mike, N., John, P. and Don, G., 2002. Combined advanced finishing and UV-laser conditioning for producing UV-damage-resistant fused silica optics. Optical Fabrication and Testing, Optical Society of America, p. OMB4.

Jung-Chou, H. and et al., 2006. Using a helical micro-tool in micro-EDM combined with ultrasonic vibration for micro-hole machining. Journal of Micromechanics and Microengineering 16, 2705.

Jung-Chou, H. and et al., 2008. Fabrication of a micro-spherical tool in EDM combined with Ni-diamond co-deposition. Journal of Micromechanics and Microengineering 18, 045010.

Kakade, S., Vijayaraghavan, L. and Krishnamurthy, R., 1994. In-process tool wear and chip-form monitoring in face milling operation using acoustic emission. Journal of Materials Processing Technology 44, 207-214.

Karow, H.H., 1993. Fabrication Methods for Precision Optics. John Wiley & Sons, Inc., New York 301–317.

Khan Malek, C., Robert, L., Boy, J.-J. and Blind, P., 2007. Deep microstructuring in glass for microfluidic applications. Microsystem Technologies 13, 447-453.

Kim, J.-D. and Kim, D.S., 1995. Theoretical analysis of micro-cutting characteristics in ultra-precision machining. Journal of Materials Processing Technology 49, 387-398.

Kirchner, H.P., 1984. Damage Penetration at Elongated Machining Grooves in Hot-Pressed Si3N4. Journal of the American Ceramic Society 67, 127-132.

Koepke, B.G., Stokes, R.J. and Honeywell Inc Hopkins Minn Corporate Research, C., 1969. A STUDY OF GRINDING DAMAGE IN MAGNESIUM OXIDE SINGLE CRYSTALS. Defense Technical Information Center.

Kopac, J. and Krajnik, P., 2006. High-performance grinding--A review. Journal of Materials Processing Technology 175, 278-284.
Kopalinsky, E.M. and Oxley, P.L.B., 1984; Oxford; UK; 9-12 Apr. Size Effects in Metal Removal Processes Mechanical Properties at High Rates of Strain Oxford; UK;, 389-396
Kozak J, R.K.P., and Wang S Z., 1994. Material removal in wire EDM of PCD blanks. . J. Eng. Ind 116, 363–369.
L. Yin, H.H., K. Ramesh, T. Huang,, 2005. High speed versus conventional grinding in high removal rate machining of alumina and alumina–titania. International Journal of Machine Tools & Manufacture 45, 897–907.
Lawn, B., 1993. Fracture of Brittle Solids, second ed., . Cambridge SolidState Science Series.
Li, K. and Liao, W., 1997. Modelling of ceramic grinding processes Part I. Number of cutting points and grinding forces per grit. Journal of Materials Processing Technology 65, 1-10.
Li, X.H., Abe, T. and Esashi, M., 2001. Deep reactive ion etching of Pyrex glass using SF6 plasma. Sensors and Actuators a-Physical 87, 139-145.
Liang, S.Y., 2004. Machining and Metrology at Micro/Nano Scale 1st International Conference on Positioning Technology, Act-city, Hamamatsu, Japan,, 23-28.
Lim, H.S., Wong, Y.S., Rahman, M. and Edwin Lee, M.K., 2003. A study on the machining of high-aspect ratio micro-structures using micro-EDM. Journal of Materials Processing Technology 140, 318-325.
Lin, C.H., Lee, G.B., Lin, Y.H. and Chang, G.L., 2001. A fast prototyping process for fabrication of microfluidic systems on soda-lime glass. Journal of Micromechanics and Microengineering 11, 726-732.
Liu, K., Li, X., Liang, S.Y. and Dong Liu, X., 2005. Nanometer-Scale, Ductile-Mode Cutting of Soda-Lime Glass. Journal of Manufacturing Processes 7, 95-101.
Liu, K. and Li, X.P., 2001. Modeling of ductile cutting of tungsten carbide. Trans.NAMRI/SME 29, 251-258.
Liu, K. and Melkote, S.N., 2006. Effect of plastic side flow on surface roughness in micro-turning process. International Journal of Machine Tools and Manufacture 46, 1778-1785.
Liu, Q., Chen, X., Wang, Y. and Gindy, N., 2008. Empirical modelling of grinding force based on multivariate analysis. Journal of Materials Processing Technology 203, 420-430.
Liu Y H, G.Y.F.a.L.J.C., 1999. Electric discharge milling of polycrystalline Diamond. Proc. Inst. Mech. Eng. B 211, 643–647.
Llanes, L., Idañez, E., Martínez, E., Casas, B. and Esteve, J., 2001. Influence of electrical discharge machining on the sliding contact response of cemented carbides. International Journal of Refractory Metals and Hard Materials 19, 35-40.
Luo, S.Y., Liao, Y.S., Chou, C.C. and Chen, J.P., 1997. Analysis of the wear of a resin-bonded diamond wheel in the grinding of tungsten carbide. Journal of Materials Processing Technology 69, 289-296.

Luo, S.Y., Liao, Y.S. and Tsai, Y.Y., 1999. Wear characteristics in turning high hardness alloy steel by ceramic and CBN tools. Journal of Materials Processing Technology 88, 114-121.

M.J. Chen, D.L., S. Dong, F.H. Zhang, 2004. Factors influencing the surface quality during ultra-precision grinding of brittle materials in ductile mode,. Key Engineering Materials 257/258, 201–206.

Mahdavinejad, R.A., 2005. EDM machining of WC-Co. Journal of Material processing Technology 162-163, 637-643.

Maksoud, T.M.A., Mokbel, A.A. and Morgan, J.E., 1999. Evaluation of surface and sub-surface cracks of ground ceramic. Journal of Materials Processing Technology 88, 222-243.

Malkin, S., 1989. Grinding technology : theory and applications of machining with abrasives. E. Horwood ; Halsted Press, Chichester; New York.

Malkin, S. and Cook, N.H., 1971. The Wear of Grinding Wheels: Part 2---Fracture Wear. Journal of Engineering for Industry 93, 1129-1133.

Malkin, S. and Guo, C., 2008. Grinding technology: theory and applications of machining with abrasives. Industrial Press.

Malkin, S. and Hwang, T.W., 1996. Grinding Mechanisms for Ceramics. CIRP Annals - Manufacturing Technology 45, 569-580.

Mamalis, A.G., Grabchenko, A.I., Magazeev, M.G., Krukova, N.V., Prohàszká, J. and Vaxevanidis, N.M., 2004. Two-stage electro-discharge machining fabricating superhard cutting tools. Journal of Materials Processing Technology 146, 318-325.

Masuzawa, T., 2000. State of the Art of Micromachining. CIRP Annals - Manufacturing Technology 49, 473-488.

Masuzawa, T., Fujino, M., Kobayashi, K., Suzuki, T. and Kinoshita, N., 1985. Wire Electro-Discharge Grinding for Micro-Machining. CIRP Annals - Manufacturing Technology 34, 431-434.

Merchant, M.E., 1945. Mechanics of metal cutting process, and type 2 chip
Journal of Applied Physics 16, 318-324.

Miklaszewski, S., Zurek, M., Beer, P. and Sokolowska, A., Micromechanism of polycrystalline cemented diamond tool wear during milling of wood-based materials. Diamond and Related Materials 9, 1125-1128.

Mitra, P.R.W.a.S.K., 2008. Investigation of Combined Electro-Osmotic and Pressure-Driven Flow in Rough Micro channels. Journal of fluid Engineering 130, 061204.

Miyashita, M., November 1985. paper presented at 1st Annual Precision Engineering Conference, North Carolina State University, Raleigh, NC, .

Mokbel, A.A. and Maksoud, T.M.A., 2000. Monitoring of the condition of diamond grinding wheels using acoustic emission technique. Journal of Materials Processing Technology 101, 292-297.

Morgan, C.J., Vallance, R.R. and Marsh, E.R., 2004. Micro machining glass with polycrystalline diamond tools shaped by micro electro discharge machining. Journal of Micromechanics and Microengineering 14, 1687-1692.

Moronuki N, B.E., 2002. Micromachining of brittle materials by ultrasonic lapping with tool wear compensation. In: Proceedings of the 3rd EUSPEN international conference, Eindhoven, The Netherlands, 399–402

Mourzina, Y., Steffen, A. and Offenhäusser, A., 2005. The evaporated metal masks for chemical glass etching for BioMEMS. Microsystem Technologies 11, 135-140.

Nachiappan Ravi and Han. Huang, 2002. Fabrication of symmetrical section micro features using the electro-discharge machining block electrode method. J. Micromech. Microeng. 12, 905-910.

Nachiappan Ravi, H.H., 2002. Fabrication of symmetrical section micro features using the electro-discharge machining block electrode method. J. Micromech. Microeng. 12, 905-910.

Nachiappan. Ravi, S., Xue Chuan, 2002. The effects of electro-discharge machining block electrode method for microelectrode machining. J. Micromech.Microeng 532-540.

Nakazawa, H., 1994. Principles of precision engineering. Oxford University Press.

Nikumb, S., Chen, Q., Li, C., Reshef, H., Zheng, H.Y., Qiu, H. and Low, D., 2005. Precision glass machining, drilling and profile cutting by short pulse lasers. Thin Solid Films 477, 216-221.

Onikura, H., Inooue, R., Okuno, K., Ohnishi,O., 2003. Fabrication of electroplated micro grinding wheel and manufacturing of microstructure with ultrasonic vibration. Key Engineering materials 238-239, 9-14.

P. Hed, a.D.F.E., 1987. Optical glass fabrication technology. 2: Relationship between surface roughness and subsurface damage," Appl. Opt. 26(21)

P. Hed, D.F.E., and J. B. Davis, 1989. Subsurface damage in optical materials: origin, measurements and removal. . Collected papers from ASPE Spring Conference on subsurface damage in glass, Tucson, AZ

P.S.Sreejith, B.K.N., 2001. Material removal mechanisms in precision machining of new materials International J. Machine tools &Manufecturing 41, 1831-1843.

Perveen, A., Jahan, M.P., Rahman, M. and Wong, Y.S., A study on microgrinding of brittle and difficult-to-cut glasses using on-machine fabricated poly crystalline diamond (PCD) tool. Journal of Materials Processing Technology In Press, Corrected Proof.

Petersen, D., Mogensen, K.B. and Klank, H., 2004. Glass Micromachining. Wiley-VCH Verlag GmbH & Co. KGaA.

Pham, D.T., Dimov, S.S., Bigot, S., Ivanov, A. and Popov, K., 2004. Micro-EDM--recent developments and research issues. Journal of Materials Processing Technology 149, 50-57.

Philbin, P. and Gordon, S., 2005. Characterisation of the wear behaviour of polycrystalline diamond (PCD) tools when machining wood-based composites. Journal of Materials Processing Technology 162-163, 665-672.

Plaza, J.A., Lopez, M.J., Moreno, A., Duch, M. and Cane, C., 2003. Definition of high aspect ratio glass columns. Sensors and Actuators a-Physical 105, 305-310.

Randi, J.A., Lambropoulos, J.C. and Jacobs, S.D., 2005. Subsurface damage in some single crystalline optical materials. Appl. Opt. 44, 2241-2249.

Ravindra, H.V., Srinivasa, Y.G. and Krishnamurthy, R., 1997. Acoustic emission for tool condition monitoring in metal cutting. Wear 212, 78-84.

Reynaerts, D., Heeren, P.-H. and Van Brussel, H., 1997. Microstructuring of silicon by electro-discharge machining (EDM) -- part I: theory. Sensors and Actuators A: Physical 60, 212-218.

S. Blackeley, R.O.S., 1990. Mechanics of material removal in diamond turning. Proceedings of the ASPE Annual Meeting, Rochester, NY,, 68-71.

Schlautmann, S., Wensink, H., Schasfoort, R., Elwenspoek, M. and van den Berg, A., 2001. Powder-blasting technology as an alternative tool for microfabrication of capillary electrophoresis chips with integrated conductivity sensors. Journal of Micromechanics and Microengineering 11, 386-389.

Shaw, M., 2003. The size effect in metal cutting. Sadhana 28, 875-896.

Shaw, M.C., 1972. Fundamentals of grinding. Proc. of Int'1 grinding Conf.: New Developments in Grinding, pittsburge,PA,April 1972,, 221-258.

Shaw, M.C., 1996. Principles of abrasive processing. Clarendon Press.

Shun-Tong, C. and et al., 2008. Fabrication of a miniature diamond grinding tool using a hybrid process of micro-EDM and co-deposition. Journal of Micromechanics and Microengineering 18, 055005.

Sin, H., Saka, N. and Suh, N.P., 1979. Abrasive wear mechanisms and the grit size effect. Wear 55, 163-190.

Slikkerveer, P.J., Bouten, P.C.P. and de Haas, F.C.M., 2000. High quality mechanical etching of brittle materials by powder blasting. Sensors and Actuators a-Physical 85, 296-303.

Son, S.M., Lim, H.S. and Ahn, J.H., 2005. Effects of the friction coefficient on the minimum cutting thickness in micro cutting. International Journal of Machine Tools and Manufacture 45(4-5), 529-535.

Soon, W.K., 2009. Modeling of the tool edge radius effect on the mechanics of micromachining. Dissertation, National University of Singapore.

Srihari, G. and Lal, G.K., 1994. Mechanics of vertical surface grinding. Journal of Materials Processing Technology 44, 14-28.

Stjernstrom, M. and Roeraade, J., 1998. Method for fabrication of microfluidic systems in glass. Journal of Micromechanics and Microengineering 8, 33-38.

Sun, X., Stephenson, D.J., Ohnishi, O. and Baldwin, A., 2006. An investigation into parallel and cross grinding of BK7 glass. Precision Engineering 30, 145-153.

Suzuki, H., Moriwaki, T., Yamamoto, Y. and Goto, Y., 2007. Precision Cutting of Aspherical Ceramic Molds with Micro PCD Milling Tool. CIRP Annals - Manufacturing Technology 56, 131-134.

T. G. Bifano, T.A.D., R. O. Scattergood, 1992. Ductile-regime grinding. A new technology for machining brittle materials. Journal of Engineering for Industry, Vol.113 (1991), 113, 184–189.

T. Nakasuji, S.K., S. Hara, H. Matsunaga, N. Ikawa, S. Shimada, 1990. Diamond turning of brittle materials for optical components. Annals of the CIRP 39(1), 89–92.

T.G. Bifano, T.A.D.a.R.O.S., 1991. Ductile regime grinding: a new technology for machining brittle materials. Journal of Engineering for Industry 113, 184–189.

T.W. Hwang, C.J.E., E.P. Whitenton, S. Malkin, 1999. High speed grinding of silicon nitride with electroplated diamond wheels. I. Wear and wheel life. Manufacturing Science and Engineering 10, 431–441.

Takahashi, T. and Funkenbusch, P.D., 2000. Micromechanics of diamond composite tools during grinding of glass. Materials Science and Engineering A 285, 69-79.

Takashi Matsumura, T.H.a.T.S., 2005. A study on cutting force in the Milling process of glass. Journal of Manufacturing Processes 7, 102-108.

Torres, C.D., Heaney, P.J., Sumant, A.V., Hamilton, M.A., Carpick, R.W. and Pfefferkorn, F.E., 2009. Analyzing the performance of diamond-coated micro end mills. International Journal of Machine Tools and Manufacture 49, 599-612.

V.C. Venkatesh, I.I., H.K. Toenshoff, T. Nakagawa, I.D. Marinescu, 1995. Observations on polishing and ultraprecision machining of semiconductor substrate materials. Annals of the CIRP 44(2), 611–618.

Verkerk, J. and Peters, J., 1977. FINAL REPORT CONCERNING CIRP COOPERATIVE WORK ON THE CHARACTERIZATION OF GRINDING WHEEL TOPOGRAPHY. Ann CIRP 26, 385-395.

W. Konig, L.C., U. Dortmund, G. Spur, H.K. Tonshoff, M. Vigneau, W.J. Zdeblick, 1990. Machining of new materials. Annals of the CIRP 39(2), 673–681.

W. Pfeiffer, T.H., , in: S. Jahanmir 1993. Damage determination and strength prediction of machined ceramics by X-ray diffraction techniques. Machining of Advanced Materials, National Institute of Standards and Technology SP 847, Government Printing Office, Washington, DC, 235–245.

Waghmare, P.R. and Mitra, S.K., 2008. Investigation of Combined Electro-Osmotic and Pressure-Driven Flow in Rough Microchannels. Journal of Fluids Engineering 130, 061204-061207.

Weng, F.T., Shyu, R.F. and Hsu, C.S., 2003. Fabrication of micro-electrodes by multi-EDM grinding process. Journal of Materials Processing Technology 140, 332-334.

Xu, H.H.K., Padture, N.P. and Jahanmir, S., 1995. Effect of Microstructure on Material-Removal Mechanisms and Damage Tolerance in Abrasive Machining of Silicon Carbide. Journal of the American Ceramic Society 78, 2443-2448.

Xu, H.K. and Jahanmir, S., 1995. Microfracture and material removal in scratching of alumina. Journal of Materials Science 30, 2235-2247.

Y. Shen, Y.L., X.P. Xu, Y. Gao, 2003. Force and energy characteristics in grinding of ceramics. Key Engineering Materials 238/239, 105–110.

Y.J. Yuan, L.G., S. Dong, 1993. Ultra-precision machining of SiCw/Al composites. Annals of the CIRP 42 (1), 107–109.

Yin, S., Ohmori, H., Uehara, Y., Shimizu, T. and Lin, W., 2004. Micro V-Groove Grinding Technique of Large Germanium Immersion Grating Element for Mid-Infrared Spectrograph. JSME International Journal Series C Mechanical Systems, Machine Elements and Manufacturing 47, 59-65.

Yoshikawa, H., 1967. Brittle–ductile behaviour of crystal surface in finishing. Journal of JSPE 35, 662–667.

Zarudi, I. and Zhang, L.C., 2000. On the Limit of Surface Integrity of Alumina by Ductile-Mode Grinding. Journal of Engineering Materials and Technology 122, 129-134.

Zhang, B., 1993. Precision grinding regime of advanced ceramics, in: Proceedings of the 1993 Annual Meeting of American Society of Precision Engineering, Seattle, Washington, DC, November 7–12. 225–229.
Zhang, B. and Howes, T.D., 1994. Material-Removal Mechanisms in Grinding Ceramics. CIRP Annals - Manufacturing Technology 43, 305-308.
Zhang, B., Zheng, X.L., Tokura, H. and Yoshikawa, M., 2003. Grinding induced damage in ceramics. Journal of Materials Processing Technology 132, 353-364.
Zhao, Q., Liang, Y., Stephenson, D. and Corbett, J., 2007. Surface and subsurface integrity in diamond grinding of optical glasses on Tetraform 'C'. International Journal of Machine Tools and Manufacture 47, 2091-2097.
Zhou, M., Ngoi, B.K.A., Yusoff, M.N. and Wang, X.J., 2006. Tool wear and surface finish in diamond cutting of optical glass. Journal of Materials Processing Technology 174, 29-33.
Zhou, Y., Funkenbusch, P.D., Quesnel, D.J., Golini, D. and Lindquist, A., 1994. Effect of Etching and Imaging Mode on the Measurement of Subsurface Damage in Microground Optical Glasses. Journal of the American Ceramic Society 77, 3277-3280.

List of Publications

Journals (Peer-Reviewed):

1. Asma Perveen, M.P. Jahan, M. Rahman, Y.S. Wong; A study on microgrinding of brittle and difficult-to-cut glasses using on-machine fabricated poly crystalline diamond (PCD) tool, International Journal of Material Processing Technology, Volume 212, Issue 3, Pages 580-593 (March 2012).

2. Asma Perveen, M.P. Jahan, M. Rahman, Y.S. Wong; Cutting Force Analysis of On Machine Fabricated PCD Tool during Glass Micro- grinding, Advanced Materials Research (Published), DOI. 10.4028/www.scientific.net/AMR.264-265.1085.

3.Asma Perveen, Y.S. Wong, M. Rahman; Fabrication of different geometry cutting tools and their effect on the vertical micro grinding of BK7 glass, Journal of Advanced Manufacturing Technology, (26 October 2011), pp. 1-15, doi:10.1007/s00170-011-3688-5.

4**.** *Asma Perveen, Y.S. Wong, M. Rahman Characterization and online monitoring of wear behaviour of on machine fabricated PCD micro-tool while vertical micro-grinding of BK7 glass. International Journal of Abrasive Technology, 2011 - Vol. 4, No.4 pp. 304 - 324.*

5. Asma Perveen, M. Rahman, Y.S. Wong; Analysis of surface and subsurface damage of micro-ground BK7 glass using on machine fabricated PCD micro-tool, International Journal of Abrasive Technology.(Accepted)

6. Asma Perveen, Y.S. Wong, M. Rahman; Force modeling of Vertical Micro grinding Incorporating single grain interaction, Journal of Material Processing Technology. (Submitted)

International Conferences:

1. Asma Perveen, Rahman. M, Y. S, Wong, Comparative Micro-grinding performance of BK-7, Lithosil and NSF14 glass using on–machine fabricated PCD tool, Proceeding of 5th international Conference on leading Edge Manufacturing in 21st Century(LEM21), 2-4th December, 2009, Osaka University Convention Centre Japan, pp.563-568.

2. Asma Perveen, M.P. Jahan, Y. S, Wong, Rahman. M, Cutting force analysis of on machine fabricated PCD tool during glass micro-grinding, The International conference on Advances in Material and Processing Technology (APMT), 26-29 October, 2009, KL, Malaysia.

3. Asma Perveen, Y. S. Wong, Rahman. M, Fabrication of PCD micro-tools using block EDM method and their application to different micro-structures in brittle and hard materials, Proceedings of the ASME 2010 ASME international Manufacturing Science and Engineering Conference (MSEC2010),12-15th October, 2010, Erie, Pennsylvania, USA.

4. *Asma Perveen, Y. S. Wong, Rahman, Wear behavior of PCD micro-tool while vertical micro-grinding of BK7 glass, Proceedings of the 11th Euspen International Conference – Como – May 2011.*

5. *Asma Perveen, M, Rahman, Y. S. Wong,Analysis of surface and subsurface damage of micro-ground Bk7 glass using on machine fabricated PCD micro-tool, Proceedings of the 12th Euspen International Conference - Stockholm-June 2012.*